DOCTORAL DISSERTATION

GEOHISTORY OF THE CENTRAL ANATOLIAN PLATEAU SOUTHERN MARGIN (SOUTHERN TURKEY)

PhD Student: Giuditta Radeff

Supervisors

Prof. Domenico Cosentino – Roma Tre University

Prof. Manfred R. Strecker – Potsdam University

Co-supervisor

Taylor F. Schildgen, PhD – Potsdam University

Roma Tre University – Department of Science
in Cotutelle de Thèse with
Potsdam University - Institute of Earth and Environmental Science

Scuola Dottorale in Geologia dell'Ambiente e delle Risorse
Sezione Geologia dell'Ambiente e delle Risorse
Ciclo XXVI

DOCTORAL DISSERTATION

GEOHISTORY OF THE CENTRAL ANATOLIAN PLATEAU SOUTHERN MARGIN (SOUTHERN TURKEY)

PhD Student: Giuditta Radeff

Supervisors

Prof. Domenico Cosentino – Roma Tre University

Prof. Manfred R. Strecker – Potsdam University

Co-supervisor

Taylor F. Schildgen, PhD – Potsdam University

Director of the Doctoral School

Prof. Claudio Faccenna

Reviewers

Dr. Gian Paolo Cavinato
IGAG – CNR

Prof. William B. Ryan
Columbia University

To Mrs. Conci,
who taught me the meaning of "important"

To Mr. Christian, Mrs. Floriana and Miss Elisabeth,
my idea of happiness

Wann immer einen die Dinge erschreckten, sei es eine gute Idee, sie zu messen.
“Die Vermessung der Welt”, Daniel Kehlmann

Quando si ha paura delle cose, bisogna misurarle.
“La misura del Mondo”, Daniel Kehlmann

TABLE OF CONTENTS

2. DIFFERENCES AND SIMILARITIES IN THE LATE MIOCENE SUBSIDENCE HISTORIES OF THE MUT AND ADANA BASINS (SOUTHERN TURKEY): A RECORD OF SURFACE UPLIFT OF THE SE MARGIN OF THE CENTRAL ANATOLIAN PLATEAU

Preface

This work is the result of a 3 years doctoral project, within the framework of a "Cotutelle de Thèse" between Roma Tre University and Potsdam University.

The project is about the Adana Basin (southern Turkey). The position of the basin, located at the southeastern margin of the Central Anatolian Plateau and close to the Arabia-Eurasia collision zone, is ideal to record fundamental Neogene topographic and tectonic changes in the easternmost Mediterranean realm.

The thesis is organized in three chapters, each one constituting a preliminary draft for a publication.

The first chapter focuses on the study of a very well time-constrained sedimentary unit constituted by an alternation of conglomerates and marls bearing a brackish-water fauna and deposited during the latest stage of the Messinian Salinity Crisis (*Lago-Mare* stage ~5.45 – 5.33 Ma). I interpret 34 seismic lines, calculate the volume of the sedimentary body and I perform a provenance analysis by means of clast counting the conglomeratic portion and measuring paleocurrent directions. My first goal is to find a trace of the Central Anatolian Plateau southeastern margin uplift recorded in the sediments of the Adana Basin. I furthermore suggest a possible mechanism leading to the uplift of the plateau margin and to the subsidence in the Adana Basin.

The second chapter focuses on the comparison between the Adana Basin and the Mut Basin, another mainly Neogene basin located on top of the Central Anatolian Plateau southern margin. Differences and similarities on the stratigraphy, present elevation of the sediments and subsidence curves of the two basin are described and commented. I apply stratigraphy, seismic stratigraphy, 3D-surface restoration, isopach map reconstruction, and volume calculation to describe the evolution of the Adana Basin and its subsidence history. I integrate the data from a field-work carried on by Prof. Domenico Cosentino (Roma Tre supervisor) with data from literature in order to reconstruct the subsidence curve for the Mut Basin. The first aim is to better define the uplift history of the Central Anatolian Plateau southern margin.

The third chapter presents new structural data collected along the NW and SE margin of the Adana Basin and integrate them with the present seismicity of the area. The analysis of the spatial and temporal variation of the deformation coupled with the analysis of the present seismotectonic setting help to better define the

tectonic evolution of the Adana Basin and to furthermore comment the possible mechanism leading to subsidence in the basin.

1.

SEDIMENTARY EVIDENCE FOR LATE MIOCENE UPLIFT OF THE SE MARGIN OF THE CENTRAL ANATOLIAN PLATEAU: ADANA BASIN, SOUTHERN TURKEY

1.1. Introduction

Orogenic plateaus are areas of high mean-surface elevation that exert a fundamental influence on climate, erosion, and sedimentation (e.g. Molnar et al. 1993; Li et al. 1997; Zhisheng et al. 2001; Carrapa et al. 2006; Strecker et al. 2007). Understanding the timing and the mechanisms leading to the uplift of these major topographic features is therefore an outstanding topic that can help improve our understanding of the connection between geodynamic processes, changes in sedimentary supply, and climate evolution. Sedimentary rocks preserved within and along the margins of orogenic plateaus provide first-order information about the spatiotemporal development of these morphotectonic provinces (e.g. Vandervoort et al. 1995; DeCelles et al. 1998; Chung et al. 1998; Metivier et al. 1998; Najman and Garzanti 2000; Wörner et al. 2002; Carrapa et al. 2006; Uba et al. 2007; Strecker et al. 2009; Decou et al. 2011). Nonetheless, it is often difficult to obtain a detailed and reliable chronostratigraphic framework for these sedimentary sequences, and to link the stratigraphic record unambiguously to major changes in topography.

The Central Anatolian Plateau, which is characterized by a well dated sedimentary record capping its southern margin (Cosentino et al. 2012; Schildgen et al. 2012b) and a thick succession of sediments bordering its south and southeastern margin, provides an optimal setting to investigate the local interactions among tectonics, climate, erosion, and surface uplift, and possibly also uplift mechanisms at the plateau margin (Schildgen et al. 2012a and b; Lüdecke et al. 2013; Mazzini et al. 2013).

The Anatolian Plateau is an integral part of the western reaches of the Himalayan orogenic belt, formed during the Cenozoic by accretion of different lithospheric plates as a result of closure and suturing of the northern and southern branches of the Neotethys Ocean (Şengör and Yılmaz 1981; Görür et al. 1984; Robertson and Dixon 1984; Şengör et al. 1984; Biryol et al. 2011). The current westward motion of the Aegean-Anatolian plate with respect to Eurasia along two major transform faults, the North Anatolian and

East Anatolian faults (Fig. 1A; Ketin 1948; McKenzie 1978; Şengör 1979; Dewey and Şengör 1979; Şengör et al. 1985), appears to be controlled by the combined effects of the retreat of the Hellenic trench and the continental collision of the Arabian and Eurasian plates. Based on different deformation styles throughout this complex region, the Anatolia has been subdivided into four principal tectonic provinces (Şengör 1985): the Northern Anatolian province, separated from the other three by the North Anatolian Fault; the predominantly extensional Western Anatolian province(McKenzie 1970, 1978; Le Pichon and Angelier 1979; Jackson and McKenzie 1984; McClusky et al. 2000; Reilinger et al. 1997, 2006); the largely contractional Eastern Anatolian province with the Eastern Anatolian Plateau (EAP; McKenzie 1970, 1978; Şengör 1980; Jackson and McKenzie 1984; Jackson 1992; McClusky et al. 2000; Reilinger et al. 1997 2006), and the Central Anatolian province, which is transitional between the Eastern Anatolian and Western Anatolian provinces (Fig. 1A; Barka and Reilinger 1997; Bozkurt 2001).

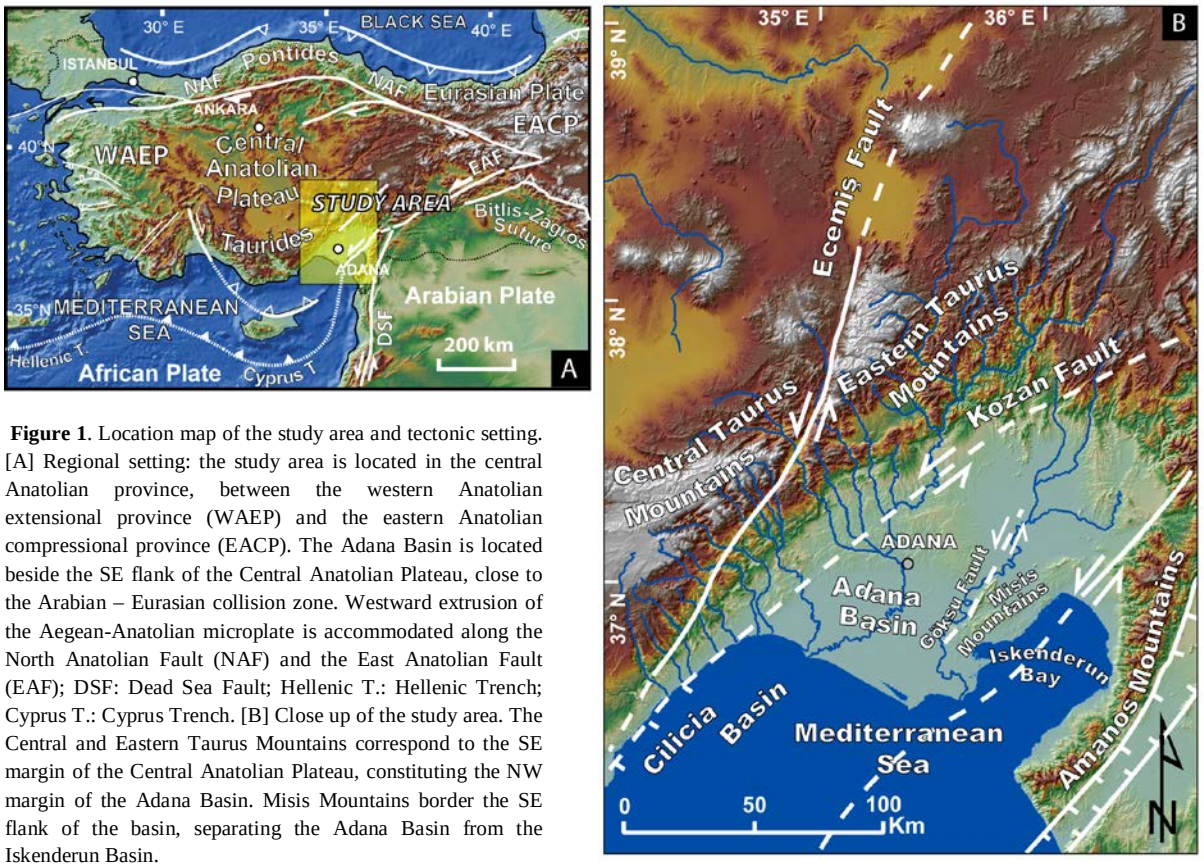

Figure 1. Location map of the study area and tectonic setting. [A] Regional setting: the study area is located in the central Anatolian province, between the western Anatolian extensional province (WAEP) and the eastern Anatolian compressional province (EACP). The Adana Basin is located beside the SE flank of the Central Anatolian Plateau, close to the Arabian – Eurasian collision zone. Westward extrusion of the Aegean-Anatolian microplate is accommodated along the North Anatolian Fault (NAF) and the East Anatolian Fault (EAF); DSF: Dead Sea Fault; Hellenic T.: Hellenic Trench; Cyprus T.: Cyprus Trench. [B] Close up of the study area. The Central and Eastern Taurus Mountains correspond to the SE margin of the Central Anatolian Plateau, constituting the NW margin of the Adana Basin. Misis Mountains border the SE flank of the basin, separating the Adana Basin from the Iskenderun Basin.

Although much attention over the past several decades has focused on the evolution of the Aegean/Western Anatolian province with respect to slab retreat (Le Pichon and Angelier 1979, 1981; Faccenna et al. 2006; Jolivet et al. 2013) and the growth of the Eastern Anatolian plateau associated with

continental collision and deeper lithospheric processes (Meissner and Mooney 1998; Şengör et al. 2003; Keskin 2003, 2006), only recently has attention been focused on the timing and mechanisms of topographic development in Central Anatolia (Cosentino et al. 2012; Schildgen et al. 2012a, 2012b, in press; Cipollari et al. 2013a and b). Given that the evolution of the Central Anatolian Plateau (CAP) is likely to have been influenced by the geodynamics of its bordering regions, studying the temporal and spatial evolution of the CAP surface uplift is crucial for understanding i) the style and timing of crustal deformation; ii) the tectonic setting of the central Anatolian province; and iii) the mechanisms leading to vertical and lateral growth of the plateau.

Mantle delamination and slab break-off following continental collision have been suggested as the likely trigger mechanisms for volcanism and uplift in Eastern Anatolia (Pearce et al. 1990; Şengör et al. 2003; Keskin 2003, 2006; Göğüş and Pysklywec 2008; Kuscu and Geneli 2010). These interpretations were based on the moderate crustal thickness of the plateau (Zor et al. 2003), which is insufficient to explain the strongly negative Bouguer gravity anomalies (Ates et al. 1999).

Break-off of the Tethyan slab is also inferred for the southern margin of Central Anatolia based on mantle tomography (Gans et al. 2009; Biryol et al. 2011) and seismicity studies (Kalyoncuoğlu et al. 2011; Imprescia et al. 2012), which indicate the absence of a slab east of Cyprus. Coupled with the broad pattern of uplift involving regional warping of late Miocene marine sediments, the current evidence points to a deep-seated uplift mechanism for this region (Cosentino et al. 2012; Schildgen et al. 2012a, 2012b, in press). However, critical for testing the likelihood of slab break-off versus other potential mechanisms of uplift, such as crustal thickening through accretion (e.g. Fuller et al. 2006), is quantifying the pattern, timing, and rate of uplift throughout the region.

Based on biostratigraphy and magnetostratigraphy of the late Miocene marine sediments capping the southern margin of the CAP, the maximum age constraint on the start of surface uplift is ~8 Ma in the vicinity of the Ermenek Basin (Cosentino et al. 2012) or 6.7 Ma farther west (Schildgen et al. 2012b). However, a minimum age for the start of uplift has not yet been defined. Fortunately, the south and southeastern margins of the CAP are flanked by the Cilicia-Adana basin complex, an areally extensive depocenter of late Oligocene to recent sediments and potential archive of tectono-sedimentary processes for

the southern margin of the CAP (Fig. 1 A and B; Schmidt 1961; Görür 1979; Yetiş 1988; Ünlügenç et al. 1991; 1993; Gürbüz and Kelling 1991, 1993; Yetiş et al. 1995; Gürbüz andÜnlügenç 2001). A well established stratigraphy, precise age constraints on the late Miocene deposits (Cosentino et al. 2010b; Cipollari et al. 2013a; Faranda et al. 2013), and proximity to the plateau border make the Adana Basin a promising target for investigating changes in sedimentation patterns and rates that may signal topographic growth of the SE margin of the CAP.

In this study, we use provenance analysis and seismic stratigraphic observations to calculate the volume of a sedimentary unit that potentially documents plateau-margin growth. Moreover, our comparison of regional patterns of vertical crustal motions, i.e., between uplift of the CAP and sedimentation/subsidence in the Adana Basin, provides additional observations to help test hypotheses concerning geodynamic mechanisms responsible for this relatively young phase of plateau development.

1.2. Tectonic setting of the Central Anatolian Plateau and the Adana Basin

The Central Anatolian Plateau (CAP) lies within the Aegean-Anatolian plate, with its northern and southern margins defined by the Pontide and Tauride orogenic belts (Fig. 1A). The CAP is the result of a multi-phase deformation history. Convergence between the African-Arabian and Eurasian plates led to the accretion of the Pontide and Tauride fold-and-thrust belts, after the closure of the Paleotethyan Ocean in the Eocene and the Neotethyan Ocean in the Eocene to middle Miocene (e.g. Şengör and Yılmaz 1981; Şengör et al. 1984; Robertson and Dixon 1984; Robertson et al. 1996; Yılmaz et al. 1998; Görür et al. 1984, 1998; Gökten and Floyd 1987; Gökten 1993). A late Eocene – early Miocene extensional tectonic phase, probably linked to retreat of the African plate (Jolivet and Faccenna 2000; Kempler and Ben-Avraham 1987; Whitney and Dilek 1997; Dilek et al. 1999; Robertson 2000), has been tentatively correlated with the Oligocene to early Miocene terrestrial sedimentation recorded in several basins throughout the Central Taurides; the onset of terrestrial deposition can be interpreted as a first step in regional topographic growth (Clark and Robertson 2002, 2005; Bassant et al. 2005; Eriş et al. 2005; Şafak et al. 2005).

A second episode of topographic development in Eastern Anatolia postdates continental collision between Arabia and Eurasia at ca. 17.5 – 20 Ma (Okay et al. 2010; Ballato et al. 2011). This event closed the gateway between the Mediterranean and Indian Ocean; the minimum age proposed for the closure of the Tethyan gateway is ca. 11 Ma (Gelati 1975; Hüsing et al. 2009), creating the Bitlis-Zagros suture zone. Continental collision has also been associated with crustal thickening (Zor et al. 2003; Angus et al. 2006; Ozacar et al. 2008), which probably contributed to isostatic uplift of the Eastern Anatolian Plateau and the westward translation of the Aegean-Anatolian plate along the right-lateral North Anatolian and the left-lateral East Anatolian faults (Şengor et al. 1985). Nevertheless, because deformation along the North Anatolian Fault Zone predates continental collision along the Bitlis-Zagros suture (Zattin et al. 2005, 2010), and because the rate of motion of the Aegean-Anatolian plate along the Africa-Arabia-Eurasia continental collision zone increases towards the Hellenic trench (Reilinger et al. 2006), Aegean slab rollback has generally been accepted as the primary force driving the current westward movement of the Aegean-Anatolian plate (Reilinger et al. 2006; Okay et al. 2008; Mart and Ryan 2002; Mart 2013).

The Adana-Cilicia basin complex is a wide depocenter within the Aegean-Anatolian plate, north of the suture between the African and Aegean-Anatolian plates, here defined by the Cyprus Trench (Aksu et al. 2005a). East of the Cyprus Trench, the geometry of the plate boundary is complicated by the East Anatolian Fault, which has been tentatively linked by different authors (e.g. Şengor et al. 1985; Dewey et al. 1986; Chorowicz et al. 1994; Poole and Robertson 1998; Aksu et al. 2005a; Reilinger et al. 2006; Yin 2010; Koç et al. 2012) to the Bitlis-Zagros suture zone towards the northeast and to the Cyprus Trench to the southwest. The Ecemiş and Kozan faults are suggested to be splays of the East Anatolian Fault; they are characterized by left lateral trans-tensional kinematics (i.e. Aksu et al. 2005b; Burton-Ferguson et al. 2005) and are presently accommodating the differential uplift of the CAP relative to the Adana Basin (Cipollari et al. 2013a). The Adana-Cilicia Basin is confined to the north and northwest by the south and southeastern margin of the CAP, corresponding to the Central and Eastern Taurus mountains; to the south and southeast, it is bordered by the Misis-Kyrenia sector (Fig. 1B). As a result of the complex tectonic setting, the Adana Basin development has been alternatively associated with i) syn- or post-collisional tectonics related to slab dynamics (Williams 1995; Robertson 2004; Aksu et al. 2005a); ii) the widespread transcurrent motion

related to the development of the East Anatolian Fault Zone (Kelling et al. 1987; Chorowicz et al. 1994); or iii) a combination of the two processes (Şengor et al. 1985; Dewey et al. 1986).

The Adana Basin (Fig. 1B) constitutes the onshore prolongation of the offshore Cilicia Basin and thus contains a unique sedimentary record of the regional Neogene tectonic events (Brinkmann 1976; Kelling et al. 1987), potentially including the continental collision between the Arabian and the Eurasian plates and the uplift of the CAP. Moreover, according to recently published data (Grossi et al. 2011; Cipollari et al. 2013a; Faranda et al. 2013), the Adana Basin records all the main steps of the Messinian Salinity Crisis (MSC), a regional tectono-climatic event with far-reaching consequences for landscape evolution and environmental conditions (Hsü et al. 1977; Clauzon et al. 1978; Lofi et al. 2005; CIESM 2008 and references therein; Bache et al. 2009; Mocochain et al. 2009; Garcia-Castellanos et al. 2011; Lofi et al. 2011). Because the main steps of the MSC are precisely dated through a combination of astronomical tuning (Krijgsman et al. 1999; Cosentino et al. 2013) and high-precision CA-TIMS zircon U-Pb geochronology (Cosentino et al. 2013), this portion of the Adana Basin sedimentary fill is very well temporally constrained. Because the stratigraphic framework of these sediments is key for understanding the timing and nature of the erosive processes along the southern flank of the CAP, we briefly review the most relevant aspects of the Messinian deposits in the next section.

1.3. The Messinian Salinity Crisis

The Messinian Salinity Crisis (MSC, Fig. 2A) is a major event that impacted the paleogeographical and environmental evolution of the Mediterranean area, as a consequence of changes in the Atlantic-Mediterranean connection during the late Miocene. Although the factors leading to the MSC are still debated, the main events that occurred during the crisis have been widely recognized and precisely dated. According to Manzi et al. (2013), the onset of the MSC occurred at 5.97 +/- 0.003 Ma, with the deposition of the first Messinian gypsum cycle, generally referred to as the Primary Lower Gypsum (CIESM 2008 and references therein). Between 5.56 ± 0.005 Ma and 5.532 ± 0.0046 Ma (Cosentino et al. 2013), likely in correspondence with the TG12 glacial peak (5.55 Ma; Shackleton et al. 1995; Hodell et al. 2001; Cosentino

et al. 2013), the isolation of the Mediterranean from the Atlantic Ocean led to evaporative drawdown of the sea level (CIESM 2008). Marginal areas of the basin were subaerially exposed and erosion created the regional intra-Messinian unconformity, also known as the Messinian Erosional Surface (MES; Guillemin and Honzay 1982; Costa et al. 1986; Cita and Corselli 1990; Escutia and Maldonado 1992; Riding et al. 1999; Guennoc et al. 2000; Roveri et al. 2001; Rouchy et al. 2003; Lofi et al. 2005; Soria et al. 2005; Cornée et al. 2006; Maillard et al. 2006; Roveri et al. 2008; Garcia-Castellanos et al. 2009; Ryan et al. 2009; Sampalmieri et al. 2010; Cosentino et al. 2010a; Cosentino et al. 2013). Coinciding with development of the MES, the post-evaporitic stage of the MSC started just before 5.532 ± 0.0046 Ma (Cosentino et al. 2013). Two post-evaporitic units, p-ev1 and p-ev2, separated by a regional unconformity called LM1 (5.42 Ma; Roveri et al. 1998, 2001, 2006, 2008) or MES2 (5.45 Ma; Cosentino et al. 2010a and b; Cipollari et al. 2013a; Cosentino and Cipollari 2012) were deposited above the MES. The lower unit (p-ev1) consists of barren laminated sediments, seep limestones (Sampalmieri et al. 2008, 2010; Iadanza et al. 2013), sediments eroded from the basin margins (Resedimented Lower Gypsum; CIESM 2008), and in the deep basins, a thick halite layer (Lofi et al. 2011, and references therein; Speranza et al. 2013). The Resedimented Lower Gypsum records a transition from hyper- to hypohaline conditions (Roveri et al. 2008; Sampalmieri et al. 2010), sometimes including a brackish-water fauna that is associated with the *Lago-Mare* event (Hsü et al. 1973; Cita et al. 1978; Rouchy 1982; Emeis et al. 1996; Orszag-Sperber 2006; Grossi et al. 2008; Faranda et al. 2013). The spreading of this brackish to fresh fauna is what characterizes the sediments of the post-evaporitic upper unit (p-ev2, Grossi et al. 2008). The switch to an essentially brackish environment has been linked to wetter conditions following glacial stage TG12 (Van Der Laan et al. 2006), which was characterized by increased precipitation and runoff throughout the Mediterranean (Orszag-Sperber et al. 2000; Rouchy et al. 2001; Griffin 2002; Pierre et al. 2006; Willet et al. 2006; Reuter et al. 2011; Cosentino et al. 2012). The enhanced production of sediments observed in some marginal basins during the *Lago-Mare* event of the MSC has been interpreted as a consequence of the climatic shift from drier to wetter conditions and the resultant increase in runoff and erosion (Willett et al. 2006; Roveri et al. 2008), perhaps coupled with tectonic activity (Cosentino et al. 2006). The end of the MSC corresponds to the re-establishment of the connection between the Atlantic and the Mediterranean and the re-flooding of the Mediterranean Basin, which occurred at the onset of the

Pliocene (5.33 Ma; Iaccarino et al. 1999a and b; Iaccarino and Bossio 1999; Orszag-Sperber 2006 and references therein; Pierre et al. 2006; Gennari et al. 2008; Cipollari et al. 2013a).

1.4. Stratigraphy of the Adana Basin

The sedimentary fill in the Adana Basin unconformably lies above Palaeozoic and Mesozoic clastic, carbonate, and ophiolitic rocks, which form the regional basement that is part of the Tauride nappes. The base of the fill consists of Oligocene fluvial and lacustrine sediments of the Karsanti Formation, pertaining to the Karsanti intermontane basin (Schmidt 1961; Gürbüz and Kelling 1993; Yetiş et al. 1995; Williams et al. 1995; Gürbüz and Ünlügenç 2001). Based on the extent and the geometry of the Oligocene-lower Miocene fluvial red beds of the Gildirli Formation, they are the first deposits that can be strictly associated with the Adana Basin proper (Schmidt 1961; Görür 1979; Yetiş 1988; Ünlügenç et al. 1991, 1993; Gürbüz and Kelling 1991, 1993; Yetiş et al. 1995; Gürbüz and Ünlügenç 2001). These units are followed by and pass laterally into shallow marine fossiliferous sandstone, siltstone, marls, and sandy limestone of the Aquitanian-Burdigalian Kaplankaya Formation (Yetiş et al. 1995; Cronin et al. 2000; Nazik 2004). The coarse marine deposits of the Kaplankaya Formation also laterally pass into the Burdigalian – Langhian, reefal Karaisali Formation (Görür 1979; Cronin et al. 2000; Nazik 2004) and the lower portion of the Çingoz Formation (Schmidt 1961). The latter is a Burdigalian – early Serravallian turbidite fan system (Görür 1979; Yetiş and Demirkol 1986; Yetiş 1988; Gürbüz and Kelling 1993; Williams et al. 1995; Yetiş et al. 1995: Gürbüz 1999; Cronin et al. 2000) deposited along the NW margin of the Adana Basin; it passes laterally into the lower portion of the Serravallian Guvenç Formation, which consists of deep marine clays passing upward into sandy, shallow marine deposits (Ünlügenç et al. 1991; Nazik and Gürbüz 1992; Gürbüz and Kelling 1993; Yetiş et al. 1995). The first regressive event from the onset of deposition in the Adana Basin is reported to have occurred in late Serravallian - early Tortonian time (Yetiş 1988; Ünlügenç 1993; Yetiş et al. 1995). This event was associated with the deposition of the continental and shallow marine deposits of the Tortonian – early Messinian Kuzgun Formation, which unconformably lies above the deep marine sediments of the Guvenç Formation. In turn, the strata of the Kuzgun Formation transition upward into a cyclical succession of anhydrites and black shales, recording a younger regressive phase resulting in the main evaporative event (Primary Lower Gypsum) of the MSC (Cosentino et al. 2010a and b)

Recently Cosentino et al. (2010a and b), Cipollari et al (2013a) and Faranda et al. (2013) used new biostratigraphic data and lithostratigraphic correlations to revise the Messinian stratigraphy of the Adana Basin (Fig. 2A). They recognized two new unconformities in the basin that can be ascribed to two different stages of the MSC (CIESM 2008): (1) the base of the Resedimented Lower Gypsum (Gökkuyu Gypsum member) corresponds to the MES, which is constrained between 5.56 ± 0.005 Ma and 5.532± 0.0046 Ma (Cosentino et al. 2013) and cuts down to either the Primary Lower Gypsum or the pre-evaporitic Tortonian-early Messinian deposits of the Kuzgun Formation (Cosentino et al. 2010a; Cipollari et al. 2013 a; Faranda et al. 2013); and (2) the base of the fluvial conglomerates and marls of the Handere Formation, which corresponds to a second erosional surface (MES2; ~5.45 Ma; Cosentino et al. 2010b; 2013) and cuts down-section to either the Primary Lower Gypsum, the Resedimented Lower Gypsum, or even the pre-evaporitic Tortonian-early Messinian deposits of the Kuzgun Formation (Cosentino et al. 2010b; Cipollari et al. 2013a; Faranda et al. 2013). Both the Resedimented Lower Gypsum (p-ev1) and the continental sediments of the Handere Formation (p-ev2) contain ostracods with Paratethyan affinities pertaining to the late Messinian *Lago-Mare* biofacies (Grossi et al. 2008; 2011). The Resedimented Lower Gypsum in the Adana Basin has been constrained by Cipollari et al. (2013a) and Faranda et al. (2013) to the *Loxoconcha mülleri* Zone (Gliozzi et al. 2010; Grossi et al. 2011), whereas the fluvial conglomerates and marls of the Handere Formation are part of the *Loxocorniculina djafarovi* Zone (Cosentino et al. 2010b; Gliozzi et al. 2010; Grossi et al. 2011; Cipollari et al. 2013a; Faranda et al. 2013). At the top of the Messinian stratigraphic succession, above a Zanclean regional flooding surface (5.33 Ma), lie the lowermost Zanclean deep-marine gray clays of the Avadan Formation (Cipollari et al. 2013a). In the S-SE part of the Adana Basin, Quaternary alluvial sediments deposited by the Seyhan and Tarsus rivers cover the older units of the Adana Basin stratigraphic succession.

We studied the sedimentary record of the Adana Basin in the light of the recently revised stratigraphy with the main purpose of: (i) finding evidence for uplift of the SE margin of the CAP, and (ii) defining the tectonic context of this depocentral area.

1.5. Methodology

1.5.1. Seismic Interpretation

Based on the integration of the classic stratigraphy proposed for the Adana Basin (Schmidt 1961; Görür 1979; Yetiş 1988; Ünlügenç et al. 1991; 1993; Gürbüz and Kelling 1993; Yetiş et al. 1995; Gürbüz 1999; Gürbüz, and Ünlügenç 2001; Nazik 2004) with the stratigraphy recently proposed by Cosentino et al. (2010a and b), Cipollari et al. (2013a), and Faranda et al. (2013) for the Messinian deposits of the Adana Basin, we outline a new depositional history derived from seismic stratigraphy (Fig. 2B). We used more than 600 km of onshore seismic reflection profiles, recording up to 7s two-way travel time (TWT), acquired and processed between 1970 and 1988 by the Turkish Petroleum Corporation (TPAO; Fig. 2B). To validate our interpretations, we correlated the different units imaged in seismic reflection profiles with surface exposures in the vicinity of the seismic lines, mainly along the uplifted margins of the Adana Basin. In addition, to check the stratigraphy imaged from the seismic profiles, we used the lithologic descriptions of a few well logs made available to us by TPAO (Adana 1; Akyar 1; Çakit 1; Dumandere 1; Yenice 1; Yenice 2).

1.5.2. Volume Calculation

To produce an isopach map of the sesimic facies corresponding to the late *Lago-Mare* facies of the Handere Formation (Fig. 3), we interpolated regions between our interpreted seismic lines using the 3D software program Petrel, which allowed us to reconstruct the top and bottom surfaces of the seismic unit. We used the surfaces as boundaries to calculate the unit volume using the software MATLAB.

1.5.3. Provenance Analysis

To understand the source areas of clasts within the conglomerates of the Handere Formation, we determined the lithologies, their percentages, and their paleocurrent directions. With the aim of identifying potential changes in the catchment areas from late Messinian to today, we compared the percentages of lithologies found in the Messinian samples with the values obtained from i) clast counting of two recent alluvial deposits and ii) exposed lithologies in the present-day catchments located on the SE margin of the CAP.

For the clast counts we sampled eight sites; six sites were sampled within the conglomerates of the Handere Formation (TOP 0, KAR 0, MEN 0, ECE 0, CER 0, IMAM 0; Fig. 4), and two sites were sampled from conglomerates of two recent river terraces located on the NW margin of the Adana Basin (GOR 0, ALA 1; Fig. 4). All pebbles contained within a $1m^2$ square were counted, amounting to a total of ~300 to 500 clasts per site (Fig. 5). Almost all pebbles were well preserved. A minor percentage presented a partly weathered surface, although this characteristic was not related to a particular lithology. However, gabbro pebbles were generally weathered (Fig. 5B), and easily disintegrated upon a hammer stroke; because these clasts are more likely to have been damaged during transport, this lithology, which we associate with an ophiolitic succession ("ophiolites" in Table 1), has probably been slightly underestimated in our analysis.

We assigned every pebble to a lithologic class after observing it with a 10x lens and recording its reaction to hydrochloric acid. In few cases, thin sections were needed to better define the lithology. These classes were further differentiated (Table 1) to compare them with the 1:500,000 "Adana" geological map (Fig. 6; MTA: AA.VV. 2002; Bilgiç and AA.VV 2002; Ulu and AA.VV 2002a and b). The lithological map of the Turkish Geological Survey (MTA) was also consulted to define the eight main lithological categories that we identified in our analysis (Table 1).

We took a total of 230 paleocurrent measurements from the conglomerates of the Handere Formation based on the imbrications of prolate clasts at 17 different sites (Fig. 7). The analysis of the paleocurrent measurements coupled with the clast counting provided rigorous constraints on the contributing areas that led to the deposition of the Handere Formation upper sub-unit.

1.5.4. Evolution of the drainage system

To link our clast counting analysis to source areas and to identify potential changes in the drainage areas that occurred between late Messinian and today, we calculated the percentages of lithologies currently outcropping in the catchments drained by streams flowing into the Adana Basin (Figs. 8 and 9). We extracted the outcropping areas of each lithology in the present drainage basins after integrating a 1:500,000-scale digital geologic map of Turkey (AA.VV. 2002; Bilgiç and AA.VV 2002; Ulu and AA.VV 2002a and b) into a Geographic Information System (ArcMap 9.3).

We also investigated how drainage systems may have evolved over time considering the uplift rates reported in Schildgen et al. (2012b) and Cipollari et al. (2013a), which we used to reconstruct the paleo-topography of the southern Central Anatolian Plateau margin and the Adana Basin at ~5.45 Ma (Fig. 10). To make this reconstruction, we separated the digital elevation model of the area in three tectonic domains: the internal portion of the plateau, the margin of the plateau, and the Adana Basin. For each tectonic domain, we derived a different equation obtained using the uplift or subsidence rate. For areas in which topography grew, we applied an exponential decrease to the modern elevations, assuming that the highest peaks today have been uplifted more than the areas of lower elevation. We applied the equations to an Advanced Spaceborn Thermal Emission and Reflection Radiometer digital elevation model (DEM) that we re-sampled to 90-m resolution using the Spatial Analyst function in ESRI's ArcMap 9.3. After topography restoration at ~5.45 Ma, we re-assembled the different tectonic domains and then extracted the river network from the new DEM. We made no attempt to restore the river offset caused by motion along the Kozan and Ecemiş faults.

1.6. Results

Our results integrate seismic stratigraphy, 3D reconstructions of the unit surfaces from the seismic lines, volume calculation of the late *Lago-Mare* sub-unit of the Handere Formation, and provenance analysis. Below, each of these aspects will be addressed separately.

1.6.1. Seismic stratigraphy

From the 34 seismic profiles that we interpreted, we distinguish five different seismic units (MS2, MS3, MS4a, MS4b, and MS5), and identify four regional erosional surfaces (U1, U2, MES1, and MES2). Next, we describe how we correlate these units and the identified erosional surfaces with what has been recently reported for the Adana Basin (Fig. 2 A and B; Williams et al. 1995; Cosentino et al. 2010b; Cipollari et al. 2013a; Faranda et al. 2013).

In all of the interpreted seismic profiles, the oldest erosional surface (U1) separates the Central Tauride basement rocks from the first seismic unit (MS2), comprising the Oligocene – Serravallian portion of the Adana Basin fill (Schmidt 1961; Gürbüz and Ünlügenç 2001; Nazik 2004). A younger erosional

surface (U2) separates MS2 and MS3. The latter is a seismic unit corresponding to Tortonian-lower Messinian deposits of the Kuzgun Formation, including the Messinian Lower Evaporites at the top. At the NW margin of the basin, Cosentino et al. (2010a,b) reported the top of MS3 to be characterized by a few, equally-spaced and high-amplitude reflectors corresponding to the Primary Lower Gypsum of the MSC (LE in Fig. 2B). Where the high-amplitude reflectors corresponding to the Primary Lower Gypsum are missing, an erosional surface cuts down to MS3. We interpret this erosional surface to be the Messinian Erosional Surface (MES). Above the MES, a peculiar seismic facies characterized by high-amplitude and discontinuous reflectors (MS4a) is tentatively correlated with the Resedimented Lower Gypsum of the MSC (CIESM 2008), which, according to Cipollari et al. (2013a) and Faranda et al. (2013), is widely exposed along the uplifted NW margin of the Adana Basin.

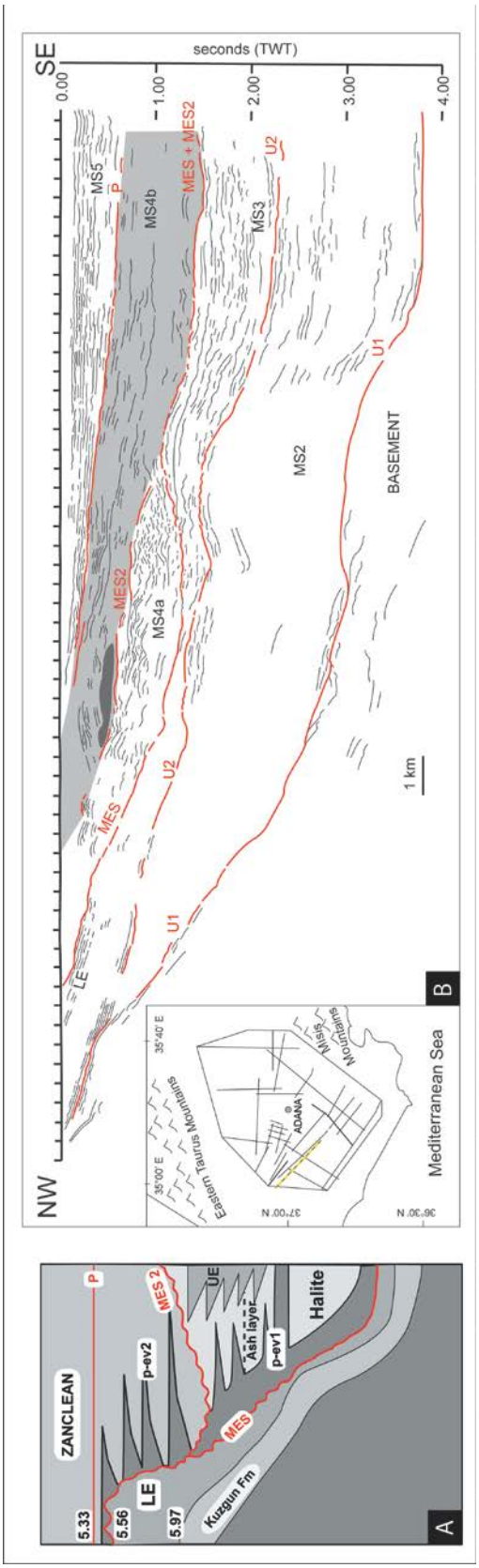

Figure 2. [A] The Messinian Salinity Crisis in the Adana Basin. 5.33: Zanclean flooding event; ca. 5.45 – 5.33: upper Lago-Mare sediments deposited; 5.56: End of 17th cycle of Lower Evaporites; subsequent sea-level drawdown, erosion of Lower Evaporites to form Messinian Erosional Surface (MES), and deposition of Resedimented Lower Evaporites (RLE). 5.97: Start of Messinian Salinity Crisis and onset of deposition of Lower Evaporites (LE). [B] Location map of the interpreted seismic profiles and line-drawing of the seismic profile highlighted in the map showing the new seismostratigraphy proposed for the Adana Basin. Separated by traces of unconformities and trangressive surfaces (in red) are the main seismostratigraphic units, including MS2: Oligo – Serravallian sequence; MS3: Tortonian Kuzgun Formation; LE: Lower Evaporites; MS4a: Resedimented Lower Gypsum; MS4b: upper Messinian Lago-Mare unit, consisting of an alternation of conglomerates and marls bearing a brackish-water fauna; MS5: Pliocene unit. Surfaces include P: base Zanclean flooding surface (5.33 Ma); MES 2: late Messinian Erosional Surface (5.45 Ma); MES: early Messinian Erosional Surface (5.60 Ma); U2: late Serravallian – early Tortonian Erosional Surface; U1: late Oligocene – early Aquitanian Erosional Surface. Lines in the map correspond to the traces of the seismic profiles used for the reconstruction of the MS4b isopach map and volume calculation. Isopach map and volume calculation have been performed for the area corresponding to the polygon in the map.

Table 1. List of the principal lithologic groups used for provenance analysis. [1]

Lithologic group	Principal lithologies from Clast Counting	Principal lithologies from MTA map
Carbonates	Microcrystalline, micritic and marly limestones; microbrecciated and fossiliferous limestones.	"Carbonate rocks", "Limestone", "Neritic limestone", "Pelagic Limestone", "Lacustrine limestone, marl, shale, etc", "Clastic and Carbonate rocks", "Carbonate rocks and Clastic rocks in place",
Other sedimentary	Sandstones, calcarenites, conglomerates, chert	"Continental clastic rocks", "Clastic rocks", "Clastic rocks, (with blocks)", "Undifferentiated continental clastic rocks", "Undifferentiated clastic rocks", "Continental rocks (marine inplaces)", "Travertine"
Volcanic	Red, green or dark grandmass with different percentages of phenocrysts; vesicular and vitreous rocks.	"Basalt", "Pyroclastic rocks", "Andesite", "Undifferentiated volcanic rocks"
Metamorphic	Schistosic rocks, marbles and quartzites.	"Marble", "Marble, schist in place", "Marble, recrystallized limestone", "Schists (Lower Triassic in place)", "Metaclastic and metacarbonate rocks", "Schists", "Schists, quartzite, marble etc.", "Gneiss, schist, amphibolites, marbles, etc.", "Schist, phyllite, etc.", "Schists (quartzite, metasiltsone, metasandstone)"
Ophiolites	Mainly gabbros, with crystals of different dimensions.	"Gabbro", "Ophiolitic rocks: peridotite", "Ophiolitic mélange", "Ophiolitic rocks: undifferentiated serpentinite, dunite, harzbugite, etc.", "Undifferentiated Harzbugite, Dunite, Serpentinite, etc.", "Serpentinites", "Ophiolitic rocks: dunite"
Intrusive	Phaneritic rocks, mainly granites.	"Granite, granodiorites"
Volcanic and sedimentary		"Volcanic and sedimentary rocks"
NC	Not Classified rocks	
Undifferentiated Quaternary		"Undifferentiated Quaternary", "Alluvium fan, slope debris, cone of dejection etc."

[1] In the first column the selected lithologic groups are listed; in the second column, all the lithologies found in analyzing the samples for clast counting are related to their pertaining group. In the third column the formations reported in the Turkish General Directorate of Mineral Research and Exploration (MTA) map are grouped in order to be comparable with the clast counting analysis.

A second intra-Messinian unconformity (MES2) cuts down to either the high-amplitude/discontinuous reflectors of the Resedimented Lower Gypsum (unit MS4a), the high-amplitude/continuous reflectors of the Primary Lower Gypsum, or the pre-evaporitic Tortonian-early Messinian deposits of the Kuzgun Formation (MS3). The seismic facies overlying the MES2 (unit MS4b) is characterized by more continuous reflectors, which should correspond to the upper sub-unit of Messinian Handere Formation (Cosentino et al. 2010b; Cipollari et al. 2013a), with its channelized coarse-grained fluvial deposits and interbedded marls. If this interpretation is correct, the MS4b seismic facies was associated with a very high sedimentation rate, because it shows a significant thickness (up to 1.4 s TWT) deposited in 120 kyr, from about 5.45 to 5.33 Ma (Cosentino et al. 2010b, 2013) (Fig. 2). At the top of MS4b, the seismic reflection lines clearly show a conformable surface (P), corresponding to the Messinian/Zanclean transition. This surface represents the early Pliocene flooding event, which happened at 5.33 Ma throughout the Mediterranean Basin (Iaccarino et al. 1999a and b; Iaccarino and Bossio 1999; Orszag-Sperber et al. 2006 and references therein; Pierre et al. 2006; Gennari et al. 2008; Cipollari et al. 2013a). That flooding surface is overlain by a seismic facies with continuous, high-frequency reflectors, corresponding to the Pliocene-lower Pleistocene marine clays of the Avadan Formation (Cipollari et al. 2013a).

1.6.2. Volume Calculation of the late *Lago-Mare* facies (Handere Formation)

We use the results of the seismic profile interpretation to identify the seismic facies MS4b, which should correspond to the coarse-grained fluvial deposits and marls of the Handere Formation based on field evidence. To estimate the volume of this thick late *Lago-Mare* sedimentary body within the Handere Formation, we first extrapolated a TWT isopach map of the corresponding seismic facies (MS4b). Because the available seismic profiles cover only a limited area of the Adana Basin, the calculated volume is a minimum value. We extrapolated an isopach map for an area of ~3500 km^2; however, within the region covered by seismic lines, the Lago-Mare deposits are present only in the SW portion of the area (Fig. 3). The time-depth conversion was done using the Vp interval velocities applied for seismic processing integrated on the interval of interest; the resulting Vp value of the MS4b seismic facies is 2700 m/s. Using this velocity, together with 3D upper and lower surfaces constructed in Petrel with the seismic lines, we calculated a

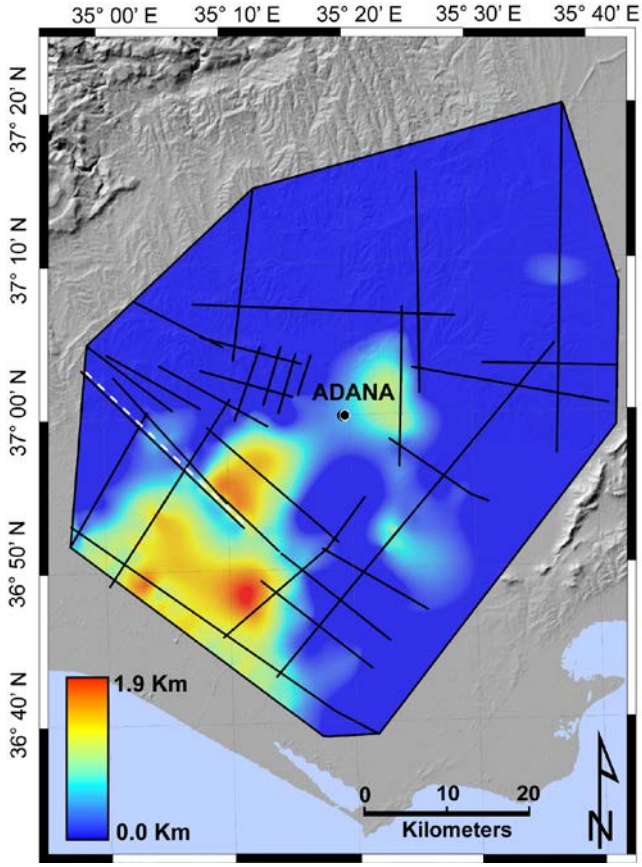

Figure 3. Isopach map of the Lago-Mare conglomerates and marls pertaining to the Handere Formation. Black lines are the trace of the available seismic profile; the dashed white line is the trace of the seismic profile in Fig. 2. Due to the poor data coverage in the areas of higher thickness, we estimate an error of ~20% on maximum thickness of 1.9 km, and ~1500 km^3 as the total volume of deposited sediments during a time span of approximately 120 kyr. Due to the relative scarcity of seismic coverage in the depocentral area of the basin and the possible error associated with the automatic surface reconstruction performed by the software, we estimate the error in the calculations to be ~20% for the thickness and 25% for the volume; therefore we calculated a corrected minimum thickness of ~1.5 km and a corrected minimum volume of ~1100 km^3. Where the sediment thickness is greatest, the local minimum sedimentation rate is therefore ~12.5 mm/yr.

1.6.3. Provenance analysis

1.6.3.1. The Handere Formation sampling sites

We sampled six sites for clast counting in the late *Lago-Mare* sub-unit of the Handere Formation (Fig. 4 and 6). All of the sampling sites show a predominant S, SE or SW paleocurrent direction, and pebbles are polymict. Sampling site MEN 0 is characterized by several channel-fill, matrix-supported conglomerates, with lenticular shapes, variable thicknesses, and erosive bases carved into grayish-brownish pelites. The setting suggests that deposition occurred in braided-river channels. The matrix consists of non-cemented sand and clay, and the degree of lithification is low. Pebbles are of different dimensions, from several millimeters to tens of centimeters, all well rounded, often imbricated, and crudely graded. The outcrops at sample locations KAR 0 and TOP 0 are very similar, characterized by braided channels with predominantly clast-supported conglomerates, with a yellowish/reddish sandy matrix, well cemented by calcite at the KAR

0 sampling site. Yellowish banks of sandstone are present. Pebbles are dimensionally slightly more homogeneous, ranging from a few millimeters up to 20 cm, rounded to well rounded, with roundness clearly depending on lithology. Samples ECE 0 and CER 0 were collected from outcrops characterized by channel-fill, non-cemented conglomerates, with a major fraction of yellowish sandstone. Pebbles are well-rounded, with grain sizes ranging from a few millimeters to 15-20 cm. CER 0 includes slightly polished *Ostrea* shells as clasts (Fig. 5D), indicating a very short transport distance from the source area. IMAM 0 is the easternmost sampling site, which is quite different from the others. The outcrop consists of ~ 30 m of conglomerates, micro-conglomerates, coarse sandstones, calcarenites, carbonate levels, sands, and a thick layer of clay affected by pedogenesis. Conglomerates are predominant; they are organized in braided channels, with a yellowish/reddish matrix. Pebbles are dimensionally more homogeneous than in the other sampling sites, with 75% of them between 2 to 3 and 15 cm in diameter. They are either cemented or not, clast- or matrix-supported. The clay horizons are non-fossiliferous on hand lens inspection.

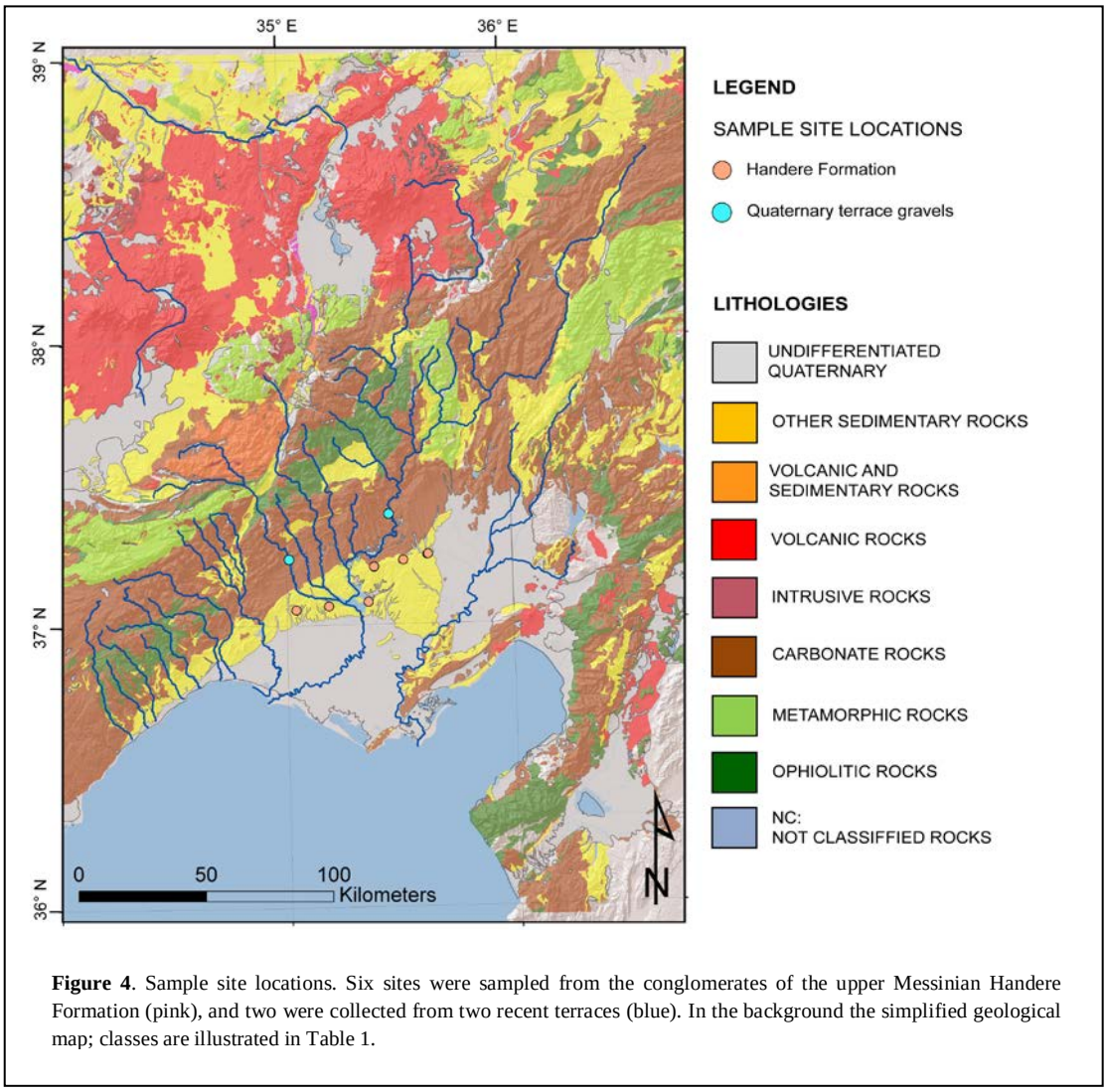

Figure 4. Sample site locations. Six sites were sampled from the conglomerates of the upper Messinian Handere Formation (pink), and two were collected from two recent terraces (blue). In the background the simplified geological map; classes are illustrated in Table 1.

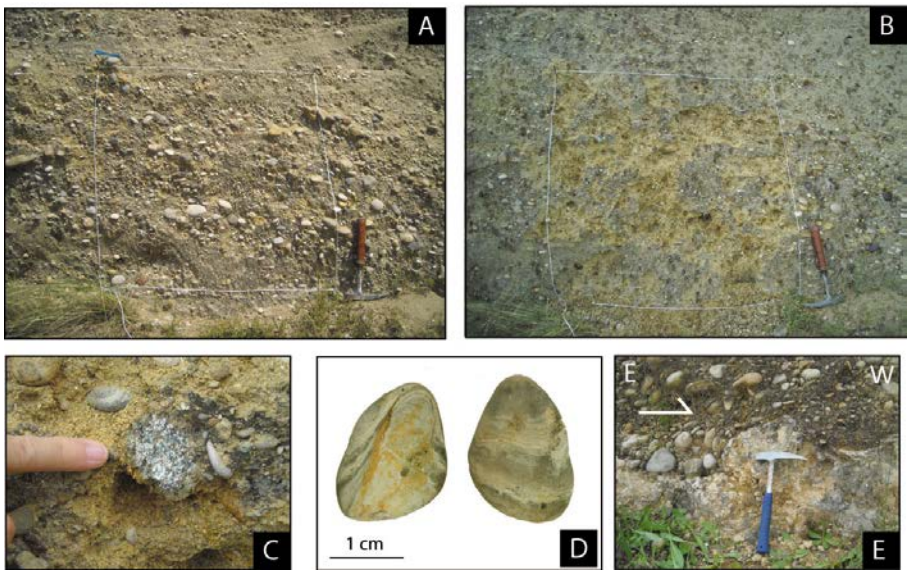

Figure 5. Field pictures. Sample site CER 0 [A] before and [B] after the sampling. The squares are 1 x 1 m wide. [C] Detailed view of CER 0 sample site. Weathering of a gabbroid pebble and [D] clast constituted by a slightly polished ostrea shell, indicating a relatively short transport from the source area. [E] IMAM 0 sample site, where paleocurrent can be inferred from the pebbles' arrangement. Large-size pebbles are all located on the left of the picture, upstream in comparison with a riverbed obstacle. In the shadow zone, downstream of the riverbed obstacole, only finer grained pebbles were deposited because of the flow pressure drop.

1.6.3.2. Provenance analysis of the clasts in the late Lago-Mare conglomerates of the Handere Formation

The percentages of the lithologies constituting the conglomerates of the Handere Formation (Table 2; Fig. 6) are quite similar, generally with a predominance of carbonates and other sedimentary rocks, including sandstones, calcarenites, conglomerate clasts, chert, volcanic rocks, and minor amounts of ophiolitic and metamorphic rocks. Qualitatively, this composition points to the SE portion of the CAP as a source area. The northeastern-most sample, IMAM 0, differs from the others. It is predominantly comprised of carbonates and other sedimentary rocks, and shows a very small percentage of volcanic rocks, with neither ophiolitic nor metamorphic rocks. Most of the paleocurrent directions record flow toward the S, SE, or SW (Fig. 7), in agreement with the provenance data. Thus, the clasts must have come into the Adana Basin from the SE margin of the CAP (Fig. 6). However, paleocurrents from IMAM 0 show flow toward the NW or W (Figs. 5E and 7), potentially indicating a source in the Misis Mountains at the present-day SE margin of the basin. Lithologically, the Misis Mountains consist predominantly of carbonates, with minor amounts of clastic and volcanic rocks. The similarity between the clast compostion of the upper Messinian conglomerates at IMAM 0 (Fig. 6) and the lithologic composition of the Misis Mountains suggests the existence of a fluvial system sourced from the Misis Mountains during the deposition of IMAM 0. This fluvial connection no longer exists today, corroborating the notion that the drainage system in this area of the Adana Basin must have changed between the late Messinian and today.

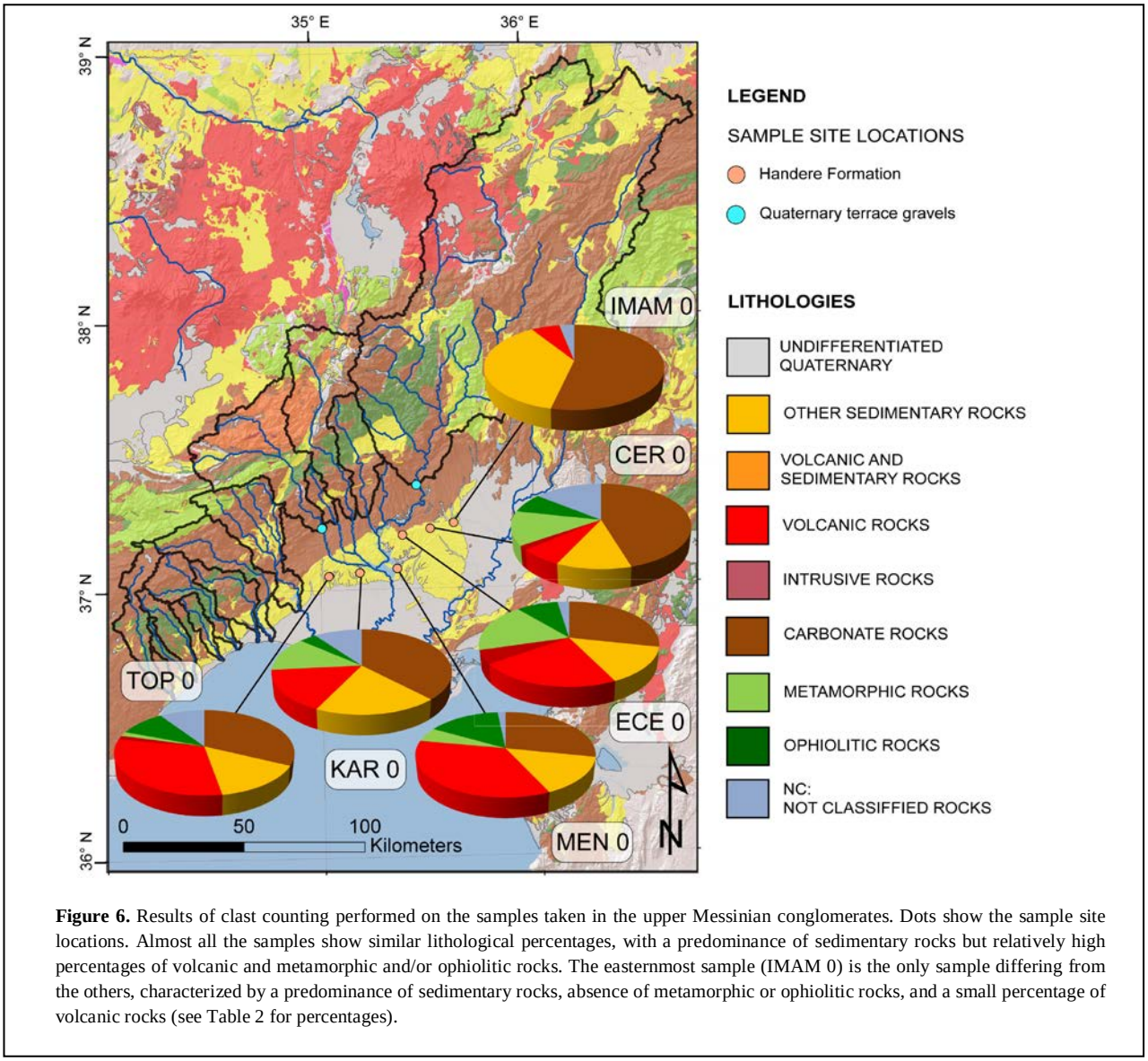

Figure 6. Results of clast counting performed on the samples taken in the upper Messinian conglomerates. Dots show the sample site locations. Almost all the samples show similar lithological percentages, with a predominance of sedimentary rocks but relatively high percentages of volcanic and metamorphic and/or ophiolitic rocks. The easternmost sample (IMAM 0) is the only sample differing from the others, characterized by a predominance of sedimentary rocks, absence of metamorphic or ophiolitic rocks, and a small percentage of volcanic rocks (see Table 2 for percentages).

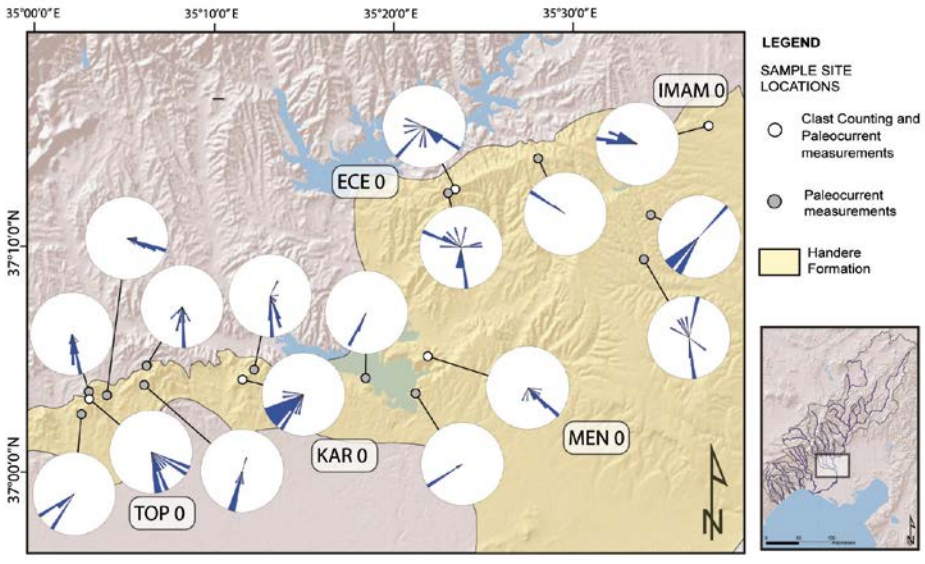

Figure 7. Paleocurrent directions measured in the Handere Formation conglomerates. White dots show the location of the measurement sites, grey dots show the location where both paleocurrent directions measurements and samples for clast counting were taken. Almost all the samples show a flow direction toward the SE/SW. The northeastern-most sector, however, shows a clear countertrend, with material being transported from SE to NW. This variation is in good agreement with the results from clast counting, showing similar lithologic percentages with the exception of the northeastern-most sample (IMAM 0).

1.6.4. Evolution of the drainage system

1.6.4.1. Present-day catchments versus present-day provenance

Before comparing the composition obtained from the provenance study in the upper Messinian conglomerates of the Handere Formation with exposed lithologies in the present-day drainage basins, we tested if the two datasets are likely to be comparable. To do this, we compared the lithologic percentages obtained from the samples taken from two recent river terraces with the composition of outcropping lithologies in the corresponding present-day drainage basins (Fig. 8). Our aim was to validate the methodology and to quantify the role of differential erosion for different lithologies.

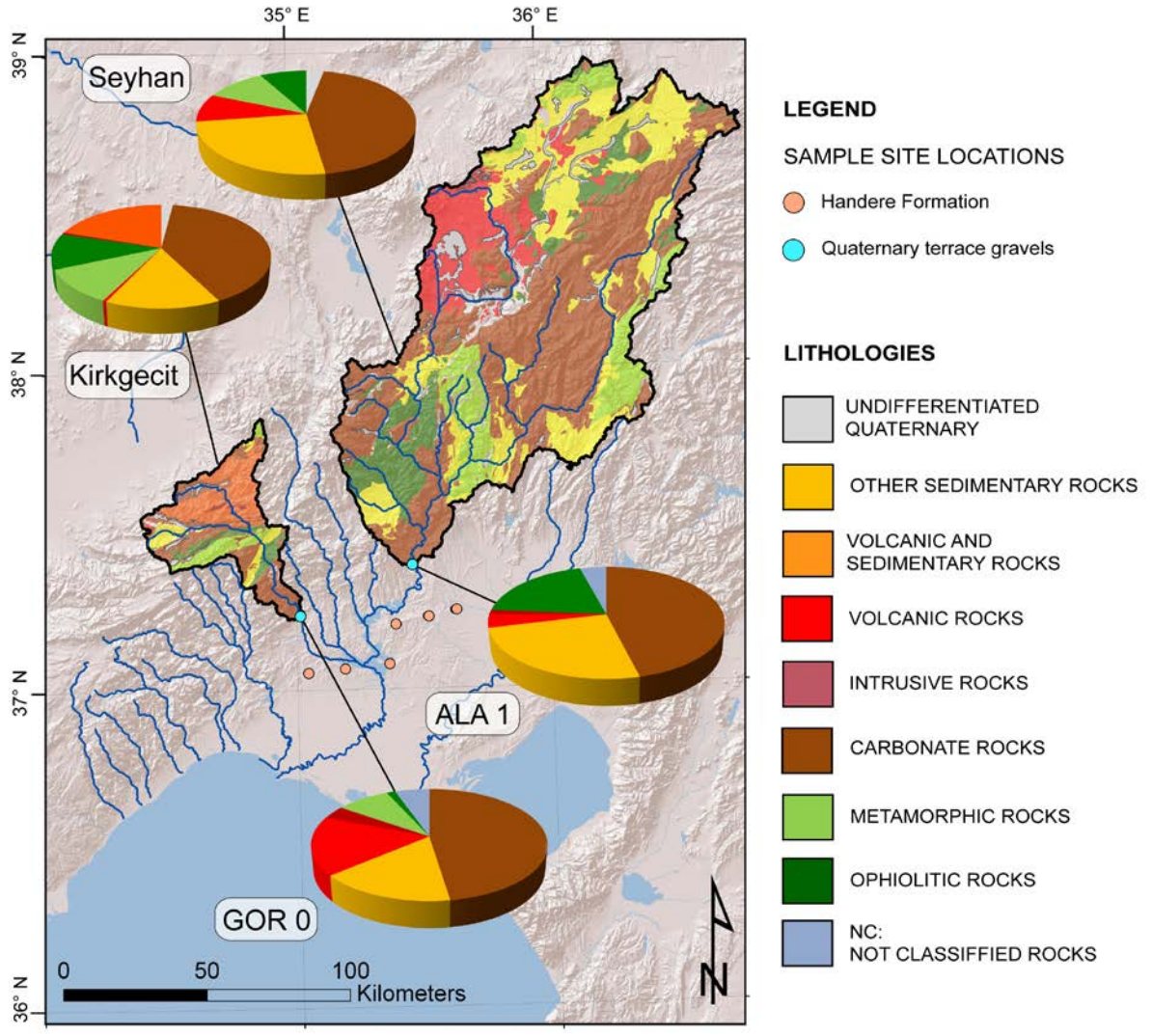

Figure 8. Lithologic percentages of present drainages versus recent fluvial terraces. Dots show the location of the sample sites. The percentages derived from clast counting performed on the conglomerates of two recent terraces (ALA1 and GOR 0) are similar to those calculated for the correspondent present drainage basins – those of the Seyhan and Kirkgecit rivers, indicating good agreement of the percentages calculated with the two different methodologies. Geological map modified from MTA "ADANA" 1:500,000-scale map.

The clast composition at both terrace-sampling sites is strongly correlated with the outcropping lithologies in the corresponding drainage basins, with a predominance of carbonates and other sedimentary rocks, and smaller percentages for the remainder (Fig. 8). The contribution of volcanic rocks is also comparable between terraces and the modern drainage basins. However, differences emerge when considering the percentages of ophiolitic and metamorphic rocks; ophiolitic rocks outcropping in the Seyhan catchment basin are 12% less than the corresponding material found at terrace site ALA 1, which contained no metamorphic clasts. The Kirkgecit catchment shows a difference in percentages of ~2% (for metamorphic rocks) and ~10% (for ophiolitic rocks) with respect to the corresponding GOR 0 terrace (Fig. 8). Nevertheless, percentages are broadly similar if the metamorphic and ophiolitic rocks are summed. Overall, the sediments in the modern river channels and the Quaternary terraces qualitatively and quantitatively correspond to the exposed lithologies in the catchment, suggesting that the role of differential erosion in affecting the composition of the sampled conglomerates is negligible.

Table 2. Percentages of the selected lithologic groups in the samples taken for clast counting.

	TOP 0	**KAR 0**	**MEN 0**	**ECE 0**	**CER 0**	**IMAM 0**	**GOR 0**	**ALA 1**[2]
Limestone	33.23	39.38	28.38	27.97	46.99	54.32	48.86	47.00
Other sedimentary	15.52	20.17	14.87	14.01	12.14	37.90	16.68	25.63
Volcanic	31.41	16.88	35.05	22.17	7.02	5.98	17.58	3.95
Igneous	1.58	0.00	0.00	5.14	1.67	0.00	3.84	1.28
Metamorphic	1.70	13.48	5.32	18.16	13.47	0.12	8.77	0.00
Ophiolites	10.10	3.78	15.19	8.58	7.68	0.00	1.41	19.86
NC	6.45	6.30	1.19	3.96	11.02	1.68	2.86	2.27
TOT	**100**	**100**	**100**	**100**	**100**	**100**	**100**	**100**

1.6.4.2. Present-day catchments versus Handere Formation clasts provenance

We calculated the percentages of exposed lithologies for all the catchments presently draining into the Adana Basin, including the Kirkgecit, Seyhan, Üçüge, Gorgun, and Eğlence rivers (Fig. 9). The exposed

[2] MEN 0, TOP 0, KAR 0, ECE 0, CER 0 and IMAM 0 were collected from the conglomerates of the Handere Formation; GOR 0 and ALA 1 were collected from two different recent terraces.

lithologies are mainly carbonates, with a smaller component of ophiolites, sandstones, conglomerates and chert. Exposures of volcanic rocks do not occur in all of the basins. Overall, carbonates, sandstones, conglomerates, and chert dominate. The present-day catchments show different percentages of the exposed lithologies when compared with the clasts of the Handere Formation upper sub-unit; the percentage of volcanic material changes the most, showing a clear reduction from the relatively large fraction represented in the upper Messinian conglomerates (~10-35%) compared with the volcanic material outcropping in the present catchments (~0-10%). This reduction of clasts of volcanic origin is offset by a major coeval increase in the proportion of carbonate rocks (from ~30-55% to ~40-75%).

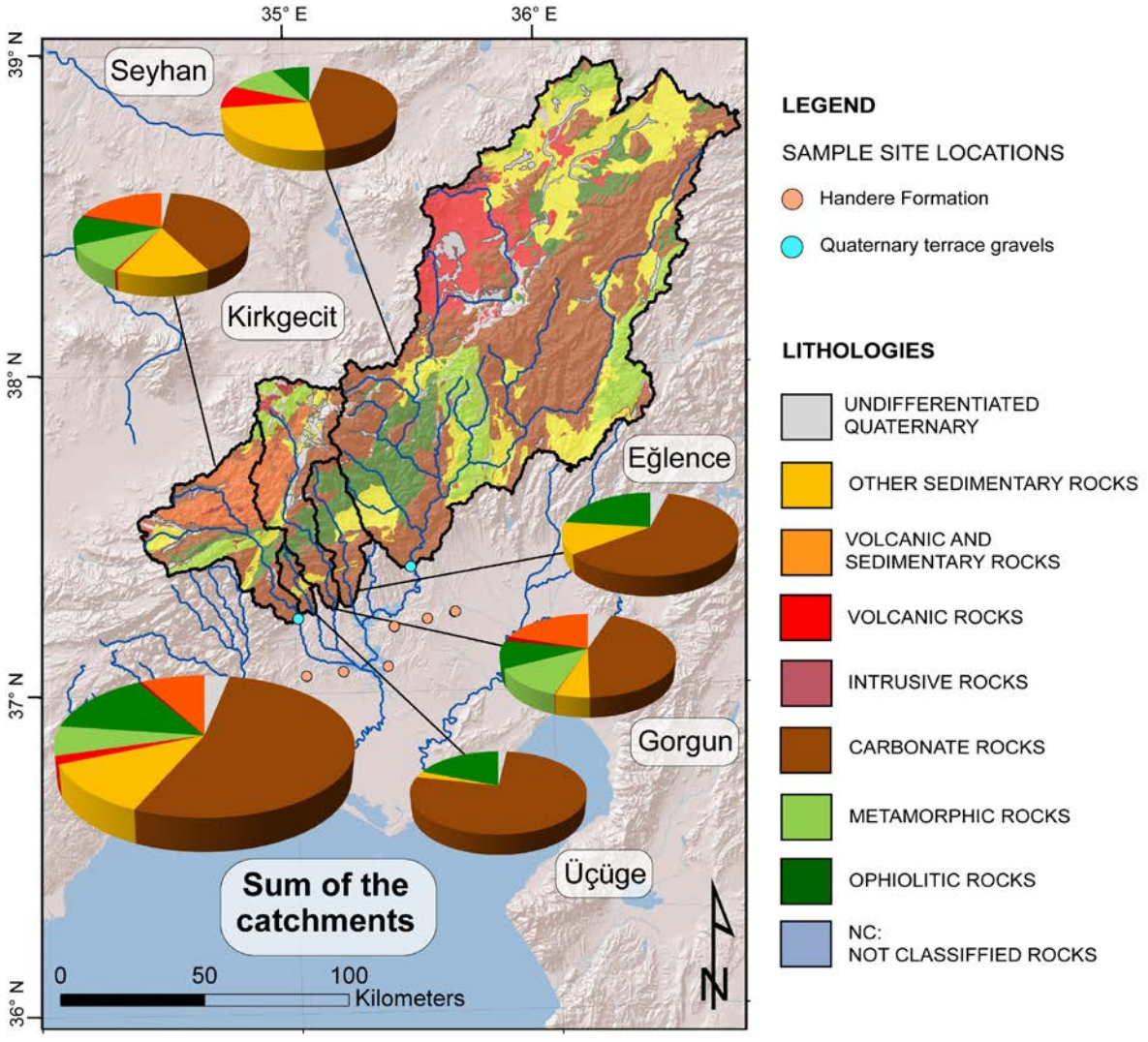

Figure 9. Lithologic percentages of the present drainage basins. A significant variation in lithologic percentages is evident when comparing this figure with Fig. 6, showing the results of clast counting performed on the upper Messinian conglomerates of the Handere Formation; the percentage of volcanic material decreases dramatically from the late Messinian to Present.

1.7. Discussion

Due to the limited transport distance of coarse sedimentary material (Kodama 1994; Ferguson et al. 1996; Wandres et al. 2004; Boggs 2009), conglomerate provenance analysis is often used to constrain the uplift and erosional exhumation history of the source area (Zapata et al. 2010). The refined Messinian stratigraphy of the Adana Basin (e.g. Cosentino et al. 2010b; Cipollari et al. 2013a; Faranda et al. 2013) provided us with the unique opportunity to recognize and stratigraphically constrain seismic facies MS4b, which can be correlated with the *Lago-Mare* facies of the Messinian Handere Formation. This seismic facies shows a two-way travel time of up to 1.4 s, corresponding to a succession of fluvial deposits up to 1.5-km thick and a local sedimentation rate of at least 12.5 mm/yr. Our volume calculation results in a minimum of 1100 km^3 deposited in ~120 kyr, over a region of ~3000 km^2.

This significant sedimentary influx into the Adana Basin approximately between 5.45 and 5.33 Ma could be explained as a consequence of (i) increased runoff/erosion as a result of enhanced precipitation during the Lago-Mare stage of the MSC; (ii) a major tectonic event inducing uplift in the surrounding areas; or (iii) a combination of both processes. To try to distinguish among these possibilities, we compared thicknesses and inferred sedimentation rates of the sediment deposited during the *Lago-Mare* stage of the MSC in the Adana Basin with coeval units deposited in different parts of the Mediterranean realm. When present, *Lago-Mare* deposits in the Eastern Mediterranean are characterized by different lithofacies. These include marlstones with interbedded turbiditic sandstones and siltstones as reported at DSDP 376, north of the Florence Rise (Hsü et al. 1978); alternations of silty clay, silt, and sand at ODP 160 – Site 968, south of Cyprus (Emeis et al. 1996); fluvial conglomerates, sandstones, and marls in Israel (Druckman et al. 1995); carbonates and conglomerates interbedded with paleosoils observed in the Pissouri Basin, southern Cyprus (Rouchy et al. 2001); dark marl deposits containing abundant carbonate gravels, caliche-like concretions and intercalations of conglomerates observed in the Polemi Basin, southern Cyprus (Rouchy et al. 2001), and, finally, clays, sandstones, and fluvial conglomerates in the upper Messinian *Lago-Mare* deposits recently found in the Messarà Plain of Crete, (Cosentino et al. 2007). Thicknesses span from ~25 m in the Pissouri and Polemi basins (Orszag-Sperber et al. 2000; Rouchy et al. 2001) to several tens of meters, as observed in the Messarà Plain (Cosentino et al. 2007), north of the Florence Rise (Hsü et al. 1978), on the Cyprus lower

slope (Emeis et al. 1996; Blanc-Valleron et al. 1998), and onshore Israel (Druckman et al. 1995). Sedimentation rates calculated for these deposits span from 0.2 mm/yr in the Pissouri and Polemi basins (calculated from Orszag-Sperberg et al. 2000, and Rouchy 2001) to 0.43 mm/yr for the Messarà Plain (Crete; calculated from Cosentino et al. 2007), and up to 0.6 mm/yr for the northern flank of the Florence rise (calculated from Hsü et al. 1978). Variability in thickness and inferred sedimentation rates increase when dealing with the Mediterranean as a whole, with more than 250 m of upper Messinian *Lago-Mare* deposits on the eastern margin of the northern Tyrrhenian Basin (Cipollari et al. 1999) and maximum thicknesses reaching up to several hundreds of meters (> 938 m) as in the case of the Mondragone 1 well, drilled onshore of the Garigliano coastal plain (eastern margin of the central Tyrrhenian Sea), in a basin controlled by active tectonics (Cosentino et al. 2006). These observations from other areas highlight the anomalous thickness of the Adana Basin *Lago-Mare* sequence, which is up to two orders of magnitude greater than the coeval Eastern Mediterranean sediments. Given that the climatic shift must have impacted the whole region, the elevated thickness should be explained with some other process that, coupled with the enhanced runoff, caused the high sediment production. At the very least, topography must have existed along the northwestern border of the Adana Basin (the CAP southern margin) at the time of deposition of the Handere Formation upper sub-unit, which places the first minimum age constraint on the onset of uplift along the southern margin of the CAP. This result is in good agreement with the maximum age for the start of plateau uplift in central Anatolia proposed by Cosentino et al. (2012) and Schildgen et al. (2012b), who dated the youngest shallow marine sediments outcropping on the top of the southern margin of the plateau to be ~ 8 and 6.7 Ma, respectively. Considering the unusually great thicknesses of the *Lago Mare* deposits in the Adana Basin, it is also likely that tectonics were active at the time of deposition.

Based on our provenance analysis, the lithologic composition of the present-day basins (Fig. 9) appears to be different from the clast composition of the upper Messinian conglomerates (Fig. 6), especially with respect to the reduced volcanic component in the present-day basins. An extensive area in the NW sector of the geologic map covering the plateau realm (Fig. 3) is mainly characterized by volcanic rocks. However, this region is disconnected from the present-day drainage system due to the high SE margin of the CAP, which defines the Mediterranean/Black Sea drainage divide. The higher percentage of volcanic material in the upper Messinian conglomerates of the Handere Formation thus suggests that during its

deposition, rivers must have drained from the internal part of the CAP to the Adana Basin. It follows that the SE margin of the plateau cannot have been a significant topographic barrier during the Messinian compared to today. This result also corroborates our hypothesis of a major change in the drainage patterns that was postulated as a result of one of the Handere Formation samples (IMAM 0) having an apparent provenance from the Misis Mountains. A reconstruction of the palaeo-topography at ~5.45 Ma corroborates this hypothesis (Fig. 10); the late Messinian drainage system relative to the restored topography shows major differences from the present drainage system, with palaeo-rivers draining the volcanic-rich areas behind the plateau margin.

Based on both our calculated sedimentation rates and provenance analysis of the clasts of the *Lago-Mare* conglomerates of the Handere Formation, we suggest that the uplift of the CAP must have started shortly before 5.45 Ma and helped to produce the voluminous upper Messinian *Lago-Mare* conglomerates and marls in the Adana Basin. Because the upper Miocene marine sediments along the axis of the southern margin of the CAP are now at more than 2 km elevation, our new results imply a maximum long-term average uplift rate of 0.37 mm/yr since 5.45 Ma at the NW margin of the Adana Basin. Considering the 8-my-old marine carbonates at 2 km elevation (Cosentino et al., 2012), the combined minimum and maximum age constraints confine the long-term average surface uplift rate to be between 0.20 and 0.37 mm/yr along the axis of the CAP southern margin.

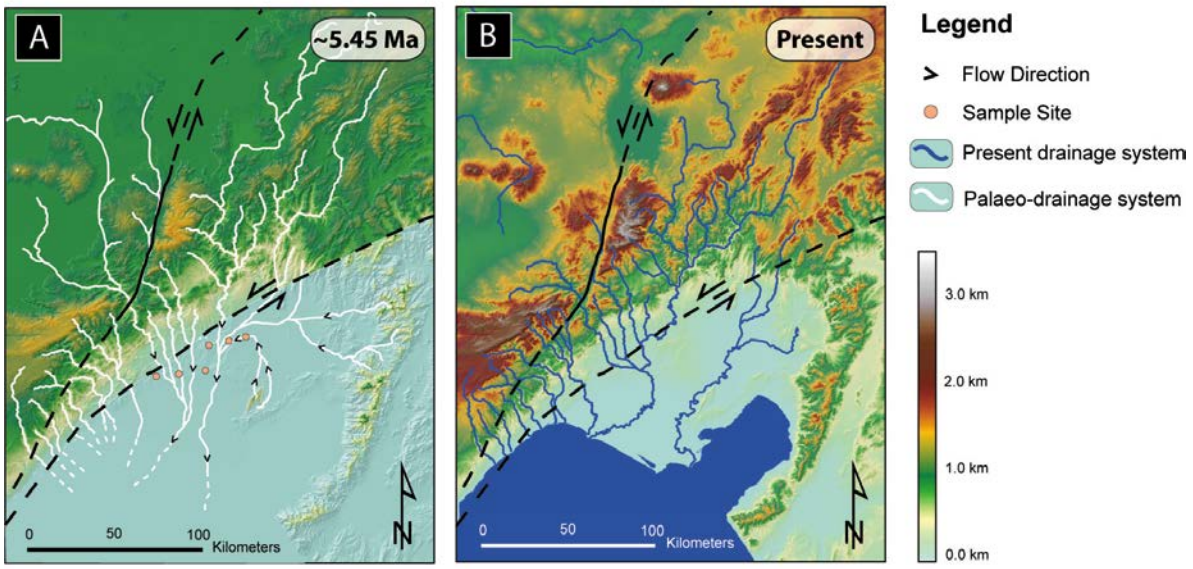

Figure 10. Palaeo (A) versus present (B) drainage systems. The traces of the Ecemiş and Kozan faults are shown in black. The sample site locations for the conglomerates of the Handere Formation are shown in (A) for reference. The palaeo-drainage system has not been restored for the possible offset related to movements on the faults.

The large sediment volumes and a rapid increase in sedimentation rate in the Adana Basin support earlier suggestions that uplift along the southern margin of the CAP largely resulted from a deep-rooted mechanism (e.g. Cosentino et al. 2012; Schildgen et al. 2012a and b). Importantly, our combined observations from the Adana Basin are consistent with analog (Bajolet et al. 2012) and numerical (Gögüş and Pysklywec 2008) models of the surface response to deep-seated processes involving lithospheric slab delamination and break-off. If we relate the geometry of these models to the tectonic setting of the Adana Basin, it would be expected that the region south of the delamination and break-off experiences rapid subsidence, while the area above the delamination and break-off is uplifted. The subsided area itself is later partially uplifted as the region reaches isostatic equilibrium. Considering the rapid sedimentation rate derived for the Adana Basin starting at 5.45 Ma, together with results demonstrating that the basin was uplifted 350 to 650 m since 5.2 or 5.3 Ma (Cipollari et al. 2013a), our new results offer corroborating evidence for the delamination/break-off hypothesis.

1.8. Conclusions

In the Adana Basin, at the southern flank of the Central Anatolia Plateau, we recognize for the first time a thick seismic facies associated with the second post-evaporitic stage of the Mediterranean MSC (p-ev2; CIESM 2008 and references therein). This facies consists of at least 1100 m^3 of conglomerates and marls deposited in a time span of ~120 kyr, between around 5.45 and 5.33 Ma (Cosentino et al. 2013), corresponding to the late *Lago-Mare* stage of the MSC (Gliozzi et al. 2010; Grossi et al. 2011). Based on the recently revised onshore stratigraphy of the Adana Basin, this unit can be correlated with the fluvial conglomerates and marls of the Handere Formation (Cipollari et al. 2013a; Faranda et al. 2013).

The provenance of the Handere Formation conglomerates documents that the majority of the clasts is sourced from the Eastern Taurus Mountains. Compared with the clast composition of Quaternary terraces and with lithologies outcropping in the present-day catchments, we infer a major change in the drainage system to have occurred between 5.45 Ma and the Quaternary. This change is corroborated by two independent lines of evidence: i) a change in paleocurrent directions, and ii) a reduction of areas overlain by

volcanic rocks that drain towards the Adana Basin. Together, these observations indicate disconnection of drainage systems sourced in both the Misis Mountains and the internal portion of the CAP since the deposition of the *Lago-Mare* conglomerates of the Handere Formation. All these observations support the hypothesis that the CAP southern margin was uplifted during the deposition of the *Lago-Mare* conglomerates, providing the large amount of material coevally deposited in the Adana Basin and creating a barrier that disconnected the internal portion of the CAP from the present drainage system.

Even if an inferred regional-scale climatic shift from dry to wetter conditions during the time of the deposition of the *Lago Mare* sediments of the MSC contributed to increased erosion and sediment supply to the Adana Basin, climate change as a sole reason for the anomalously high sedimentation rates is unlikely, since similarly large increases in sedimentation rates are not observed throughout the eastern Mediterranean. In addition, the NW margin of the Adana Basin (the SE margin of the CAP), which we demonstrate was the source area for most of the Handere Formation conglomerates, was still below sea level until at least 8 Ma (Cosentino et al. 2012). For these reasons, we interpret the high sedimentation rate in the Adana Basin to be predominantly tectonically controlled, and tightly linked to uplift of the SE margin of the CAP, which had started by ~5.45 Ma. Our results therefore provide for the first time a minimum age constraint for the timing of this important phase of topographic development along the southern plateau margin of Central Anatolia. Because slab delamination and break-off models (e.g. Gögüş and Pysklywec 2008; Bajolet et al. 2012) illustrate uplift and subsidence in regions that are equivalent to the tectonic setting of the southern CAP margin and the neighboring Adana Basin, our results corroborate earlier suggestions that these deep lithospheric processes provide a viable uplift mechanism for the southern margin of the CAP.

2.

DIFFERENCES AND SIMILARITIES IN THE LATE MIOCENE SUBSIDENCE HISTORIES OF THE MUT AND ADANA BASINS (SOUTHERN TURKEY): A RECORD OF SURFACE UPLIFT OF THE SE MARGIN OF THE CENTRAL ANATOLIAN PLATEAU

2.1. Introduction

The complex interactions between plate boundaries, deep-rooted processes, and surface morphology is an outstanding topic for the understanding of the relations intervening between geodynamic and landscape evolution through time (e.g. Scheidegger and Ai 1986; Wells et al. 1988; Daradich et al. 2003; Cloething et al. 2005; Faccenna et al. 2011). The link is particularly evident in those areas where these interactions have led to the development of major topographic features, such as the Ethiopian, the Altiplano-Puna, or Tibetan plateaus. Even though plateaus are not necessarily associated with plate margins, the occurrence of many of these remarkable landscape elements in the vicinity of different types of plate boundaries points to a variety of mechanisms that may govern the growth of these features (e.g. Allmendinger et al. 1997; Giese et al. 1999; Clark and Royden 2000; Yuan et al. 2000: Tapponier et al. 2001; Yang and Liu 2002; Goudie 2005; Schurr et al. 2006; Schildgen et al. 2007, 2009; Hoke and Garzione 2008; Yuan et al. 2013).

The convergence zone of the African and Arabian plates with Eurasia is marked by a wide zone of high-topography, expressed from east to west by the Tibetan, the Iranian, and Anatolian plateaus. Anatolia is a wide region located within the Alpine-Himalayan collision zone, resulting from the convergence and collisional processes that involved the African-Arabian and Eurasian plates during Cretaceous to Eocene times (Şengör and Yılmaz 1981; Şengör et al. 1983, 1984; Görür et al. 1984; Robertson and Dixon 1984; Robertson and Woodcock 1986; Robertson 2000; Clark and Robertson 2002; Aksu et al. 2005a; Kelling et al. 2005). Anatolia appears to be part of a lithospheric plate moving westward with respect to the adjacent Eurasian, African and Arabian plates (i.e. Reilinger et al. 1997, 2006; McClusky et al. 2000), with movement accommodated by two major intacontinental transform faults, the North Anatolian Fault (NAF) and the East Anatolian Fault (EAF; Ketin 1948; McKenzie 1978; Şengör 1979; Dewey and Şengör 1979; Şengör 1979; Şengör et al. 1985). It is characterized by a complex tectonic setting (Fig. 1): Western Anatolia is governed

by the slab pull of the Hellenic Trench and associated extension, whereas Eastern Anatolia is mainly characterized by shortening related to the continental collision of the Arabian and Eurasian plates (e.g. Şengor 1985; Biryol et al. 2011); in the middle, Central Anatolia act as a "transition zone" mainly characterized by the presence of a major topographic feature, the Central Anatolian Plateau (CAP).

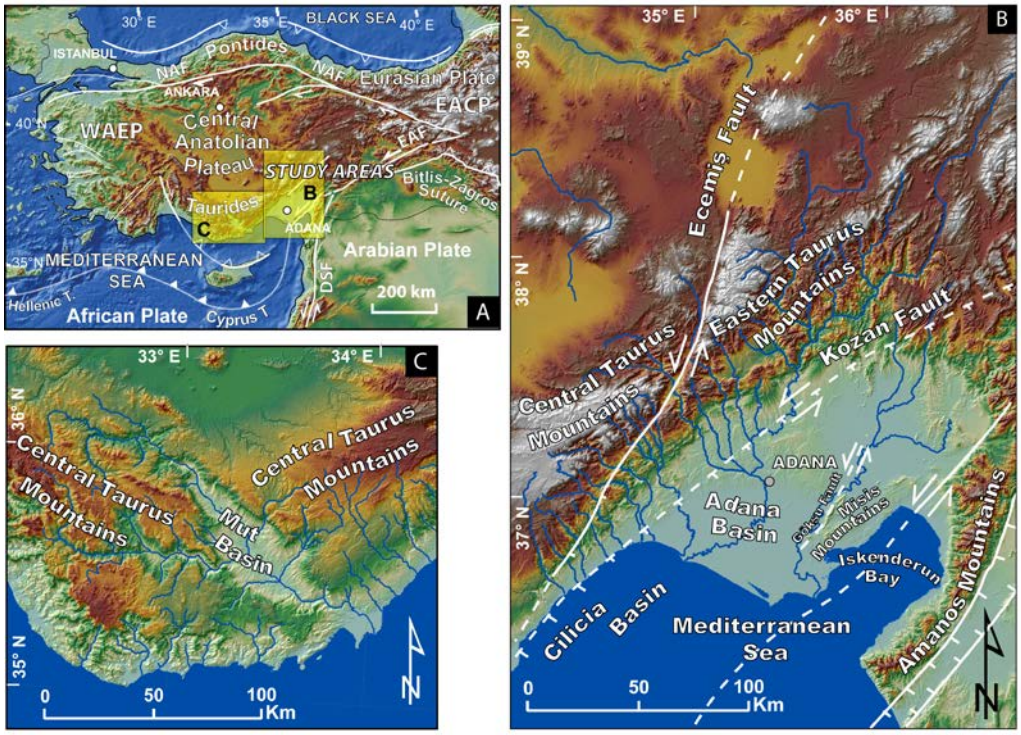

Figure 1. Location map of the study areas and tectonic setting. [A] Regional setting: the study areas are located in the central Anatolian province, between the western Anatolian extensional province (WAEP) and the eastern Anatolian compressional province (EACP). The Adana Basin is located beside the SE flank of the Central Anatolian Plateau, close to the Arabian – Eurasian collision zone. Westward extrusion of the Aegean-Anatolian microplate is accommodated along the North Anatolian Fault (NAF) and the East Anatolian Fault (EAF); DSF: Dead Sea Fault; Hellenic T.: Hellenic Trench; Cyprus T.: Cyprus Trench. [B] Close up of the Adana Basin study area. The Central and Eastern Taurus Mountains correspond to the SE margin of the Central Anatolian Plateau, constituting the NW margin of the Adana Basin. Misis Mountains border the SE flank of the basin, separating the Adana Basin from the Iskenderun Basin. [C] Close up of the Mut Basin study area. The basin is nestled on top of the Central Anatolian Plateau southern margin.

The southern boundary of the Central Anatolian Plateau CAP is defined by the Tauride fold-and-thrust belt, created by the progressive accretion of several continental fragments during the Alpine orogeny (e.g. Şengör and Yılmaz 1981; Şengör et al. 1984; Robertson and Dixon 1984; Robertson et al. 1996; Yılmaz et al. 1998; Görür et al. 1984, 1998; Gökten and Floyd 1987; Gökten 1993; Kelling et al. 2005). The Taurides are externally bordered by a deep depocenter, the Adana-Cilicia Basin, a wide E-W elongated forearc basin (i.e. Jackson and McKenzie 1984; Aksu et al. 2005b); on top of the southern Taurides lies the Mut Basin.

Depocenters located in the vicinity of plate boundaries or major topographic features are key locations to study the evolution of the surrounding regions through time, as their sedimentary infilling potentially records the main tectonic and climatic events that occurred since the start of deposition. Moreover, because basins evolve independently in different geodynamic contexts (e.g. Bally et al. 1982), their sedimentary records could help to define the tectonic setting of the region in which they developed.

Whereas it is generally accepted that the Mut Basin evolved as a supra-sutural basin on the already accreted Taurides nappes (Kelling 2000; Eriş et al. 2005; Şafak et al. 2005), different models have been proposed for the Adana Basin, which is located southeast of the Tauride range, where it is likely affected by both the Bitlis-Zagros collision zone and the strike-slip kinematics of the East Anatolian Fault Zone. The development of the Adana Basin has been suggested to relate to: (1) transcurrent kinematics in the Africa-Eurasia-Arabia triple junction region (Şengor et al. 1985; Dewey et al. 1986; Karig and Kozlu 1990; Chorowicz et al. 1994; Kempler and Garfunkel 1994); (2) flexure induced by renewed thrusting in the Taurides (Williams et al. 1995); (3) intracontinental sagging (Kelling et al. 1987); (4) forearc extension and subduction roll-back (Robertson 2004); and (5) the evolving Tauride fold–thrust belt, whereby the Adana Basin represented first the foredeep and then, after the advancing of the thrust front, a piggy back basin (Aksu et al. 2005b; Burton-Ferguson et al. 2005).

Deposition in the Mut Basin started in the early Oligocene (Tanar and Gökçen 1990; Şafak et al. 2005) and extends through the late Tortonian (Cosentino et al. 2012), while in the Adana Basin, deposition ranges from the late Oligocene (Schmidt 1961; Görür 1979; Yetiş 1988; Ünlügenç et al. 1991; Ünlügenç 1993; Gürbüz and Kelling 1991; 1993; Yetiş et al. 1995; Gürbüz and Ünlügenç 2001) to the lower Pleistocene (Cipollari et al. 2013a). The current location of the depocenters, situated on either side of the Tauride suture zone, coupled with the timing of sedimentation, point to a genesis at least partly related to the convergence and collision of the African and Eurasian plates. The similar geodynamic context of the Mut and Adana basins, together with their partially contemporaneous sedimentation, allows for a comparison between the tectono-sedimentary evolution in each region. Specifically, the basins may each contain a record of continental collision between the Arabian and Eurasian plates, the onset of the East Anatolian Fault, and the uplift of the southeastern margin of the Central Anatolian Plateau.

To help constrain the timing of these important tectonic events, and to better assess the geodynamic context of the Adana Basin, we study and compare the Neogene evolutions of the Mut and Adana basin. To this end, we present new data on the stratigraphy and subsidence history of the Mut Basin. We also apply stratigraphy, seismic stratigraphy, 3D-surface restoration, isopach map reconstruction, and volume calculation to describe the evolution of the Adana Basin and its subsidence history. We then compare results for the two areas to better constrain the tectonic evolution of the area and to unravel the uplift mechanisms of the southeastern margin of the Central Anatolian Plateau.

2.2. Tectonic setting of the Mut and Adana basins

Starting of convergence between the African and Arabian plates led to the closure of the Paleotethys and part of the Neotethys along a collision zone complicated by the presence of several microplates located between the two major margins (e.g. Şengör and Yılmaz 1981; Robertson and Dixon 1984; Aksu et al. 2005a; Kelling et al. 2005; Robertson and Mountrakis 2006). The Pontides and Taurides orogenic belts therefore accreted as a consequence of collision and generated two arc-shaped weak zones. Deformation along the Taurides fold-and-thrust belt show a sud-vergent trend, accompanied by an analogous progressive rejuvenation of collision-related basins. (Clark and Robertson 2005).

The onset of collision in the Bitlis and Zagros, resulting from the continental collision of the Arabian and Eurasian plates, is still debated (Faccenna et al. 2013; McQuarrie and van Hinsbergen 2013) but most authors report an age between Oligocene and lower Miocene (i.e. Pearce et al. 1990; Jolivet and Faccenna 2000; Agard et al. 2005, 2011; Okay et al. 2010; Ballato et al. 2011;). By middle Miocene time, convergence accommodated by subduction no longer occurred in the Bitlis region (Şengör et al. 2003; Keskin 2003). By ~11 Ma, the gateway between the Mediterranean and the Indian Ocean no longer existed (Hüsing et al. 2009).

Continental collision between the Arabian and Eurasian plates along the Bitlis-Zagros suture zone led to a rearrangement of the region, probably causing slab delamination and/or break-off, (Gans et al. 2009; Biryol et al. 2011; Cosentino et al. 2012; Schildgen et al. 2012; in press), and an acceleration of slab retreat along the Hellenic Trench (e.g. Faccenna et al. 2006; Schildgen et al. in press). These events may in turn

have helped to generate the North and East Anatolian faults (e.g Ketin 1948; McKenzie 1978; Şengör 1979; Dewey and Şengör 1979; Şengör et al. 1985), which bring together two arc-shaped deformation zones that help accommodate the convergence of the Eurasian and African plates and the stress caused by the pull of the Hellenic Trench (e.g. Barka 1992; 2000; Zattin et al. 2005; Okay et al. 2008).

The Mut and Adana basins are located, respectively, within and adjacent to the central Taurus fold-and-thrust belt (Fig. 1). Orogenic extension giving rise to supra-sutural sedimentary basins started throughout the Taurides during the late Eocene–early Miocene (Akay and Uysal 1988; Aksu et al. 1992; Görür 1992; Williams and Unlugenç 1992; Robertson and Grasso 1995). The sedimentary record of the Mut and Adana basins overlie the older basement units of the fold-and-thrust belt with an angular unconformity. Both basins have been filled mainly during Neogene times.

The Oligocene – Middle Miocene infilling of the Mut Basin is tilted and faulted due to continued extension, but is sub-horizontal in its middle to late Miocene portion (Cosentino et al. 2012). Deformation that followed the middle Miocene was, therefore, almost purely vertical.

The Adana Basin lies between the Eastern Taurus Mountains and the East Anatolian Fault (Fig. 1); it is bounded to the northwest by the transtensional Kozan Fault (i.e. Aksu et al. 2005b; Burton-Ferguson et al. 2005) and to the southeast by the Misis Mountains. The Oligocene – Serravallian infilling of the Adana Basin is tilted toward SE and faulted along the margin with the Misis Mountains. Stratigraphic and seismostratigraphic evidence relates the deformation of the Oligocene-Serravallian deposits to the growth of the Misis Mountains, which occurred between late Serravallian and Messinian times (Mulder et al. 1975; Kelling et al. 1987; Gökçen et al. 1988; Aksu et al. 2005b; Burton-Ferguson et al. 2005; Hall et al. 2005). Younger deposits in the Adana Basin are gently tilted towards the S-SE (Yalcın and Görür 1984). Seismicity of the area suggests that the SE margin of the Adana Basin is still tectonically active and characterized by transtensional kinematics (Harvard CMT Catalogue; Dziewonski et al. 1981; Ergin et al. 2004; Over et al. 2004; Ekström et al. 2012).

2.3. Stratigraphy

2.3.1. Surface stratigraphy for the Adana Basin

The Oligocene fluvial and lacustrine sediments of the Karsanti Formation pertaining to the Karsanti intramontane Basin mark the onset of the sedimentary deposition in the Adana Basin (Schmidt 1961; Gürbüz and Kelling 1993; Yetiş et al. 1995; Williams et al. 1995; Gürbüz and Ünlügenç 2001). Within the confines of the modern Adana Basin, the first deposits of the basin Neogene succession (Fig. 2a) are the Oligocene-lower Miocene fluvial red beds of the Gildirli Formation (Schmidt 1961; Görür 1979; Yetiş 1988; Ünlügenç et al. 1991; 1993; Gürbüz and Kelling 1991; 1993; Yetiş et al. 1995; Gürbüz, andÜnlügenç 2001), followed by and laterally interfingering with the shallow marine fossiliferous sandstone, siltstone, marls, and sandy limestone of the Aquitanian-Burdigalian Kaplankaya Formation (Yetiş et al. 1995; Nazik 2004). The coarse marine sediments of the Kaplankaya Formation laterally pass into the Burdigalian – Langhian, reefal Karaisali Formation (Görür 1979; Nazik 2004) and the lower portion of the Çingoz Formation (Schmidt 1961), which represents a Burdigalian – early Serravallian turbidite fan system (Görür 1979; Yetiş and Demirkol 1986; Yetiş 1988; Gürbüz and Kelling 1993; Williams et al. 1995; Yetiş et al. 1995: Gürbüz 1999). The Cingoz Formation is deposited along the NW margin of the Adana Basin and interfingers with the lower portion of the Serravallian Guvenç Formation, which consists of deep marine clays passing upward to sandy, shallow marine deposits (Ünlügenç et al. 1991; Nazik and Gürbüz 1992; Gürbüz and Kelling 1993; Yetiş et al. 1995). The maximum thicknesses reported in literature for this Oligocene-Serravallian sequence (Table 1), ranges from 2.9 km (Yalçın and Görür 1984, and references therein) to 4.6 km (Schmidt 1961).

At late Serravallian - early Tortonian time (Yetiş 1988; Ünlügenç 1993; Yetiş et al. 1995) the first regressive event within the Adana Basin stratigraphy is recorded. Namely, the continental and shallow marine deposits of the Tortonian – early Messinian Kuzgun Formation, with their maximum thickness of ~ 1000 m (Schmidt 1961; Table 1), unconformably lie above the deep marine sediments of the Guvenç Formation, which passes conformably upward to a cyclical succession of anhydrites and black shales recording the main evaporative event (Primary Lower Evaporites) of the Mediterranean Messinian Salinity Crisis (MSC; CIESM 2008; Cosentino et al. 2010 b). Where present, Primary Lower Evaporites are cut by a first intra-Messinian unconformity, followed by the deposition of the Resedimented Lower Evaporites (Gökkuyu Gypsum member). This unconformity corresponds to the Messinian Erosional Surface (5.56 ±

0.005 Ma – 5.532± 0.0046 Ma; Cosentino et al. 2013), which cuts down to either the Primary Lower Evaporites or the pre-evaporitic Tortonian-early Messinian deposits of the Kuzgun Formation (Cosentino et al. 2010a). A second intra-Messinian unconformity has been recognized at the base of the fluvial conglomerates and marls of the Handere Formation (MES2; ~5.45 Ma; Cosentino et al. 2010b, 2013), which cuts down to either the Primary Lower Evaporites, the Resedimented Lower Primary Lower Evaporites, or the pre-evaporitic Tortonian-early Messinian deposits of the Kuzgun Formation (Cosentino et al. 2010b; Cipollari et al. 2013a; Faranda et al. 2013). Both the Resedimented Lower Evaporites (p-ev1) and the continental sediments of the Handere Formation (p-ev2 pp) contain ostracods with Paratethyan affinities pertaining to the late Messinian Lago-Mare biofacies. The Resedimented Lower Evaporites in the Adana Basin has been attributed by Cipollari et al. (2013a) and Faranda et al. (2013) to the *Loxoconcha mülleri* Zone (Gliozzi et al. 2010; Grossi et al. 2011), whereas the fluvial conglomerates and marls of the Handere Formation pertain to the *Loxocorniculina djafarovi* Zone (Cosentino et al. 2010b; Gliozzi et al. 2010; Grossi et al. 2011; Cipollari et al. 2013a; Faranda et al. 2013). The total thicknesses of the gypsum levels (combining the Primary and Resedimented Lower Evaporites) is between 100 and 900 m (Yalçın and Görür 1984). Above a Zanclean regional flooding surface (5.33 Ma), lie the epibathyal to outer circalittoral marine gray clays of the Avadan Formation which was referred to the lowermost Zanclean, followed by littoral marine lower Pleistocene sediments (Cipollari et al. 2013a). The last stratigraphic discontinuity observed in the basin is middle Pleistocene in age, and is followed by the continental deposition of sediments transported by the Seyhan and Tarsus rivers started at upper Pleistocene (Cipollari et al. 2013a).

2.3.2. Surface stratigraphy for the Mut Basin

The Neogene deposits of the Mut Basin (Fig. 2b) start with an Oligocene-lower Miocene continental succession resting unconformably on a highly deformed substratum pertaining to tectonic units of the central Taurides (i.e. Ophiolite nappe, Bozkir unit, Bolkar unit, Hadim nappe, and Geyikdağı unit; Akay and Uysal, 1988). This continental succession records the presence of an elevated land area at the southern margin of the Anatolian block as a consequence of the last phases of the Tauride orogeny and the tectonism that affected the Central Taurides during the late Oligocene-early Miocene (Monod 1977; Özgül 1976; Poisson 1977; Woodcock and Robertson 1982; Robertson and Woodcock 1986).

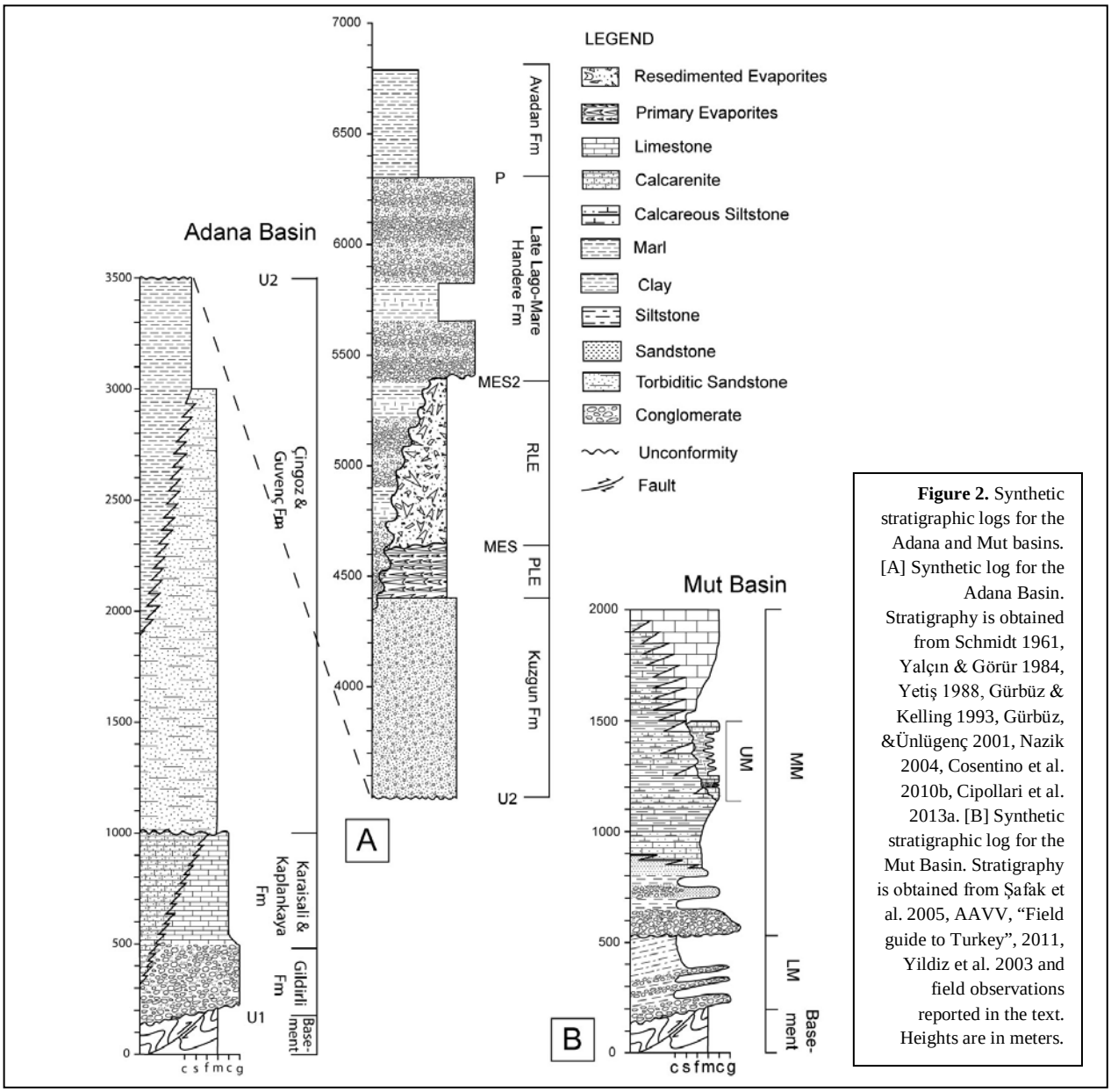

Figure 2. Synthetic stratigraphic logs for the Adana and Mut basins. [A] Synthetic log for the Adana Basin. Stratigraphy is obtained from Schmidt 1961, Yalçın & Görür 1984, Yetiş 1988, Gürbüz & Kelling 1993, Gürbüz, &Ünlügenç 2001, Nazik 2004, Cosentino et al. 2010b, Cipollari et al. 2013a. [B] Synthetic stratigraphic log for the Mut Basin. Stratigraphy is obtained from Şafak et al. 2005, AAVV, "Field guide to Turkey", 2011, Yildiz et al. 2003 and field observations reported in the text. Heights are in meters.

Safak et al. (2005) identified two megasequences within the Oligocene-late Miocene sedimentary infill of the Mut Basin. The lower megasequence (Oligocene-early Miocene p.p.) consists mainly of continental deposits, which were grouped into the Yenimahalle and Fakirca formations. The upper megasequence (early Miocene p.p.-late Miocene) is mainly characterized by marine sediments (Köselerli and Mut formations), conformably resting on continental and lagoonal deposits of the Derinçay Formation.

Field work carried out recently in the Mut Basin allowed us to distinguish a younger megasequence in the sedimentary succession of the Mut area. In some places south of the town of Mut, an erosional truncation surface cuts the gently tilted middle and upper Miocene marine deposits. On top of this younger erosional truncation surface, which in places reaches nearly to the base of the modern valley, shallow- to

deeper-water marine deposits define the third and uppermost megasequence in the Mut sedimentary succession. The deposits pertaining to this megasequence partially correspond to the Plio-Pleistocene sections described in Yildiz et al. (2003).

For this reason, in this paper we distinguish the sedimentary infill of the Mut Basin in three megasequences: (1) lower megasequence (early Oligocene-early Miocene p.p.; Rupelian-late Aquitanian); (2) middle megasequence (early Miocene p.p.-late Miocene p.p.; late Burdigalian-late Tortonian); and (3) upper megasequence (early Pliocene-early Pleistocene; late Zanclean-Calabrian).

2.3.2.1. Lower megasequence (early Oligocene-early Miocene p.p.; Rupelian-late Aquitanian)

This megasequence was separated into the Yenimahalle and Fakirca formations (Tanar and Gökçen 1990; Şafak et al. 2005). The Yenimahalle Formation is the oldest continental unit infilling the Tertiary Mut Basin. The base of the formation consists mainly of coarse-grained sediments, with clasts coming from the Meso-Cenozoic sedimentary cover of the Tauride units. Şafak et al. (2005) interpreted deposition of the lower Yenimahalle sediments in a relatively deep, partly anoxic, lacustrine setting characterized by frequent grain flows coming from the prograding fan deltas on the northern margin of the lake. Shallower lake conditions led the sedimentation of the upper Yenimahalle Formation, as testified by the occurrence of lake margin facies and storm deposits (Şafak et al. 2005). Although Eocene faunal elements are abundant in the coarse-grained deposits of the formation, leading Gedik et al. (1979) to assign it an Eocene age, the occurrence in the fine-grained intercalations of younger endemic ostracod fauna allowed Tanar (1989) and Tanar and Gökçen (1990) to consider the Yenimahalle Formation to be early to middle Oligocene in age.

The fine-grained sediments of the Fakirca Formation (mainly marls and siltstone) yielded mainly lacustrine ostracod assemblages, which Tanar (1989) and Tanar and Gökçen (1990) correlated to late Oligocene-early Miocene ostracod biozones. According to Tanar (1989), the ostracod assemblages found in the uppermost part of the Fakirca Formation (Aquitanian), together with some benthic and planktic foraminifera, indicate lagoon to littoral marine settings, which indicate a late Aquitanian transgressive event in the Mut Basin.

The lower megasequence was affected mainly by transtensional tectonics and was gently folded before the deposition of the Derinçay Formation. The erosional truncation surface separating the lower and

middle megasequences (Fakirca/Derinçay transition) was interpreted as a major sequence boundary within the Neogene deposits of the Mut Basin (Eriş et al. 2005), with abrupt change in facies from lake-lagoonal (Fakirca Formation) to fluvial deposits (Derinçay Formation).

The total thickness of the lower megasequence in the Mut area was estimated to be 350 m by Şafak et al. (2005), whereas Tanar and Gökçen (1990) suggested 180 m for Yenimahalle and Fakirca formations.

2.3.2.2. Middle megasequence (early Miocene p.p.-late Miocene p.p.; late Burdigalian-late Tortonian)

The middle megasequence of the Mut Basin (early Miocene p.p.-late Miocene) lies unconformably over the Fakirca Formation and the basement units of the Taurides. The base of the middle megasequence commences with continental fluvial deposits (Derinçay Formation) that pass upsection to coastal-, shallow water-, and deeper-marine sediments of the Köselerli and Mut formations (Tanar and Gökçen 1990; Şafak et al. 2005).

The facies of the Derinçay Formation mainly pertain to low sinuosity fluvial associations, and are characterized by coarse-grained redbeds and red mudstones, with subordinate marls, calcareous sandstones, palaeosols, and lignitic horizons (Eriş et al. 2005; Şafak et al. 2005). Alluvial fan and braidplain deposits, together with meander belt fluvial associations, have been recognized in the lower-middle part of the Derinçay Formation (Eriş et al. 2005; Şafak et al. 2005). Farther up in the succession, coastal flood-plain, shoreface, tidal flat, and inner shelf facies were identified just beneath the Derinçay/Köselerli transition (Şafak et al. 2005).

The Derincay Formation mainly crops out in the northwest and eastern parts of the Mut Basin. This formation shows great thickness variations; the maximum thickness is about 300 m northwest of Mut (Şafak et al. 2005). In other places the Derinçay Formation is missing.

The upper Derincay Formation passes upwards and laterally into the deeper marine deposits of the Köselerli and Mut formations. These formations where deposited in a shallow- to deeper-water carbonate depositional system developed in the Mut Basin as a consequence of the marine transgression that affected Central Taurides during the late Burdigalian. Shallow-water limestones sedimented in the inner (shallower) part of a carbonate-ramp setting (coral reef, rhodalgal and bryomol limestones of the Mut Formation), whereas deeper-water marls and resedimented clastic limestones characterized the deposition on the outer

(deeper) carbonate-ramp setting (deeper marine marls of the Köselerli Formation). In some places, mainly in the Mut-Ermenek area, the Köselerli Formation contains patch-reefs and carbonate mounds.

The rich planktonic foraminifera assemblages from the lower part of the Köselerli Formation span from late Burdigalian to Langhian (Şafak et al. 2005), whereas in the middle (Olupkinar section) and upper part of the Köselerli Formation (Basyayla section) fossil assemblages span from late Langhian (Cipollari et al.,2013a) up to late Tortonian (Cosentino et al. 2012). In particular, the highest marine marls cropping out in the northern part of the Mut Basin (Basyayla section) show a well-constrained late Tortonian age (8.10-8.35 Ma, Cosentino et al. 2012).

Considering the lateral interfingering between Mut and Köselerli formations, thickness measurements in the Gezende, Olupkinar, Ermenek and Mut areas, and thickness data from the literature (Gedik et al. 1979; Tanar and Gökçen 1990; Şafak et al. 2005; Dalkiliç and Balci 2009), we estimate the total thickness of these shallow- to deeper-water marine deposits to be around 1100 m.

2.3.2.3. Upper megasequence (early Pliocene-early Pleistocene; late Zanclean-Calabrian).

The upper megasequence of the Mut Basin (early Pliocene-early Pleistocene) lies unconformably over deposits mainly pertaining to Mut and Köselerli formations. In the vicinity of the towns of Haciametli, Sarikavak, and Yenisu (E and SE of Mut), the base of the upper megasequence is well exposed. Near Haciametli and Yenisu, a lag deposit, which consists mainly of pebbles from Mut limestones, separates the deposits of the middle megasequence from onlapping younger marine sediments, mainly calcarenite, marls, and marly limestones. In some places, a spectacular angular unconformity separates the middle (MM) and upper (UM) megasequences. In the Haciametli section, the bedding (strike and dip) of the MM is N227°, NW30°, whereas the UM lies with bedding planes N078°, SE31°. In the Yenisu area, we measured the MM\UM angular unconformity in two different stratigraphic sub-sections: YEN-A and YEN-J. In YEN-A, which corresponds to the highest sub-section sampled in the Yenisu area (908 m of elevation), the bedding plane of the MM (Mut Formation) is N347°, NE10°, whereas the UM lies with bedding attitude N220°, NW10°. In the lowermost part of the Yenisu section (YEN-J subsection, at 294 m of elevation), UM shows bedding attitude N306°, NE06° and rests unconformably onto MM (Köselerli Formation) that lies with bedding planes N068°, SE10°.

Yildiz et al. (2003) analyzed some stratigraphic sections in the Haciametli and Sarikavak areas to better define the age of the younger infilling of the Mut Basin. The micropaleontological results from both foraminifera and calcareous nannofossils point to a Calabrian age (early Pleistocene) for the Haciametli section, whereas the Sarikavak section shows fossil assemblages that span from late Zanclean (early Pliocene) up to the Calabrian (early Pleistocene). Although younger ages, different lithologies, and different fossil content, Yildiz et al. (2003) related the analyzed sections to the Köselerli Formation of the Mut Basin, extending to the early Pleistocene the age of this formation, previously defined as late Burdigalian-Serravallian.

Taking into account (1) the erosional surface at the base of the late Zanclean-Calabrian deposits of the Mut Basin, (2) the lag deposit separating MM and UM, (3) the angular unconformity between MM and UM, and (4) the different lithologies of the UM deposits if compared to the Köselerli Formation, we suggest formally distinguishing the upper megasequence into a new formation that we call the "Sarikavak Formation". The lower boundary of the Sarikavak Formation is an erosional surface cut into the MM down to the Köselerli Formation. The upper boundary is a younger erosional surface covered in places by colluvium or alluvial deposits.

We estimate the thickness of the Sarikavak Formation to be around 330 m. According to differences in the vertical distribution of the main lithofacies, the Sarikavak Formation is distinguishable in three different members. These members from the bottom to the top are: (1) the Hocali Member, (2) the Kürkçü Member, and (3) the Yenisu Member.

The lower Hocali Member is characterized by well-stratified thin-bedded calcarenites, showing well-developed cross-bedding structures, and in some places thin intercalations of marls, especially close to the boundary with the Kürkçü Member. The fossil content is mainly due to oysters and echinoids, suggesting a shallow-water marine environment. The thickness of the Hocali Member is 90 m.

The middle Kürkçü Member is mainly characterized by a rhythmic alternation of marls and calcareous marls, showing a general deepening-upward trend. The fossil content is characterized mainly by echinoids, molluscs and benthic foraminifera in the lower and middle part of this member, whereas planktic foraminifera and fish scales characterize the upper part. Some slumped beds were identified close to the transition to the Yenisu Member. The thickness of the Kürkçü Member is around 200 m.

The upper Yenisu Member is characterized by massive biocalcarenites, with lithothamnium, echinoids, and molluscs. The thickness of this member is around 40 m.

2.4. Data and Methods

2.4.1. Seismic interpretation

We interpreted more than 600 km of onshore seismic reflection profiles acquired in the Adana Basin and processed by the Turkish Petroleum Corporation (TPAO).

We integrated the stratigraphy compiled by different authors (Schmidt 1961; Görür 1979; Yetiş 1988; Ünlügenç et al. 1991; 1993; Gürbüz and Kelling 1993; Yetiş et al. 1995; Gürbüz 1999; Gürbüz and Ünlügenç 2001; Nazik 2004; Cosentino et al. 2010a and b; Cipollari et al. 2013a; Faranda et al. 2013) and the seismic stratigraphy described in the first chapter for the Adana Basin to interpret seismic lines. The interpretations were validated correlating the new seismostratigraphic units with surface outcrops located close to the seismic profiles and employing the lithologic description of a few well logs made available by the TPAO (Adana 1; Akyar 1; Çakit 1; Dumandere 1; Yenice 1; Yenice 2).

2.4.2. 3D surfaces, isopach maps and volume calculation

We interpolated areas between our interpreted seismic profiles using the 3D software program Petrel to reconstruct the main surfaces separating the different seismostratigraphic units. We exported our 3D reconstructed surfaces as ASCII files that we loaded in ArcGis 9.3. We calculated the thicknesses of each sedimentary body subtracting the heights of the top surfaces from those of the bottom surfaces, therefore obtaining a two-way-time (TWT) isopach maps. Conversion from TWT to thicknesses was made using the interval velocities calculated for each sedimentary body. Values were obtained using the interval velocities used in processing and provided on the seismic profiles; interval velocities were recalculated for the interval of interest with a resolution of 1 ms. We applied one single value for each sedimentary body; these values are consistent with those used by Aksu et al. (2005b). We used the isopach maps to calculate the total volume of each seismostratigraphic unit using an ad-hoc set-up routine in Matlab 7.1.

2.4.3. Subsidence curves

To reconstruct the subsidence history of Mut and Adana sedimentary basins, we first calculated the cumulative subsidence and then we partitioned the subsidence due to tectonics and that due to sediment loading assuming local Airy isostasy (*backstripping* method, Allen and Allen 1990). We calculated cumulative subsidence by decompacting the sedimentary columns following the procedure described by Sclater and Christie (1980). We used their parameters for surface porosities and rates of exponential decrease in porosity with depth (Table1 and 2). The compacted sedimentary column for the Mut Basin was made by integrating our data on the youngest deposits of the basin (Sarikavak Formation) with data from Şafak et al. (2005) and Yldiz et al. (2003; Fig. 2b). Thicknesses used for the Adana Basin compacted sedimentary column (Fig. 2a) were obtained by integrating (i) thicknesses derived from time-depth conversion of interpreted seismic profiles (Fig. 3c; Oligocene – Pliocene section) and (ii) data from literature (Pliocene – Quaternary section; Cipollari et al. 2013a)

Tectonic subsidence was calculated using equation (1) from Steckler and Watts (1978):

$$Y = S\left(\frac{\rho_m - \rho_s}{\rho_m - \rho_w}\right) + [W_d - \Delta_{SL}] - \Delta_{SL}\frac{\rho_w}{\rho_m - \rho_w}$$

where Y is the depth to the basement of a water-loaded basin, S is the total thickness of the sedimentary column corrected for compaction, ρ_m, ρ_s, ρ_w are mantle, mean sedimentary column and water densities, W_d is the paleo-water depth, and Δ_{SL} is the paleo-sea level relative to the present. The mean sedimentary column density (ρ_s) was obtained using data from Sclater and Christie (1980).

2.5. Results

2.5.1. Seismic interpretation

Although the seismic stratigraphy for the Adana Basin was outlined in the first chapter and correlated with the recently revised stratigraphy for the basin (Cosentino et al. 2010b; Cipollari et al. 2013a; Faranda et al. 2013; illustrated in Fig. 3), here, we describe in greater detail how the the different

seismostratigraphic units and regional unconformities vary across the basin. In the first chapter we identified four regional unconformities (U1, U2, MES, MES2) and a transgressive surface (P) separating five seismostratigraphic units (MS2, MS3, MS4a, MS4b, MS5). Unfortunately, with the exception of U1, the surfaces crop out only on the NW area of the Adana Basin; a major portion of the basin is covered by the Quaternary-Recent fluvial sediments of the Seyhan and Ceyhan rivers. Our interpretation on the SE part of the basin is therefore less constrained and more tentative.

2.5.1.1. Seismostratigraphic units

2.5.1.1.1. MS1

This sesimic facies is characterized by high amplitude, very discontinuous reflectors showing a chaotic pattern. The few traceable reflectors are highly deformed. MS1 outcrops along the NW and SE margins of the basin. In its upper part, it is erosionally truncated and therefore defines an unconformity surface named U1. On surface exposures, U1 corresponds to the basal angular unconformity of the basin, separating the Central Tauride basement rocks from the Oligocene – Serravallian portion of the Adana Basin filling (Schmidt 1961; Williams et al. 1995; Gürbüz and Ünlügenç 2001; Nazik 2004; Burton-Ferguson et al. 2005). We therefore correlated the portion of the seismic profiles located below U1 with the basement. Toward the SE margin of the basin, MS1 is characterized by high angle discontinuities showing a reverse offset here interpreted as pertaining to a transpessive flower structure (Fig. 3b).

2.5.1.1.2. MS2

This seismostratigraphic unit is characterized by relatively high amplitude, continuous to discontinuous reflectors. Its moderate deformation includes folding in the NW portion of the basin and faulting in the SE portion. In the NW portion of the Adana Basin (Fig. 3a) it onlaps the erosional unconformity (U1) that truncates MS1, but in the depocentral portion of the basin, the contact becomes a paraconformity and is difficult to trace. In the SE area of the basin (Fig. 3b), the boundary between MS1 and MS2 is complicated by the presence of several high angle discontinuities showing both reverse and normal offsets, characterized in one case by the presence of a series of reflectors arranged in a wedge-shaped

geometry fulfilling a small graben that we tentatively attribute to a younger seismostratigraphic unit, MS3. MS2 is clearly truncated by the "U2" erosional surface. As already mentioned in the first chapter, we interpreted this seismostratigraphic unit as the subsurface expression of a seismic mega-sequence spanning from Oligocene to Langhian and including the Gildirli, Karaisali, Kaplankaya, Çingoz and Guvenç formations.

2.5.1.1.3. MS3

This seismostratigraphic unit is characterized by undulating, continuous and discontinuous reflectors with increasing continuity toward the depocentral portion of the basin. In the westernmost section, it directly onlaps onto the U2 and U1 unconformities, ending with a wedge-shaped pinch out geometry towards the SE (see also Burton-Ferguson et al. 2005) before it reaches the southeastern portion of the basin. A limited wedge-shaped sedimentary body imaged in between the faulted southeastern portion of the basin could pertain to MS3, although in the absence of subsurface constraints, this interpretation is tentative. Exclusively towards the NW margin of the basin, seismostratigraphic unit MS3 is capped by a few, very continuous, equally spaced, high amplitude reflectors (PLE; Fig. 3a). At the top, MS3 is erosionally truncated. The absence of subsurface control in this area of the basin did not allow us to definitively exclude the presence of MS3 on top of the deformed southeastern portion of MS2.

We correlated unit MS3 with the Tortonian – Messinian Kuzgun Formation and, supported by strong control on surface stratigraphy, we interpreted the few anomalously high amplitude reflectors locally present on the uppermost portion of MS3 to be the Messinian Primary Lower Evaporites identified by Cosentino et al. (2010b) in the northwesternmost sector of the basin.

2.5.1.1.4. MS4a

Seismic facies MS4a is very distinct, characterized by discontinuous, high amplitude reflectors, showing a chaotic pattern. This facies is present only in the northwestern portion of the basin and ends towards the SE with disorganized downlaps above the erosional unconformity (MES) on top of MS3. As all the previous seismostratigraphic units, MS4a is erosionally truncated on top. We correlated this seismostratigraphic unit with the Resedimented Lower Evaporites, which occur at the base of the Messinian Salinity Crisis post-evaporitic stage (CIESM 2008; Cosentino et al. 2010b).

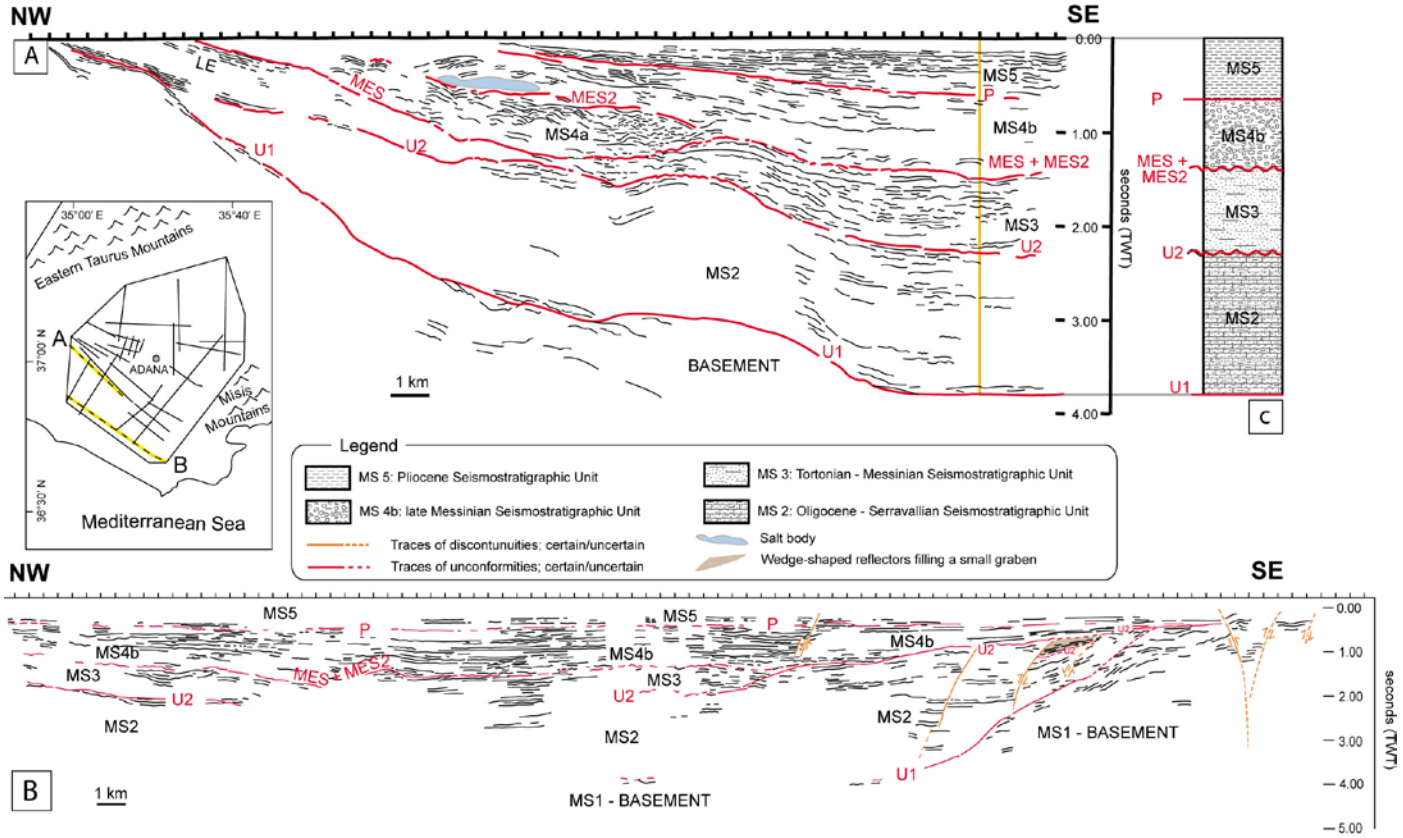

Figure 3. Location map of the interpreted seismic profiles and line-drawing of two seismic profiles highlighted in the map illustrating the seismostratigraphy applied to the Adana Basin. [A] Goes from the northwestern portion of the basin to its depocenter; it shows geometries and relationships of all the seismic facies described in the text; [B] is located SW from [A], in a more depocentral area. Separated by traces of unconformities and trangressive surfaces (in red) are the main seismostratigraphic units; MS2: Oligo – Serravallian sequence; MS3 Tortonian Kuzgun Formation; LE: Lower Evaporites; MS4a: Resedimented Lower Evaporites; MS4b: Late Messinian Lago-Mare unit, constituted by an alternation of conglomerates and marls bearing a brackish-water fauna; MS5 Pliocene unit. Surfaces; P: base Zanclean flooding surface (5.33 Ma). MES 2: late Messinian Erosional Surface (~5.45 Ma). MES: early Messinian Erosional Surface (5.60 Ma). U2: late Serravallian – early Tortonian Erosional Surface. U1: late Oligocene – early Aquitanian Erosional Surface. Lines in the map correspond to the traces of the seismic profiles used for the reconstruction of the 3D surfaces and isopach map, which have been calculates for the area corresponding to the polygon in the map. [C] Simplified stratigraphic log used for the reconstruction of the subsidence curve (lithologies are higlhy simplified).

2.5.1.1.5. MS4b

This seismostratigraphic unit is widespread throughout the basin. It is characterized by relatively continuous reflectors, unconformably overlying either MS4a (above MES2 erosional surface) or MS3 (above MES erosional surface). On the northwestern portion of the line interpreted in Fig. 3a, an acoustically transparent seismic body deflecting the overlying seismic reflectors was correlated by Cipollari et al. (2013a) with a salt body present in the subsurface. We interpret the deformed reflectors as the result of halokinesis and we therefore presume that the salt is not in-place. Seismostratigraphic unit MS4b has been correlated with the conglomerates and marls bearing a late Lago-Mare brackish fauna that have been interpreted by Grossi et al. (2011) and Cosentino et al. (2010b) as pertaining to the second post-evaporitic stage of the Messinian Salinity Crisis.

2.5.1.1.6. MS5

Seismostratigraphic unit MS5 consists of high amplitude, very continuous reflectors. It onlaps seismostratigraphic unit MS4b, but the contact is not erosional. Cipollari et al. (2013a) correlated this unit with the Pliocene-lower Pleistocene marine clays of the Avadan Formation.

2.5.1.2. Seismostratigraphic surfaces

2.5.1.2.1. U1

This surface is correlated with the basal unconformity of the Adana Basin, and is characterized by steeply dipping slopes along the basin margins that flatten to near-horizontal in the depocentral zone. The surface truncates the underlying seismostratigraphic unit MS1 and is onlapped by units MS2 and MS3 along the NW margin of the basin (Fig. 3a). Towards the SE, the contact between the basement and the overlying sequences has been deformed: a series of shortening structures separates MS1 from MS2, complicating the recognition of the boundary. A few interrupted reflectors suggest a tectonic contact between the basement and the younger units at the SE margin (Fig. 3b). However, the interpretation there is further complicated by the poor seismic resolution, and in the absence of subsurface control, any conclusion is speculative.

2.5.1.2.2. U2

This second unconformity is characterized in the seismic profiles by an almost continuous, very high amplitude reflector, with the exception of the deepest portion of the basin, where it becomes a paraconformoty and is difficult to trace. It correlates on surface with a Serravallian-Tortonian unconformity at the base of the Kuzgun formation (Yetiş 1988; Ünlügenç 1993; Yetiş et al. 1995). Along the SE portion of the basin, it is disrupted by a series of discontinuities interpreted as thrust faults (Fig. 3b).

2.5.1.2.3. MES

A third, more complex, angular unconformity divides MS3 from the MS4a and MS4b seismostratigraphic units. The pattern of the MES is very irregular; it truncates the underlying MS3 and presents both onlaps and downlaps on top. Cosentino et al. (2010b) correlated the MES unconformity surface to the intra-Messinian unconformity observed throughout the Mediterranean and separating the two major stages of the Messinian Salinity Crisis (Guillemin and Honzay 1982; Costa et al. 1986; Cita and Corselli 1990; Escutia and Maldonado 1992; Riding et al. 1999; Guennoc et al. 2000; Roveri et al. 2001; Rouchy et al. 2003; Lofi et al. 2005; Soria et al. 2005; Cornée et al. 2006; Maillard et al. 2006; Roveri et al. 2008; Ryan 2009; Garcia-Castellanos et al. 2009; Sampalmieri et al. 2010; Cosentino et al. 2010a; Cosentino et al. 2013)

2.5.1.2.4. MES2

This angular unconformity separates MS4a from MS4b in the proximity of the NW margin of the basin, and merges towards the depocenter with the MES, putting MS3 in direct contact with MS4b. The underlying units are erosionally truncated, whereas units overlying MES2 onlap onto it. The MES2 unconformity surface has been observed in surface exposures (Cosentino et al. 2012b), where it separates the Resedimented Evaporites from the late Lago-Mare conglomerates and marls, therefore defining a second intra-Messinian unconformity separating the first and second post-evaporitic stages of the Messinian Salinity Crisis (Cosentino et al. 2012a and b).

2.5.1.2.5. P

This conformable surface separates MS4b from MS5. Cipollari et al. (2013a) interpreted it as a transgressive surface, and demonstrated that it correlates with the Messinian/Zanclean transition. Therefore, the surface marks the Early Pliocene flooding event separating the late Lago-Mare sediments from the Pliocene clays of the Avadan Formation.

2.5.2. 3D surfaces and Isopach maps

The reconstructed 3D surfaces (Fig. 4) all show a deepening toward SE, in the direction of the Cilicia Basin. U1, corresponding to the basal unconformity of the Adana Basin, extends through the subsurface for almost 3300 km^2 of the area of interest. It shows a gradual deepening from NE to SW, whereas from NW to SE, it first deepens on a relatively gentle slope and then gets steeper while re-emerging on the SE flank of the basin, delineating an asymmetric trough (see also Burton-Ferguson et al. 2005). The unconformity seems to show an undulating pattern along the NW portion of the basin, but the scarce seismic coverage makes this difficult to verify.

U2 is located near the surface at the NE portion of the basin, and it deepens up to 3s TWT in the SW portion; on a NW-SE transects, it is more symmetric than U1, but maintains a steeper SE flank compared with the NW flank.

MES and MES2 are more complex surfaces, both characterized by a major depocenter at the SW portion of the basin, but distinguished also by the presence of smaller depressions generating surfaces that look rougher than the previous ones. These two discontinuites diverge only locally, in a small area located on the west side of the basin (black rectangle in Fig. 4).

P is a surfaces present only in the SE margin of the basin, relatively smooth, deepening towards Mediterranean.

The Oligocene – Serravallian sequence of the Adana Basin, MS2, displays thicknesses increasing from NW to SE (Fig. 5), with maximum values arranged along a belt roughly parallel to the Taurus Mountains and Misis Mountains and reaching up to 4.1 km (Table1).

The Tortonian – Messinian sequence, MS3, is thicker in the central portion of the basin, although greater values are probably an artifact due to the poor data coverage and quality of the area.The Messinian

Resedimented Lower Evaporites, MS4a, reworks and re-deposits at least a portion of MS3 (Fig. 5) and shows a limited depositional area, localized along the NW portion of the basin.

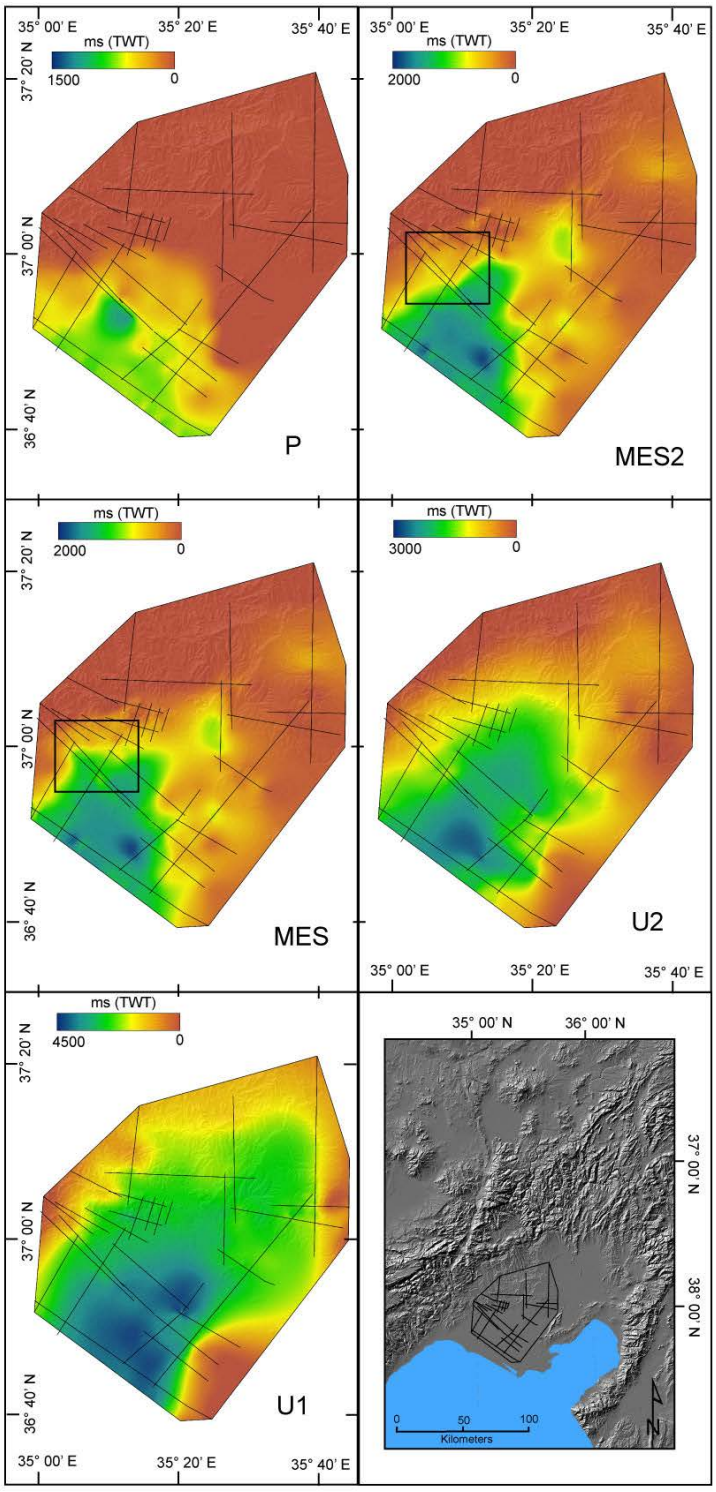

Figure 4. Discontinuities and transgressive surfaces recognized in the Adana Basin. Bottom right is the location map of the area of interest. P: base Zanclean flooding surface (5.33 Ma). MES2: late Messinian Erosional Surface (~5.45 Ma). MES: early Messinian Erosional Surface (5.60 Ma); black squares outline the small area where MES and MES2 differ. U2: late Serravallian – early Tortonian Erosional Surface. U1: late Oligocene – early Aquitanian Erosional Surface. Lines in the map correspond to the traces of the seismic profiles used for the reconstruction of the 3D surfaces and isopach maps, which have been calculated for the area corresponding to the polygon in the map.

The maximum thickness of this seismostratigraphic unit is 830 m. The late Lago-Mare seismic facies, MS4b, shows impressive thicknesses with respect to its time of deposition, with maximum values

reaching up to almost 2.0 km of material deposited in ~120 kyr (Chapter 1).The isopach map of MS4b shows a patchy pattern of sediments, with an overall increase in thicknesses toward the SE. Pliocene sediments (MS5) are present only in the SE portion of the basin; thickness generally increase from NW toward the Mediterranean.

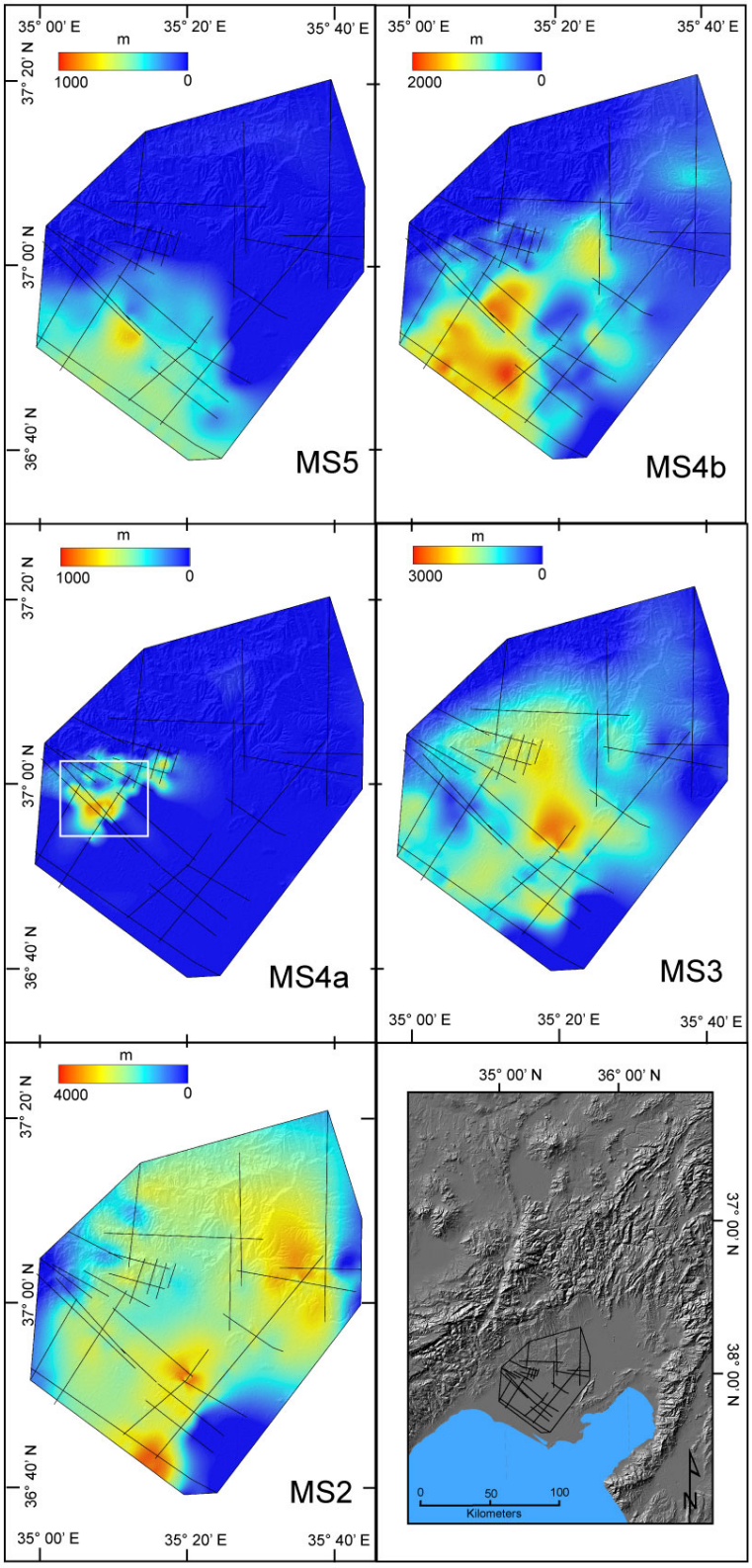

Figure 5. Isopach maps for the main seismostratigraphic units recognized in the Adana Basin. Bottom right is the location map of the area of interest. MS5 Pliocene unit. MS4b: Late Messinian Lago-Mare unit, constituted by an alternation of conglomerates and marls bearing a brackish-water fauna. MS4a: Resedimented Lower Evaporites; in the white square, the reduced depositional area of MS4a. MS3 Tortonian-Messinian sequence, constituted by the Kuzgun Formation and Lower Messinian Evaporites. MS2: Oligo – Serravallian sequence..

2.5.3. Volume calculations and deposition rates

We determined the total volume of each seismostratigraphic unit by using the raster of the isopach maps; we calculated the areas over which the units are present and we plotted these two values with the time-span of deposition on the histogram in Fig. 6A. Using these data, we calculated the depositional rates for each seismostratigraphic unit, as the result of the local thickness divided by the time-interval of deposition (Fig. 6B).

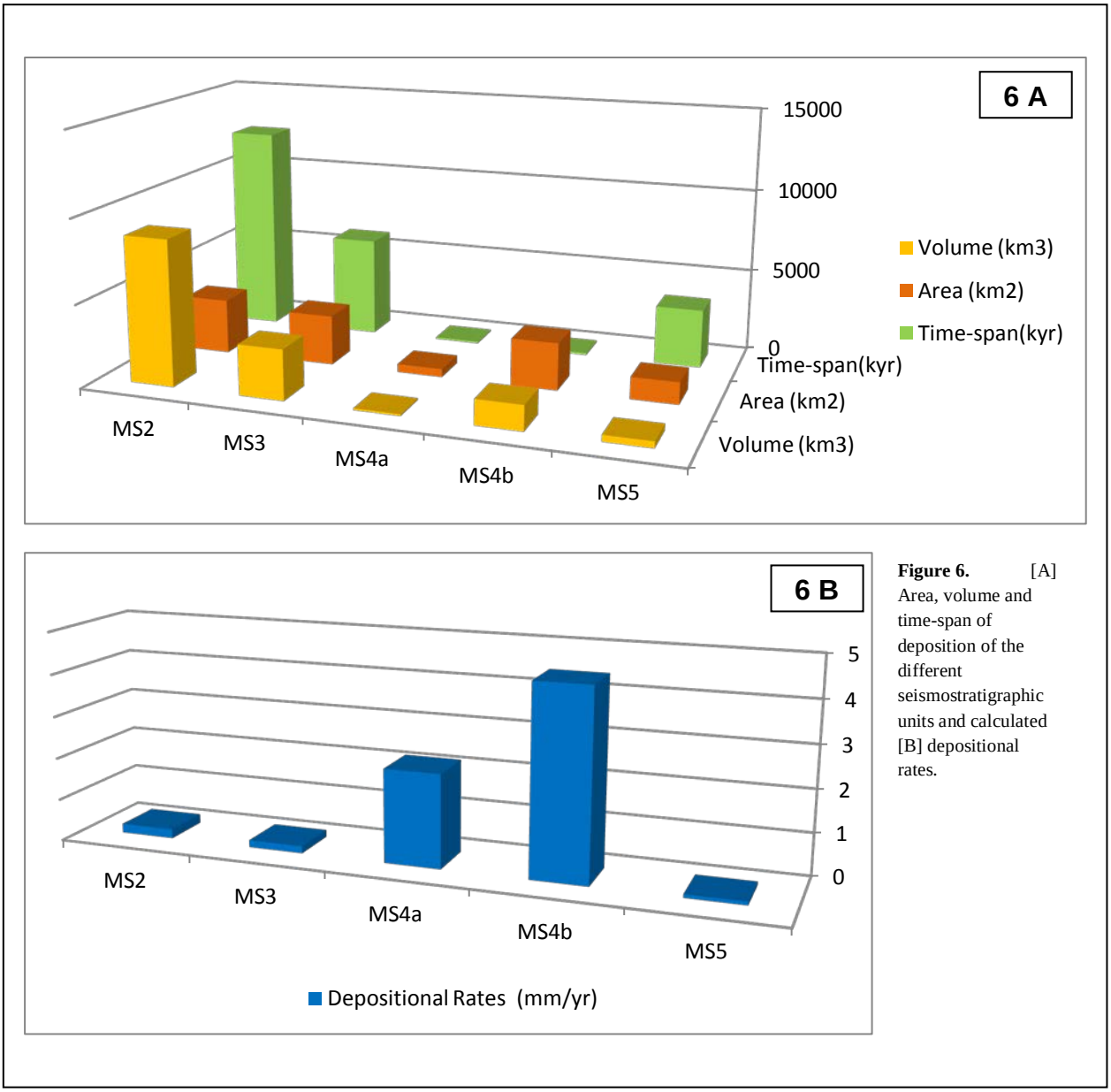

Figure 6. [A] Area, volume and time-span of deposition of the different seismostratigraphic units and calculated [B] depositional rates.

From our calculations, seismostratigraphic units MS2 and MS3 are characterized by a high volume of sediments deposited over a long time interval, resulting in relatively low depositional rates reaching up to ~0.21 for MS2 and ~0.17 mm/yr for MS3. MS4a has a relatively low amount of sediments (~ 100 km^3)

deposited over a restricted area and time-span, resulting in a relatively high depositional rate of 2.2 mm/yr. MS4b is characterized by a high volume of sediments (~ 1500 km^3) spread over a extensive area and a very short time interval of deposition; the depositional rates resulting from this calculations are the highest of the basin at ~4.5 mm/yr. Local sedimentation rates are even higher because the unit thickness varies. Seismostratigraphic unit MS5 has a limited volume of sediments deposited over a relatively broad area, with the lowest sedimentation rate in the basin of only ~0.08 mm/yr.

2.6. Subsidence Curves

2.6.1. Subsidence curve for the Adana Basin

Fig. 7a shows the subsidence curves we derived for the Adana Basin. Dark-gray-shaded areas show depositional periods while light-grey-shaded areas show non depositional and/or erosional episodes.

Deposition in the Adana Basin started during the late Oligocene, with sedimentation of an Oligocene – Serravallian Megasequence (MS2), comprising: (1) Oligocene – Lower Miocene continental deposits of the Karsanti and Gildirli formations; (2) Aquitanian – Langhian marine sediments of the Kaplankaya and Karaisali formations; (3) the Burdigalian – early Serravallian turbidite fan system of the Çingoz Formation; and (4) Serravallian deep marine clays of the Guvenç Formation. The deposition of MS2 leads to a total subsidence in the basin of ~4.0 km, with ~2.5 km (~60%) of this total related to tectonic subsidence.

A first episode of erosion is recorded at the Serravallian – Tortonian boundary (U2), with a tectonic uplift of ~0.7 km (Fig. 7a). It is followed by a second depositional event starting in the Tortonian (Yetiş 1988; Ünlügenç 1993; Yetiş et al. 1995), with the deposition of the continental – shallow marine sediments of the Kuzgun Formation. Along more marginal areas of the basin, these deposits conformably underlie the Messinian Primary Lower Evaporites, corresponding to the onset of the MSC; however, the Primary Lower Evaporites are absent in the depocentral portion of the basin (Fig. 3c), where they were probably never deposited, resulting in a flat pattern on the showed subsidence curve (Fig. 7a). The total subsidence of this second depositional event (MS3) corresponds to ~1.1 km, ~30% of which is tectonic subsidence. The drawdown of Mediterranean at ~5.56 Ma related to the Messinian Salinity Crisis results in the Adana Basin's tectonic subsidence curve showing a major phase of relative uplift, related to the removal of the water column.

The Messinian Salinity Crisis in the depocentral area of the Adana Basin is solely represented by the late Lago-Mare sediments of the Handere Formation (Fig. 3a and c), which have been deposited in the basin starting from ~5.45 Ma. This depositional event is clearly shown in the subsidence curve, and is characterized by a major increase in the subsidence rate. The subsidence rate slows down again at 5.33 Ma, in correspondence with the Pliocene reflooding of Mediterranean. The total subsidence experienced by the Adana Basin between ~5.45 and 5.33 Ma is ~1.7 km, with an additional ~0.2 km during lower Pliocene. The last part of the curve relates to the youngest sediments found in the Adana Basin and implies the onset of uplift of the Adana Basin at ~5.2 – 5.3 Ma (Cipollari et al. 2013a). Sedimentation stops again during middle Pleistocene (Cipollari et al. 2013a).

2.6.2. Subsidencce curve for the Mut Basin

The time versus depth plot in Fig. 7b shows the subsidence curves for the Mut Basin. Deposition starts with the Lower Megasequence, consisting of the mainly continental sediments of the Yenimahalle and Fakirca formations (Rupelian – late Aquitanian; Tanar 1989, Tanar and Gökçen 1990, Safak et al. 2005) and stops at the early Miocene, with the development of the first unconformity. Total subsidence of Lower Megasequence corresponds to ~0.5 km, ~0.3 km , 60% of which is tectonic subsidence. The time-gap in the sedimentary record goes from late Aquitanian to late Burdigalian, after which sedimentation restarts with the deposition of the Middle Megasequence (late Burdigalian – late Tortonian; Safak et al. 2005), mainly consisting of the marine sediments of the Köselerli and Mut formations (total subsidence equal to ~1.4 km, of which ~57% is tectonic subsidence). A second, period of non-deposition and erosion starts at some point after ~8.0 Ma, the age of the youngest sample of the Middle Megasequence dated so far (Cosentino et al. 2012); the sample was deposited in a littoral environment and lies today at ~2000 m a.s.l. (Cosentino et al. 2012; Cipollari et al. 2013b). This erosional episode is accompanied by an important phase of uplift that ends in the early Pliocene, when renewed deposition leads to sedimentation of the Upper Megasequence, which shows a total subsidence of ~0.2 km and ~0.15 tectonic subsidence. Deposits of the Upper Megasequence span from late Zanclean to Calabrian and lie today at elevations from 294 to ~1200 m a.s.l..

2.7. Discussion

Reconstruction of the main erosional and transgressive surfaces recognized in the Adana Basin and estimate of the isopach maps for the seismostratigraphic units allowed us to make some observation about the evolution of the depocenter.

A clear reduction of the depositional area through time is outlined by the 3D reconstructed surface, with the youngest surfaces deepening in the subsurface only in the SW portion of the basin, delineating also a shift in the depositional system towards this direction. Changes in the isopach maps through time support this observation, showing a pattern that suggests a progressive filling of the landward portions of the basin. In agreement with Kelling et al. (1986), we interpret this reduction in the depocentral area and shift in accomodation space towards the SW over time as related to the oblique convergence of the Arabian-Eurasian collision zone occurring ~200 km east of the basin and consequent uplift of the northeastern portion of the basin.

The oldest unconformity surface (U1), which separates the basement from the first sediments deposited in the Adana Basin, shows a SW-NE directed undulating pattern along the northwestern portion of the basin; we tentatively interpret this surface as a preserving remnants of the paleo-drainage system that led to the deposition of the Oligocene fluvial sediments, even though the scarce seismic coverage make this interpretation tenuous. Nonetheless, this hypothesis is in good agreement with the notion of an already – partially- exhumed Taurus thrust front at the onset of early Miocene deposition (e.g.Williams et al. 1995; Burton-Ferguson et al. 2005), and with the clast composition of the Gildirli Formation conglomerates, showing that this succession is mainly sourced from the Taurus Mountains (Görür 1985, 1992).

Our analysis of seismic stratigraphy shows that the NW margin of the Adana Basin, constituted by the Central and Eastern Taurus, behaved differently from the SE margin, represented by the Misis Mountains. Seismic reflectors imaged along the northwestern margin, and pertaining to the Oligocene-Serravallian megasequence, are slightly tilted towards SE (Fig. 3a), whereas the equivalent reflectors are highly deformed near the SE margin (Fig. 3b). Tilting of the northwestern portion of the basin has been attributed to a regional warping due to the uplift of the Central Anatolian Plateau southeastern margin (e.g.

Cosentino et al. 2012; Schildgen et al. 2012a and b). Deformation of the SE portion of the basin supports the notion of a post-Serravallian tectonic event, involving only this margin of the basin, already noticed both in the field and from seismic interpretation by other authors (Kelling et al. 1987; Gökçen et al. 1988; Burton-Ferguson et al. 2005). The structures we mapped in seismic profile b in Fig. 3, that cut through MS2, are high angle faults generated by a complex kinematic regime; whereas some horizons show reverse offset, the small, tectonically controlled graben implies an extensional component. Aksu et al. (2005) and Burton Ferguson et al. (2005) have referred this deformation to an early Tortonian – Messinian shortening phase related to the advancement of the Tauride thrust front and leading to the uplift of the Misis Mountains and the separation of the Adana and Iskenderun basins. Indeed, stratigraphic evidence (Kelling et al. 1987; Gökçen et al. 1988) shows a connection of the two basins up to late Serravallian and a disconnection during and after the Messinian Salinity Crisis, implying that a phase of uplift of the Misis Mountains occurred between early Tortonian and late Messinian. This event led also to the steepening of the southeastern flank of the basal unconformity (U1 erosional surface) and explains the higher thickness of seismostratigraphic unit MS2 in this portion of the basin. Higher isopach values concentrated along the SE portion of the Adana Basin during the Oligocene-Serravallian can be explained by a wider trough consisting of the shared depocenter of the Adana and Iskenderun basins (Kelling et al. 1987; Gökçen et al. 1988; Aksu et al. 2005; Burton-Ferguson et al. 2005). Nevertheless, the high angle dip of the discontinuities cutting the Oligocene – Serravallian seismostratigraphic unit, their limited extension at depth, and their reverse and normal offset do not support deformation related to thrust front propagation.

The uplift of the Misis Mountains is contemporaneous with i) the formation of a late Serravallian-early Tortonian unconformity throughout the Adana Basin (U2; Fig. 3), accompanied by ~0.7 km of tectonic uplift (Fig. 7a); ii) the end of marine deposition in Eastern Anatolia (Gelati et al. 1975; Hüsing et al. 2009) and iii) the onset of westward extrusion of Anatolia along the North and East Anatolian Faults (i.e. Dewey and Şengor 1979; Şengor et al. 1985, 2005). We speculate that regional tectonic re-organization following continental collision between the Arabian and Eurasian plates and westward extrusion of the Aegean-Anatolian microplate affected the Misis area, where local transpession related to the development of the East Anatolian Fault appears to have uplifted the Misis Mountains. Uplift of the Misis Mountains through tranpession is also supported by the presence of a positive flower structure cutting through the basement

units (Fig. 3b). The present day stress regime acting at the SE border of the Adana Basin is dominantly a transtension (Harvard CMT Catalogue; Over et al. 2004); the contact between the youngest portion of the basin filling and the basement is therefore probably still tectonic, but low resolution of the seismic profile near the surface prevents us from making a more definitive interpretation. The late Serravallian- early Tortonian tectonic phase of Eastern Anatolia, coupled with a major sea-level drop at the end of Serravallian, which coincides with the Mi-5 isotope event and the deep-sea hiatus NH4 (Hilgen et al. 2005; Faranda et al. 2013) were likely the causes of the erosional episode that occurred in the Adana Basin at this time.

In contrast to the Adana Basin, the Mut Basin experienced almost continuous subsidence from the early Oligocene to late Miocene, interrupted only by the development of a minor late Aquitanian-late Burdigalian discontinuity surface (Şafak et al. 2005) that was not accompanied by tectonic uplift (Fig. 7). The Mut Basin subsidence curve doesn't show any gap in sedimentation at the base of Tortonian. Considering that the Mut Basin is ~200 km west of the Adana Basin, and hence farther from the Arabian-Eurasia collision zone, this clear difference between the subsidence histories of the Mut and Adana basins corroborates the supposition that the late Serravallian – early Tortonian erosional episode observed only in the Adana Basin is at least partly related to the collision between Arabia and Eurasia.

The subsidence curves of the Mut and Adana Basin significantly diverge after the Tortonian. Some time after ~8Ma (Cosentino et al. 2012; Cipollari et al. 2013a) sedimentation stops in the Mut Basin, while it experiences a phase of tectonic uplift (Fig. 7b). Over the same time interval, sedimentation proceeds in the Adana Basin, with the Tortonian-Messinian sequence (MS3, MS4a, and MS4b). Tortonian sediments of the Mut Basin are today found at ~2.0 km a.s.l. (Cosentino et al. 2012; Schildgen et al. 2012a and b), and are unconformably overlain by Zanclean to Calabrian marine deposits lying today at elevations from 294 m a.s.l. to ~1200 m a.s.l.. These stratigraphic relationships imply that the late Tortonian – Early Pliocene Mut Basin erosional episode was accompanied by at least ~0.8 km uplift, with a resulting uplift rate of ~0.2 mm/yr, as previously noted by Schildgen et al. (2012a).

In the Adana Basin, the Tortonian-Messinian succession shows higher thicknesses towards the center of the basin (Fig. 5), suggesting that after the development of U2 and the growth of the Misis Mountains, the Adana Basin became an independent depocenter (separated from the Iskenderun Basin) with well-defined

margins. The two intra-Messinian unconformities recorded in the Adana Basin, MES and MES2, diverge only in the NW portion of the basin (outlined rectangle in Fig. 4), where the presence of Resedimented Lower Evaporites separates them, and converge in the other areas of the basin.

Above the MES unconformity surface, our seismic interpretations demonstrate that the Messinian evaporitic unit in the onshore Adana Basin is discontinuous and laterally limited to an area of less than 500 km^2 (MS4a; Fig. 5 and 6); this observation has major consequences for petroleum geology, because traditionally, Messinian evaporites and salt have been considered the be the main seal for the Eastern Taurus petroleum system (Demirel 2004; Çíftçí et al. 2012). Deposition of MS4a (Resedimented Lower Evaporites) is also marked by a major increase in the sedimentation rate (Fig. 6b) due to the reduction of the depositional area (outlined rectangle in Fig.5) and to the limited time of deposition (Fig. 6a). The irregular pattern of the MES and the subsequent deposition of a spatially limited sedimentary body at high sedimentation rates point to the generally accepted scenario depicted for the marginal basins during the first post-evaporitic stage of the Mediterranean Messinian Salinity Crisis, characterized by "evidence for a substantial relative sea-level drop in the Mediterranean with subaerial exposure, and erosion of evaporitic basins formed during the previous step" (CIESM 2008). Aksu et al. (2005b) and Çíftçí et al. (2012) outlined the presence of thick Messinian units constituted by halite and thin anhydrite and limestone interbeds in the Cilicia Basin, that possibly places it amongst the MSC's deep basins setting (e.g. Clauzon et al. 1996; CIESM 2008; Ryan 2009). If these interpretations are correct, future connection of the seismic stratigraphy of the Adana Basin with that of the Cilicia Basin could shed new light on the relationship between marginal and deep basins during the MSC.

A major increase in the sedimentation rate occurs in the Adana Basin after the development of the MES2 erosional surface, with the deposition of MS4b (late Lago-Mare conglomerates and marls of the Handere Formation (Fig. 6 and 7). This episode is characterized by the presence of a thick and voluminous sequence (MS4b; Fig. 3) deposited in a short time-span over a large portion of the area of interest (Fig. 5 and 6). MS4b shows the highest depositional rates for the Adana Basin, with an average value of 4.5 mm/yr and local depositional rates of up to 12.5 mm/yr (Chapter 1). Moreover, it shows the greatest tectonic subsidence rates, reaching up to 19.5 mm/yr (Fig. 7a).

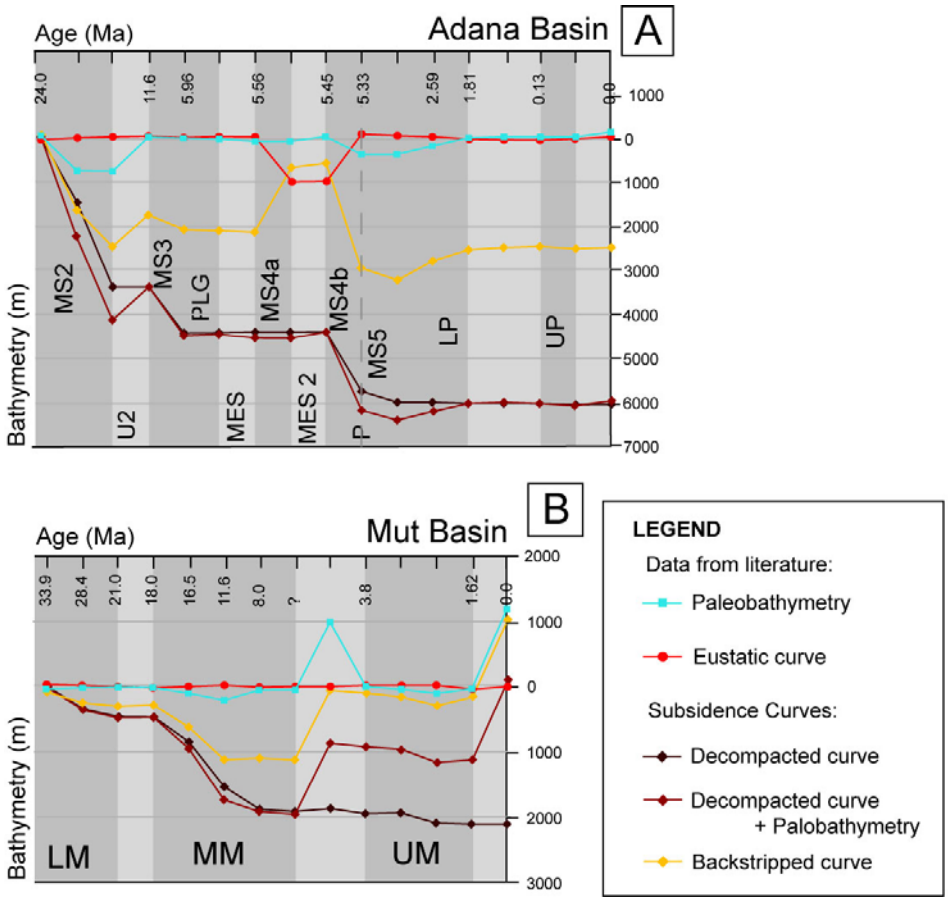

Figure 7. Subsidence curves for the Adana and Mut basins. Time axis not to scale. Dark-grey areas correspond to depositional phases, whereas light-grey areas show erosional/non-depositional phases; dashed grey line corresponds to a transgressive surface. In blue, the paleobathymetry (Nazik 2003; Şafak et al. 2005; Cosentino et al. 2010b; Cosentino et al. 2012; Cipollari et al. 2013a) and in red, the eustatic variations, (Miller et al. 2005). Dark brown line shows the decompacted curve, obtained from decompacting the different units through time using Sclater & Christie (1980) parameters for the exponential relation between porosity and depth. Light brown line is a sum of the decompacted values and the palebathymetry, illustrating the depth of the bottom of the basin through time. In yellow, the backstripped curve, obtained using the Steckler & Watts (1978) equation. Airy type isostatic adjustment is assumed, and the curve shows the purely tectonic subsidence, deprived of the fraction related to the sediment load. [A] Subsidence curve for the Adana Basin. Initial thicknesses for reconstruction of the subsidence curves have been derived integrating the results from time-depth conversion of the seimsic lines presented in this work (Fig 2c) with data from Cipollari et al. (2013) for the youngest period. MS2: Oligocene – Serravallian sequence; MS3 Tortonian-Messinian sequence, consisting of the Kuzgun Formation and lower Messinian Evaporites; MS4a: Resedimented Lower Evaporites; MS4b: Late Messinian Lago-Mare unit, consisting of an alternation of conglomerates and marls bearing a brackish-water fauna; MS5: Pliocene unit. LP: Lower Pleistocene unit; UP: Upper Pleistocene unit. [B] Subsidence curves for the Mut Basin. Time axis not to scale. Initial thicknesses for reconstruction of the subsidence curves have been derived from Şafak et al. 2005; AAVV, "Field guide to Turkey" 2011; Yildiz et al. 2003 and field observations reported in the text. Heights are in meters (Fig 6). LM: Lower Megasequence; MM: Middle Megasequence; UM: Upper Megasequence.

In the first chapter we interpreted the deposition of this huge amount of material, which occurred in conjunction uplift in the Mut Basin, as a clear signal for the uplift of the CAP south-southeastern margin. This interpretation is corroborated by a provenance study of the late-Lago Mare conglomerates of the

Handere Formation (MS4b), which reveals that the clasts are mainly derived from the interior and the SE margin of the Central Anatolian Plateau.

The subsidence rate in the Adana Basin decreased to ~0.09 mm/yr at 5.33 Ma, with the onset of Pliocene deposition, which is characterized by the lowest observed sedimentation rates (0.08 mm/yr; Fig. 7A). Tectonic uplift started at some time before the lower Gelasian for the Adana Basin (Fig. 7A; Cipollari et al. 2013a). The recognition of a Quaternary Upper Megasequence in the Mut Basin, characterized by lower Calabrian marine sediments unconformably lying above late Tortonian shallow marine sediments necessarily implies a second phase of uplift for the Mut Basin (Fig. 7b).

Sediments deposited during the Calabrian (early Pleistocene) at around sea level in the Mut Basin are now found at an elevation up to ~1.2 km, implying an uplift rate of ~0.7 mm/yr since their deposition (Schildgen et al. 2012a), a rate that agrees with the river incision rate calculated from surface exposure ages on strath terraces (Schildgen et al. 2012a). The total tectonic uplift related to the two phases of uplift experienced by the Mut Basin since the late Miocene is ~2 km, height at which we nowadays find the upper portion of the Middle Megasequence. In contrast, tectonic uplift experienced by the Adana Basin from the upper Pliocene to today is ~0.75 km.

We suggest that decoupling of the subsidence history of the Mut and Adana basins was achieved by the development of a major morphotectonic boundary, which allowed the Mut Basin to be uplifted with the southern margin of the CAP while the Adana Basin was subsiding and creating the accommodation space for the sediments derived from erosion of the uplifting plateau margin. The same boundary must have also accommodated the differential uplift of the Mut Basin relative to the Adana Basin from the early Zanclean until today (Cipollari et al. 2013 a). Although part of this differential uplift may have occurred along a broadly warping region (e.g. Cosentino et al. 2012; Schildgen et al. 2012a and b), the best candidate for accommodating such substantial differential vertical motion is the Kozan fault, which parallels the NW margin of the Adana Basin and is characterized by transtensional kinematics (e.g. Aksu et al. 2005).

The concomitant occurrence of rapid uplift of the south and southeastern margin of the Central Anatolian Plateau coupled with the fast subsidence experienced by the adjacent Adana Basin during

Tortonian-Messinian times and followed by uplift of both the plateau margin and the Adana Basin starting from the lower Pleistocene support earlier suggestions that uplift along the southern margin of the CAP largely resulted from a deep-rooted mechanism (e.g. Cosentino et al. 2012; Schildgen et al., 2012a and b). The notion of topography supported by a deep-rooted process in this region is corroborated by both analog and numerical models (Gögüş and Pysklywec 2008), showing a very good agreement between the topography resulting from modeled lithospheric slab delamination and break-off and the topography of the Central Anatolian Plateau/ Adana Basin region. If we relate the geometry of these models to the tectonic setting of the Mut and Adana Basin, it would be expected that the region south of the delamination and break-off experiences rapid subsidence (Adana Basin), while the area above the delamination and break-off is uplifted (Mut Basin), as outlined from the reconstruction of the basins' subsidence curves. The subsided area itself (Adana Basin) is later partially uplifted as the region reaches isostatic equilibrium.

2.8. Conclusions

Our interpretation of 34 seismic profiles acquired in the Adana Basin and the reconstruction of the subsidence curves for the Mut and Adana basins allowed us to recognize the main tectonic events occurred at Neogene time in this portion of Eastern Mediterranean.

High angle faulting of the Oligocene-Serravallian seismostratigraphic unit in the Adana Basin, transpessional deformation of its SE margin (Misis Mountains), and the development of a late Serravallian – early Tortonian erosional surface are all elements pointing to a major tectonic phase acting on the basin the middle-late Miocene transition. We correlate our observations with the tectonic re-organization following continental collision between the Arabian and Eurasian plates and subsequent westward extrusion of the Aegean-Anatolian microplate. Continental collision of the Arabian and Eurasian plates, consequent closure of the Tethyan gateway between the Indian Ocean and the Mediterranean sea and the occurrence of a major sea-level drop at the end of Serravallian have repercussions on the sedimentation of the Adana Basin, which experienced a period of non-sedimentation and erosion accompanied by a phase of tectonic uplift. The same regional event triggered the westward extrusion of the Aegean-Anatolian microplate, resulting in the transpessional deformation of the Misis Mountains; deformation was accomodated by the previously deposited sediments through the development of a series of high angle normal and reverse faults.

After ~8 Ma, sedimentation stopped in the Mut Basin, and the depocenter was uplifted at least 0.8 km before the start of the upper megasequence. Deposition continued during this interval in the Adana Basin, which records all the main events of the Messinian Salinity Crisis. Sedimentation in the Adana Basin was restricted to a relatively small area during the initial 5.56 to ~5.45 Ma post-evaporitic stage of the MSC, during the deposition of the Resedimented Lower Evaporites.

A major amount of sediments was delivered from the Taurus Mountains to the Adana Basin during the late post-evaporitic stage of the Adana Basin, with local subsidence rates reaching up to 19.5 mm/yr. This event, coupled with the ongoing uplift of the Mut Basin, located on top of the southern Central Anatolian Plateau, suggests that the first phase of uplift of the south and southeastern margin of the CAP occurred between ~ 8 Ma and ~5.45 Ma. The Adana Basin started to uplift at 5.3-5.2 Ma, at a slower rate with respect to the southern margin of the CAP.

The recognition of an early Pliocene – early Pleistocene Upper Megasequence in the Mut Basin outcropping today between ~294 and 1200 m elevation implies a second phase of uplift, characterized by an uplift rate of ~0.7 mm/yr, which occurred roughly contemporaneously with a deceleration of the uplift rate in the Adana Basin from 0.06 – 0.13 mm/yr to 0.02-0.13 mm/yr (Cipollari et al. 2013a). The NE-SW trending Kozan Fault, with its transtensional kinematic component, likely helped to accomodate the differential uplift of the Mut Basin relative to the Adana Basin.

Based on analogies with both numerical and analogue models we suggest slab delamination as the possible mechanism for the first phase of uplift experienced by the southern margin of the Central Anatolian Plateau, with concurrent major subsidence in the Adana basin. This mechanism would be in good agreement also with the second, Quaternary phase of uplift, characterized by the differential rise of topography on the south and southeastern margin of the plateau and on the Adana Basin.

3.

PRESENT DAY SEISMICITY AND STRUCTURAL SETTING OF THE ADANA BASIN (SOUTHERN TURKEY)

3.1. Introduction

The Adana Basin (southern Turkey) is a wide mainly Neogene depocenter bounded by the Central and Eastern Taurus Mountains to the W and to the N and by the Misis Mountains to the E-SE (Fig.1); to the SW it passes to the offshore Inner Cilicia Basin. The Taurus Mountains (Taurides) reach up to 3.0 km, whereas the Misis Mountains are only 0.7 km high. This significant difference in elevation reflects a different geological history. The Taurus mountain chain is part of the Alpine-Himalayan orogenic belt and was accreted during Cretaceous – Eocene times (Şengör and Yılmaz 1981; Şengör et al. 1983, 1984; Görür et al. 1984; Robertson and Dixon 1984; Robertson and Woodcock 1986; Robertson 2000; Clark and Robertson 2002; Aksu et al. 2005; Kelling et al. 2005); today it constitutes the southern boundary of an high-elevated area denominated the Central Anatolian Plateau. Taurides at the NW margin of the Adana Basin constituted a paleo-topographic high as early as Oligocene (e.g. Williams et al. 1995) but the last phase of uplift that led to its present elevation didn't occur before late Tortonian times (Cosentino et al. 2012). The Misis Mountains are a structural high separating the Adana Basin from the Iskenderun Basin. Stratigraphic and seismostratigraphic data firmly suggest that the Adana and Iskenderun basins (Fig. 1) formed a single depocenter called the Çukurova Basin (Kelling et al. 1987; Gökçen et al. 1988) from Oligocene to, at least, late Langhian times; from Messinian times the two depocenters were disconnected (e.g. Kelling et al. 1987; Gökçen et al. 1988). The Misis Mountains represent a structurally elevated segment of the Cukurova basin-fill constituted by Oligocene-Miocene highly deformed sediments (Gökçen et al. 1988).

The mechanisms leading to the diachronous development of the two margins of the Adana Basin as well as the geodynamic setting in which the basin developed are still poorly understood (e.g. Over et al. 2004; Aksu et al. 2005). The basin is entirely located on the Aegean – Anatolian plate (e.g. Aksu et al. 2005), close to the plate's SE boundary. This region has been affected by different tectonic events; the Aegean-Anatolian microplate is, in fact, the result of: i) the convergence between the Eurasian and African plates and intervening microplates, leading to the development of the Pontide and Tauride fold-and-thrust belts (Şengör

and Yılmaz 1981; Şengör et al. 1983, 1984; Görür et al. 1984; Robertson and Dixon 1984; Robertson and Woodcock 1986; Robertson 2000; Clark and Robertson 2002; Aksu et al. 2005; Kelling et al. 2005); ii) the continental collision between the Arabian and Eurasian plates leading to the development of the Bitlis-Zagros suture zone occurred at ca. 17.5 – 20 Ma (e.g. Okay et al. 2010; Ballato et al. 2011) and iii) the consequent development of two major intra-continental transform faults, the North and East Anatolian Faults (McKenzie 1972; Tapponier 1977; Şengor et al. 1985; Dewey et al. 1986).

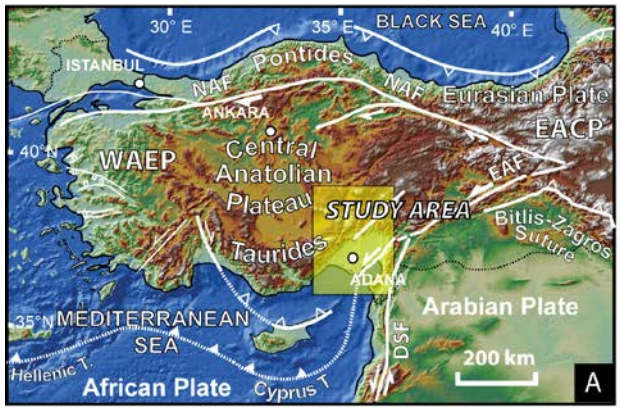

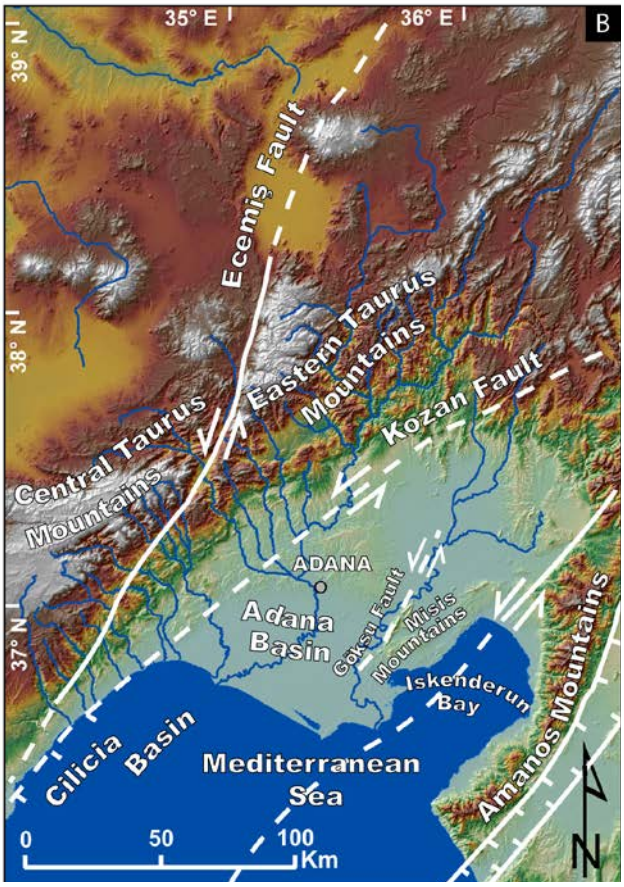

Figure 1. Location map of the study area and tectonic setting. [A] Regional setting. The Adana Basin is located beside the SE flank of the Central Anatolian Plateau, close to the Arabian – Eurasian collision zone. Westward extrusion of the Aegean-Anatolian microplate is accommodated along the North Anatolian Fault (NAF) and the East Anatolian Fault (EAF); DSF: Dead Sea Fault; Hellenic T.: Hellenic Trench; Cyprus T.: Cyprus Trench. [B] Close up of the study area. The Central and Eastern Taurus Mountains correspond to the SE margin of the Central Anatolian Plateau, constituting the NW margin of the Adana Basin. Misis Mountains border the SE flank of the basin along the Göksu Fault, separating the Adana Basin from the Iskenderun Basin.

Deep-rooted processes associated with plate rearrangement further complicate this setting: P-wave tomography shows fast seismic anomalies in correspondence of the subducted portion of the African lithosphere along the Cyprus trench (Faccenna et al. 2006; Gans et al. 2009; Biryol et al. 2011). The eastern termination of the subducting African slab is located east of Cyprus, near the transition to the Arabian–Eurasian collision front that is underlain by large volumes of hot asthenosphere marked by slow velocity perturbations (Şengor et al. 2003; Faccenna et al. 2006; Byriol et al. 2011). The presence of a slab window (Faccenna et al. 2006, 2013; Keskin 2007) would have allowed the northward and vertical (to shallow

depths) motion of asthenospheric hotter material sourced from beneath the slab (i.e., underneath the Arabian continent; Keskin 2007) or as far as the Afar plume (Ethiopia, Faccenna et al. 2013). One of the consequences of this rising astenospheric flow would be the uplift of the Central Anatolian Plateau (Cosentino et al. 2012). In this context, the Adana Basin is located beside the Central Anatolian Plateau and relatively close to both the Arabian-Eurasian collision zone and the East Anatolian Fault. From ~ 5.3- 5.2 Ma the Adana Basin started to uplift, but at a lower rate with respect to the adjacent margin of the Central Anatolian Plateau (Cosentino et al. 2012; Cipollari et al. 2013). If and how the aforementioned deep-rooted processes have contributed to the subsidence and final uplift of the Adana Basin or on the development of its margins is not yet clear. Better constrain the evolution of the basin margins would therefore be crucial to define the geodynamic setting in which the Adana Basin evolved and possibly comprehend the mechanisms responsible for the high subsidence recoded during Neogene times in the basin.

We measured and analyzed several structural elements in the Aquitanian-Messinian deposits outcropping along the NW and SE areas of the Adana Basin and we compared them with the present seismicity of the region. Our main aims were to better understand the current tectonic setting of the region along both the NW and SE margin of the Adana Basin, to spot the possible differences between the two margins and link them to present and past geodynamic contexts.

3.2. Geological setting

The Adana Basin filling is composed by a ~6000 to ~8000 m thick sedimentary succession spanning late Oligocene to Recent (e.g. Gürbüz et al. 1999; Burton-Ferguson et al. 2005). The central portion of the basin is compactly covered by the Quaternary fluvial sediments deposited by the Seyhan and Ceyhan rivers. Along the NW side of the basin Neogene deposits extensively outcrop and strata are generally dipping gently to the south (Yalcın and Görür 1984), whereas along its SE margin only a few patches of highly deformed Neogene sediments outcrop. The mainly Neogene sedimentary filling of the Adana Basin unconformably overlies a basement constituted by deformed and thrust-emplaced Paleozoic and Mesozoic units (Schmidt 1961; Yetiş et al. 1995 and references therein; Cronin et al. 2000). From the base to the top, the sedimentary successions characterizing the Neogene sediments outcropping on the NW side of the basin are constituted by an Oligocene – lower Miocene fluvial deposit (Gildirli Formation; Schmidt 1961; Görür 1979; Yetiş 1988;

Ünlügenç et al. 1991, 1993; Gürbüz and Kelling 1991; 1993; Yetiş et al. 1995; Gürbüz andÜnlügenç 2001) passing laterally and upward to the Aquitanian-Burdigalian marine deposits of the Karaisali and Kaplankaya formations, constituted by reefal carbonate, fossiliferous sandstone, siltstone, marls, and sandy limestone (Görür 1979; Yetiş et al. 1995; Nazik 2004). These deposits pass laterally and upward to the Burdigalian – Serravallian turbidite fan system pertaining to the Çingoz Formation (Schmidt 1961; Görür 1979; Yetiş and Demirkol 1986; Yetiş 1988; Gürbüz and Kelling 1993; Williams et al. 1995; Yetiş et al. 1995: Gürbüz 1999), which in turn passes laterally and upwards to the predominantly deep marine clays of the Serravallian Guvenç Formation (Ünlügenç et al. 1991; Nazik and Gürbüz 1992; Gürbüz and Kelling 1993; Yetiş et al. 1995). Above a late Serravallian-early Tortonian angular unconformity witnessing the first regressive event in the Adana Basin (Yetiş 1988; Ünlügenç 1993; Yetiş et al. 1995) the Tortonian-Messinian shallow marine sediments of the Kuzgun Formation are present (e.g. Schmidt 1961), in some portion of the basin conformably capped by a cyclical succession of anhydrites and black shales recording the main evaporative event of the Mediterranean Messinian Salinity Crisis (CIESM 2008; Cosentino et al. 2010b). Above the Tortonian – Messinian deposits, on top of a first intra-Messinian unconformity, the Resedimented Lower Evaporites of the Gökkuyu Gypsum member, and above a second intra-Messinian unconformity an up to 1.9 km thick succession of conglomerates interbedded with marls pertaining to the late *Lago-Mare* stage of the Messinian Salinity Crisis (~5.45 – 5.33 Ma; Cosentino et al., 2012b; Chapter 1) predating the Pliocene refilling of the Mediterranean, which led to the deposition of the Pliocene – lower Pleistocene mainly epibathyal marine deposits of the Avadan Formation (Cipollari et al. 2013a). Unconformably capping the succession are the Quaternary-Recent fluvial sediments aforementioned. To the E of the Adana Basin, Miocene successions are incorporated in highly deformed structures along the eastern portion of the Misis Mountains. Gökçen et al. (1988) subdivided this succession in a lower Aquitanian olistrostromal unit, a middle Burdigalian–Langhian unit, named Karataş Formation, constituted by mainly turbiditic deposits confidently correlated with the Çingoz and Guvenç formation of the Adana Basin (Burton-Ferguson et al. 2005) and an upper, mainly Tortonian succession named Kızıldere Formation correlated with the Kuzgun Formation (Burton-Ferguson et al. 2005).

The major structural elements present in the area are NE-SW oriented. The Taurus Mountains constituting the NW margin of the Adana Basin are divided in Central and Eastern Taurus by the Ecemiş

Fault, a regional transtensional fault that is currently retained to accomodate the wastward motion of the Aegean-Anatolian plate (e.g. Jaffey and Robertson et al. 2001; Piper et al. 2010). The NW margin of the basin is traced by the Kozan Fault (Fig.1), another left-lateral transtensional element partitioning the displacement of the East Anatolian Fault (Aksu et al. 2005b; Burton-Ferguson et al. 2005). The SE margin of the basin is also retained to be fault-controlled and defined by the Göksu Fault (Ergin et al. 2004) or Misis-Ceyhan Fault (Over et al. 2004), two of a group of NE-SW oriented strike-slip structures contributing to partitioning the displacement of the East Anatolian Fault (Ergin et al. 2004; Over et al. 2004).

3.3. Methodology

We used the modern earthquake parameters (location, magnitude and depth) to give an overview of the present seismicity in the Adana region (Fig. 2; Harvard CMT Catalogue; Ergin et al. 2004; KOERI National Earthquake Monitoring Center). Where data were available we plotted the earthquake focal mechanisms (Fig. 3; Dziewonski et al. 1981; Cronin 2004; Ergin et al. 2004; Ekström et al. 2012). We manually mapped the main linear topographic discontinuities of the area on an Advanced Spaceborn Thermal Emission and Reflection Radiometer digital elevation model (DEM) that was previously processed using the Spatial Analyst function in ESRI's ArcMap 9.3 in order to better outline the macro-scale structures. We grouped the discontinuities with respect to their strike direction and we extracted the average strike direction value for each group using the Spatial Statistics Tools in ArcMap 9.3 (Fig. 4a).

We measured the meso-scale fault planes (Fig. 6) and, where possible, their kinematic structures (mainly calcite steps; Fig. 10) during a fieldwork carried on in May 2012 (Fig. 7, 8 and 9). We took a total of 747 measurements whereof 461 faults. We performed a statistic analysis using the software Daisy3 [version 4.93.06, Salvini et al. 1999; Salvini 2008] and we extracted the average strike directions of the main fault populations (Fig. 4 b) in order to compare them with the average strike directions obtained with the macro-scale analysis. We grouped the stations in 11 sites (Fig. 5) taking into account the age of the rocks and their spatial distribution. Within the NW portion of the Adana Basin, 7 sites pertain to the late Oligocene-Serravallian succession, including 1 site in the conglomerates of the Aquitanian – Burdigalian Gildilri Formation, 3 sites in the limestones and marls of the Burdigalian – Langhian Karaisali and Kaplankaia formations, 3 sites in the sandstones-dominated turbidites of the Çingoz Formation, 1 site in the upper

portion of the Kuzgun Formation (late Tortonian - early Messinian in age) and 2 sites in the late Messinian *Lago-Mare* deposits; just one site has been found along the SE portion of the Adana Basin pertaining to the Langhian-Serravallian turbiditic sandstones of the Karataş Formation (Gökçen et al. 1988) correlated with the Langhian – Serravallian Çingoz and Güvenç formations outcropping in the northwestern portion of the basin (Burton-Ferguson et al. 2005).

Using fault slickenlines, the age of faulted sediments, comparison with modern earthquake focal mechanisms (Harvard global CMT catalogue; Ergin et al. 1999) and a limited record of the latest seismicity in Turkey (earthquake database of the period going from 10.10.2013 – 09.12.2013; Kandilli Observatory and Earthquake Research Institute of the National Earthquake Monitoring Center [KOERI NEMC]), we identify the changing style of deformation in the Adana region through time and space along with its seismotectonic setting.

3.4. Data and results

3.4.1. Spatial distribution, depth, magnitude and focal mechanisms solution of the earthquakes

The earthquake databases used in this work report different types of events: the CMT Catalogue reports only events with magnitude greater than 5.0, Ergin et al. (2004) reports fault-plane solutions and epicenters for the earthquakes with magnitudes greater or equal than 4.0, whereas the data taken from the KOERI Catalogue have magnitudes greater than 1.0 and, in this work, are relative to a very short time span (Fig. 2). Interestingly, the earthquakes characterized by higher magnitudes are all concentrated around the Misis Mountains and are usually related to relatively deep (20 km < depth < 40 km) events (Fig. 2).

If we consider only those events reported from Ergin et al and in the CMT Catlogue (i.e. events with magnitude major or equal to 4.0), the NW margin of the Adana Basin seems to be completely aseismic; however, when we consider lower magnitude events, this margin shows the occurrence of very high frequency/low energy earthquakes. Low magnitude earthquakes, mostly characterized by shallow depth occur almost daily throughout the Adana region.

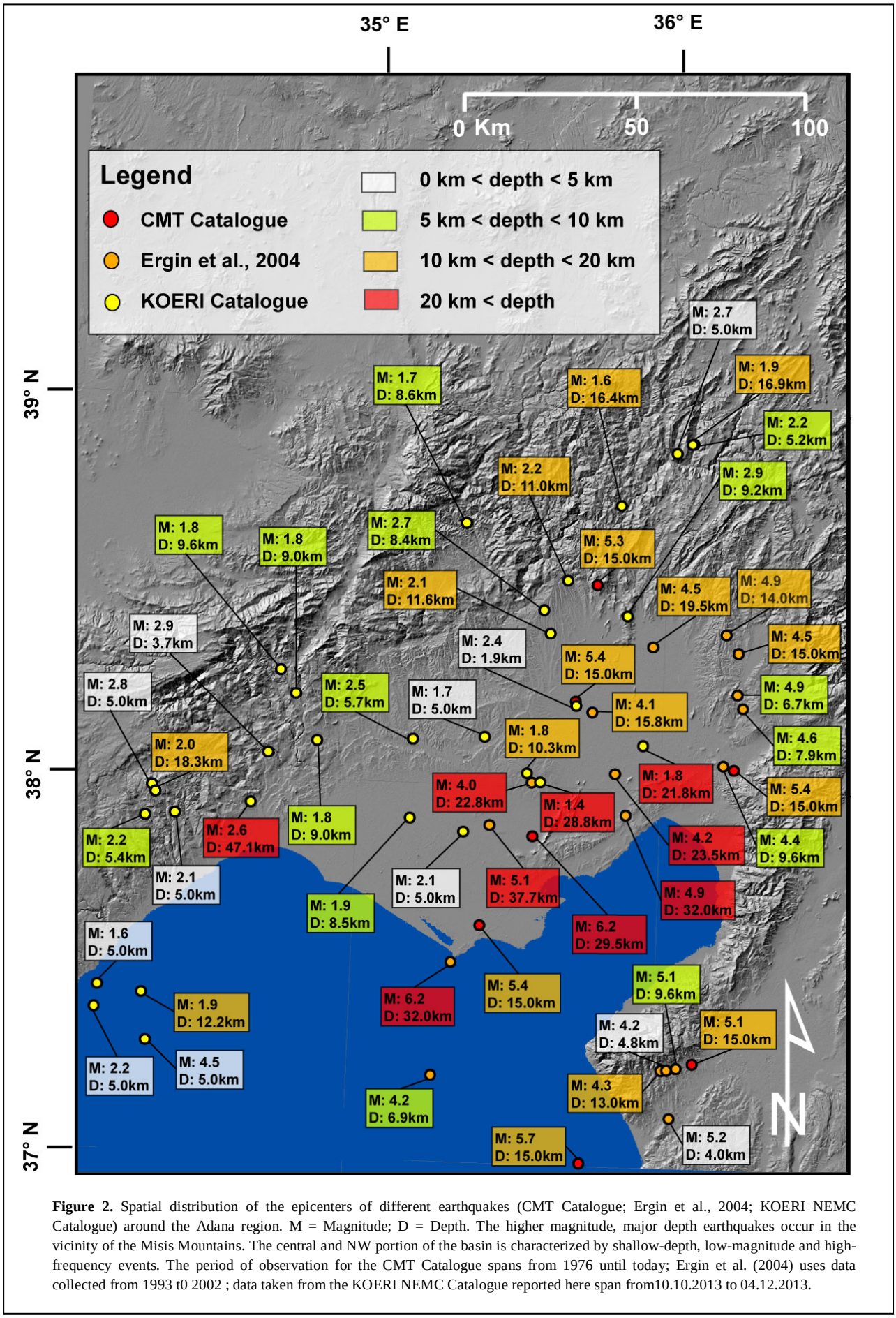

Figure 2. Spatial distribution of the epicenters of different earthquakes (CMT Catalogue; Ergin et al., 2004; KOERI NEMC Catalogue) around the Adana region. M = Magnitude; D = Depth. The higher magnitude, major depth earthquakes occur in the vicinity of the Misis Mountains. The central and NW portion of the basin is characterized by shallow-depth, low-magnitude and high-frequency events. The period of observation for the CMT Catalogue spans from 1976 until today; Ergin et al. (2004) uses data collected from 1993 t0 2002 ; data taken from the KOERI NEMC Catalogue reported here span from10.10.2013 to 04.12.2013.

Spatial distribution of the modern earthquake focal mechanisms (CMT Catalogue; Ergin et al. 2004) show homogeneous patterns in the different tectonic domains; the Adana Basin and Misis Mountains area are characterized mainly by transcurrence with a mostly subordinate dip-slip component; in just one case pure extension is showed. Toward the NE margin of the Adana Basin, the focal mechanisms mainly show almost pure extension and fault planes oriented NNW-SSE, NW-SE or NE-SW. Earthquakes occurred in the Amanos region show a predominant oblique movement, mainly transtensional toward the south.

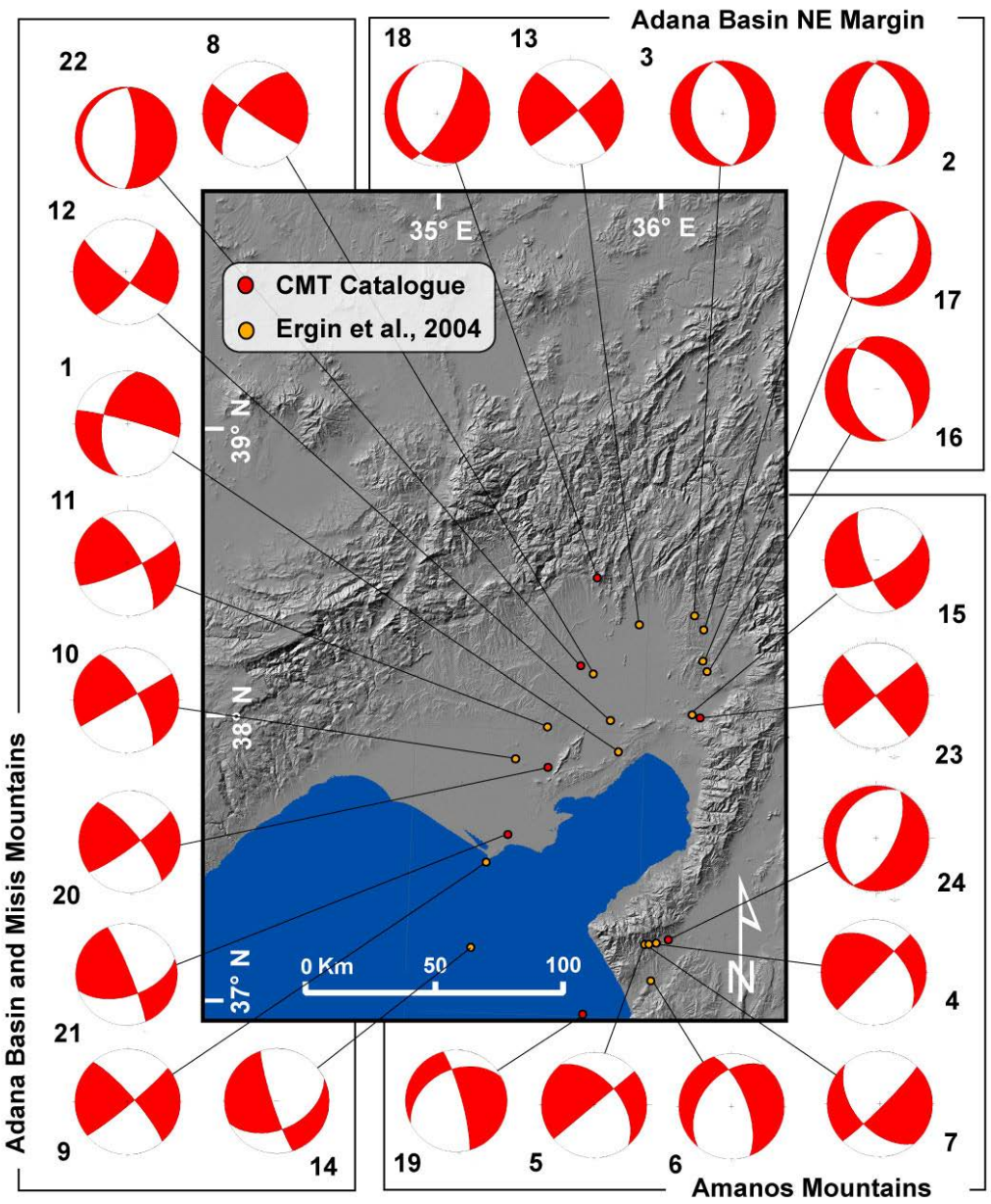

Figure 3. Spatial distribution of the modern earthquake focal mechanisms around the Adana region. The area in the vicnity of the Misis Mountains is characterized by transcurrence and transtension. The period of observation for the CMT Catalogue spans from 1976 until today; Ergin et al. (2004) uses data collected from 1993 t0 2002.

3.4.2. Fault measurements

3.4.2.1. Discontinuity trends on the macro- and meso-scale

The topographic linear discontinuity visible and mapped on a 30-m resolution DEM show four main orientations (Fig. 4a); the majority of the linear discontinuities trend NE-SW and can be divided into two sub-groups (~39° and ~ 67°); the other two relevant orientations trend NW-SE: one group is more WNW – ESE oriented (~106°), whereas the other is more NNW – SSE oriented (~160°).

Trends of the faults measured in the field (Fig. 4b) are clearly consistent with the trends of the discontinuities mapped on the DEM (Fig. 4b; ~37°; ~63°; 96°; ~150°); nevertheless, the meso-scale analysis outline the occurrence of two other groups of faults: one shows an almost pure NW-SE trend (~121°), whereas the other shows a NNE-SSW trend (~6°).

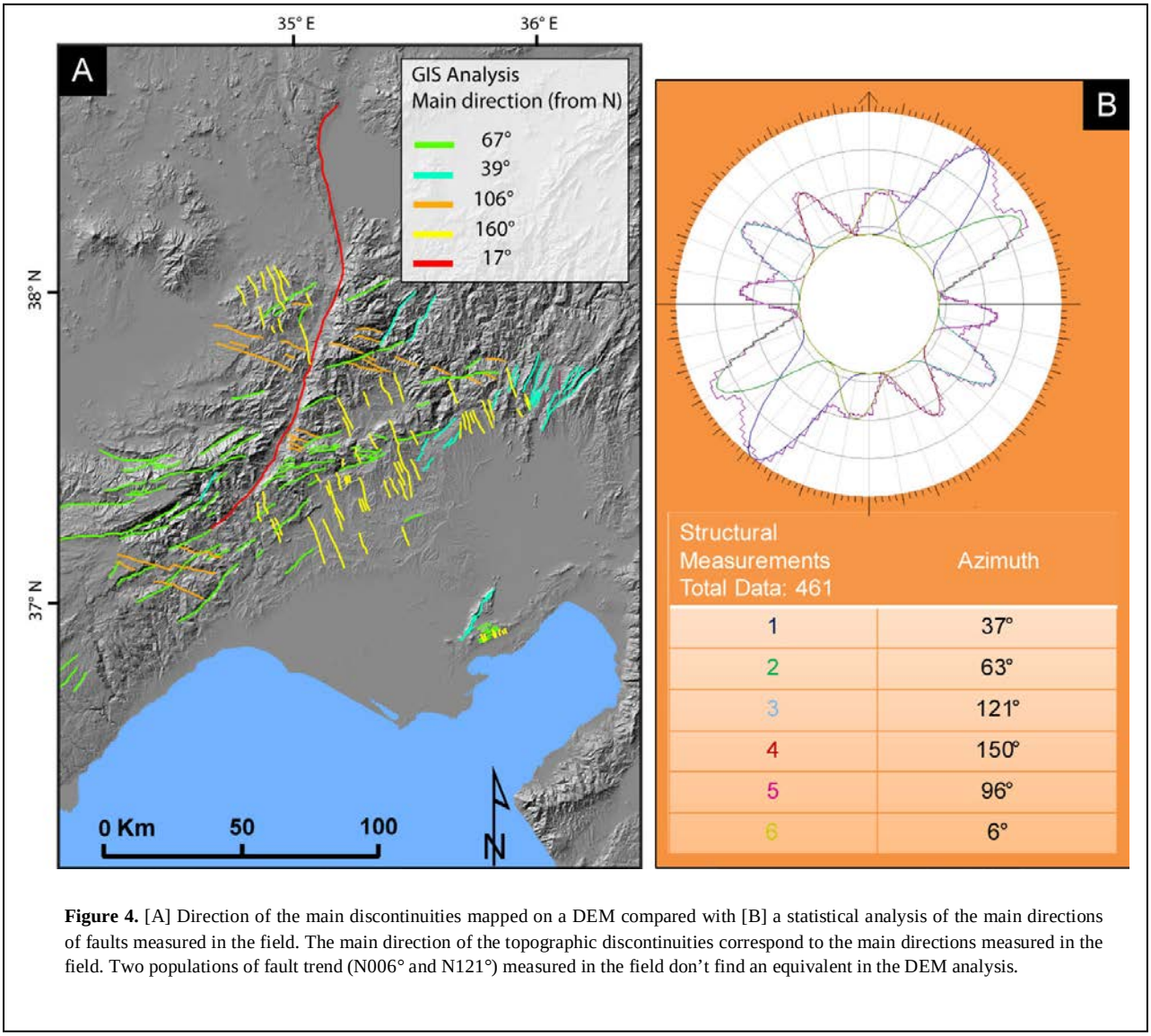

Figure 4. [A] Direction of the main discontinuities mapped on a DEM compared with [B] a statistical analysis of the main directions of faults measured in the field. The main direction of the topographic discontinuities correspond to the main directions measured in the field. Two populations of fault trend (N006° and N121°) measured in the field don't find an equivalent in the DEM analysis.

3.4.2.2. Direction Analysis of the measured faults

If we plot the poles of the measured faults on a Schmidt lower hemisphere projection, dividing them with respect to the stratigraphic age of the deformed deposits (first and third column in Fig. 6), we can observe that the elements measured in the youngest rocks, located in the internal portion of the basin show four main clustered populations of faults, two trending NW-SE (~120° and ~155°), one trending NNE-SSW (~5°), and a fourth trend WSW-ENE oriented (~70°), less clustered and mainly noticed in the uppermost portion of the Tortonian – Messinian Kuzgun Formation. To be noted that the directions of two of these four populations exactly correspond to the two trends not detected from the macro-scale analysis performed on a DEM mostly along the margins of the Adana Basin (Fig. 4).

Elements measured in the older deposits on the NW portion of the Adana Basin show major complications, probably related to the occurrence of multiple phases of deformation; for this reason we decided to filter the data removing those elements whose trend corresponded to the three main trends detected in the faults cutting the late Messinian sediments. Filtered data don't show major changes in the main trends of the elements collected in the Aquitanian – Langhian deposits. Nevertheless, the data pertaining to the Langhian-Serravallian interval show a major consistency, with a predominance of NE-SW oriented structures clustered into two sub-trend; one sub-trend is common to all the structures measured in the Aquitanian-Serravallian deposits (~60°-65°) and the other sub-trend is found exclusively in the Langhian-Serravallian sediments (~30°). A third WNW-ESE trend (~95°) characterizes the elements measured in the Langhian-Serrvavallian NW deposit. Overall, the faults measured along the NW portion of the basin generally show high angle dips.

Faults measured on the SE portion of the basin also show a predominance of NE-SW directed structures (~40°) with a subordinate presence of NW-SE oriented structures (~125°); nevertheless, data are better clustered with respect to the elements measured in the coeval deposits outcropping on the NW portion of the basin and faults show an overall shallower dip, with the NE-SW oriented structures dipping ~60° and the NW-SE trending elements ~30°.

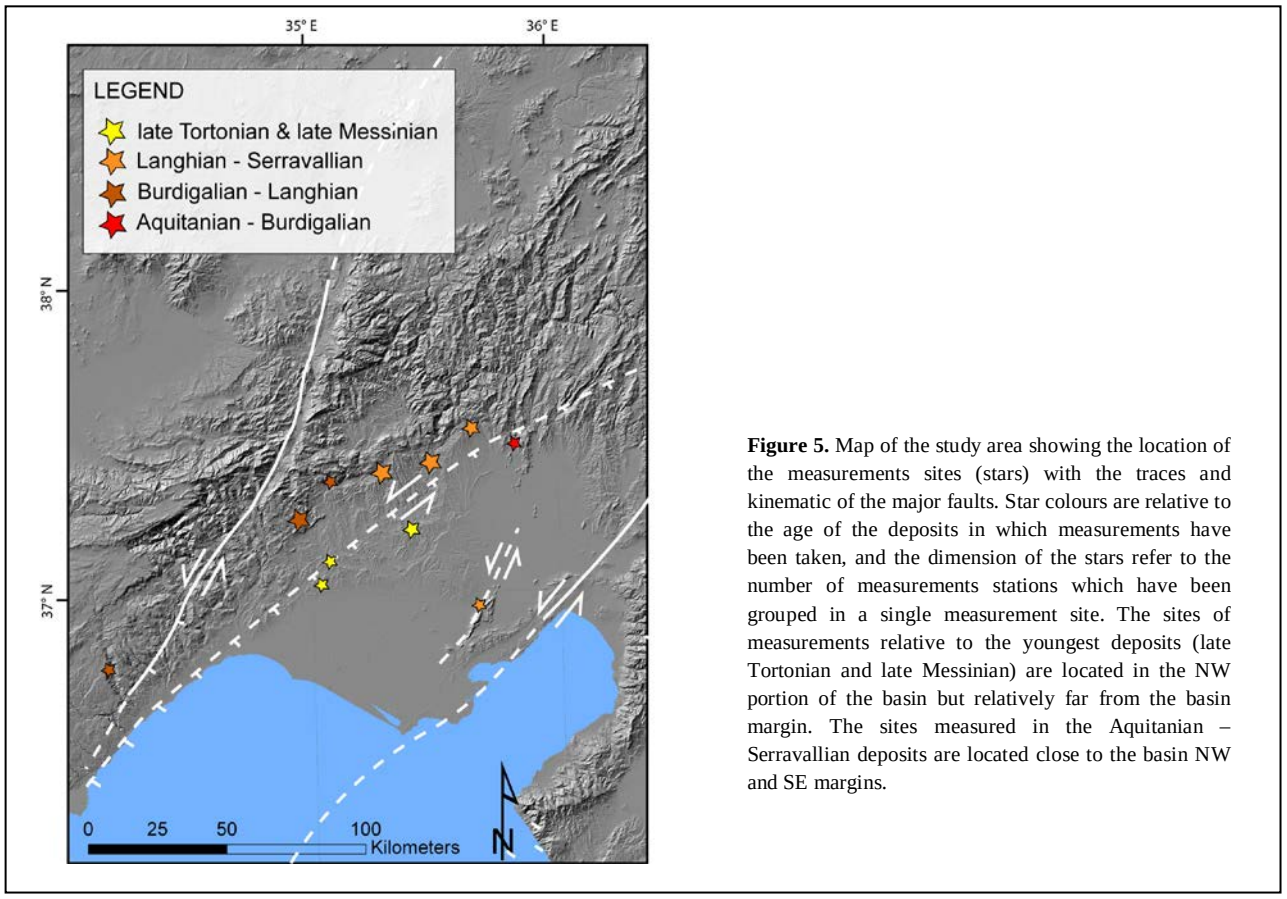

Figure 5. Map of the study area showing the location of the measurements sites (stars) with the traces and kinematic of the major faults. Star colours are relative to the age of the deposits in which measurements have been taken, and the dimension of the stars refer to the number of measurements stations which have been grouped in a single measurement site. The sites of measurements relative to the youngest deposits (late Tortonian and late Messinian) are located in the NW portion of the basin but relatively far from the basin margin. The sites measured in the Aquitanian – Serravallian deposits are located close to the basin NW and SE margins.

3.4.2.3. Kinematic Analysis of the measured faults

In the field, the deformation of the NW and SE portions of the Adana Basin look completely different. The NW area mainly shows extension-related structures, with a predominance of high angle normal faults (Fig. 7) frequently showing a subordinate strike-slip component which can be both right-lateral or left-lateral (Fig. 7A and 7D). Localized open to close asymmetric antiforms (Fig. 8A), high angle reverse faults (Fig. 8 B, C) showing a very limited offset (Fig. 8 B, C and D) and long wavelength folds (Fig. 8 E) are secondary compression-related structures. The limited extension of localized antiforms coupled with the strong tilting of the strata (Fig. 8A), the concurrent occurrence of normal and reverse faults with dip patterns reminding flower structures (Fig. 8B), the steep slope of the reverse fault planes (Fig. 8 A and B) and their limited offset (Fig. 8 D) induced us to interpret these structures as related to transpression. Along the SE portion of the Adana Basin deformation has often overturned the beds creating tight recumbent folds (Fig. 9) cut by numerous faults (Fig. 9 A).

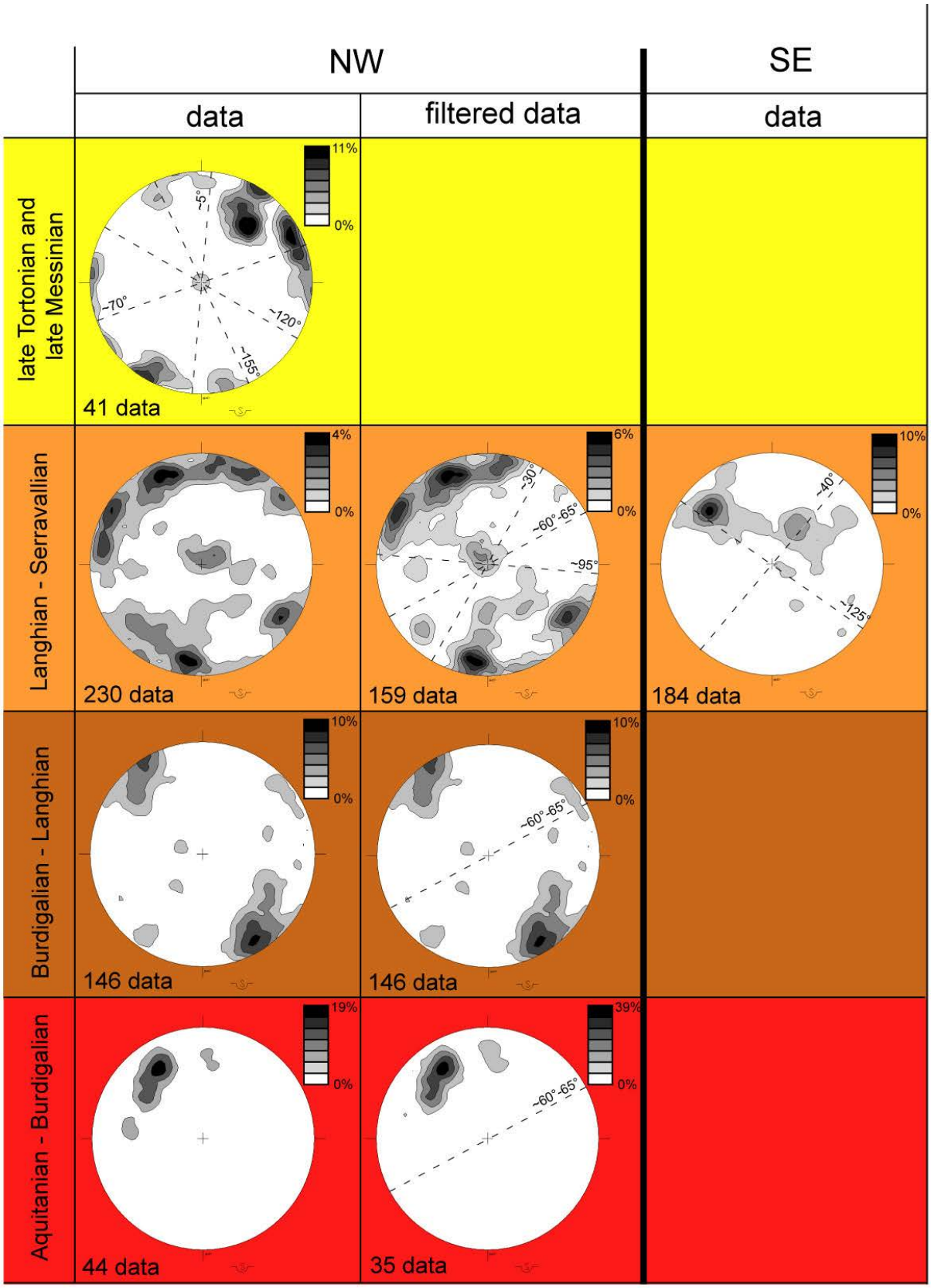

Figure 6. Fault poles of the measured elements plotted on a Schmidt projection (lower hemisphere) with respect to the age of the deposits in which fault were measured. The first two columns are relative to the NW portion of the Adana Basin; the first column shows all the measured data, whereas the second column shows filtered data. The third column pertains to the SE portion of the basin.Dotted lines show the trends of the main fault populations.

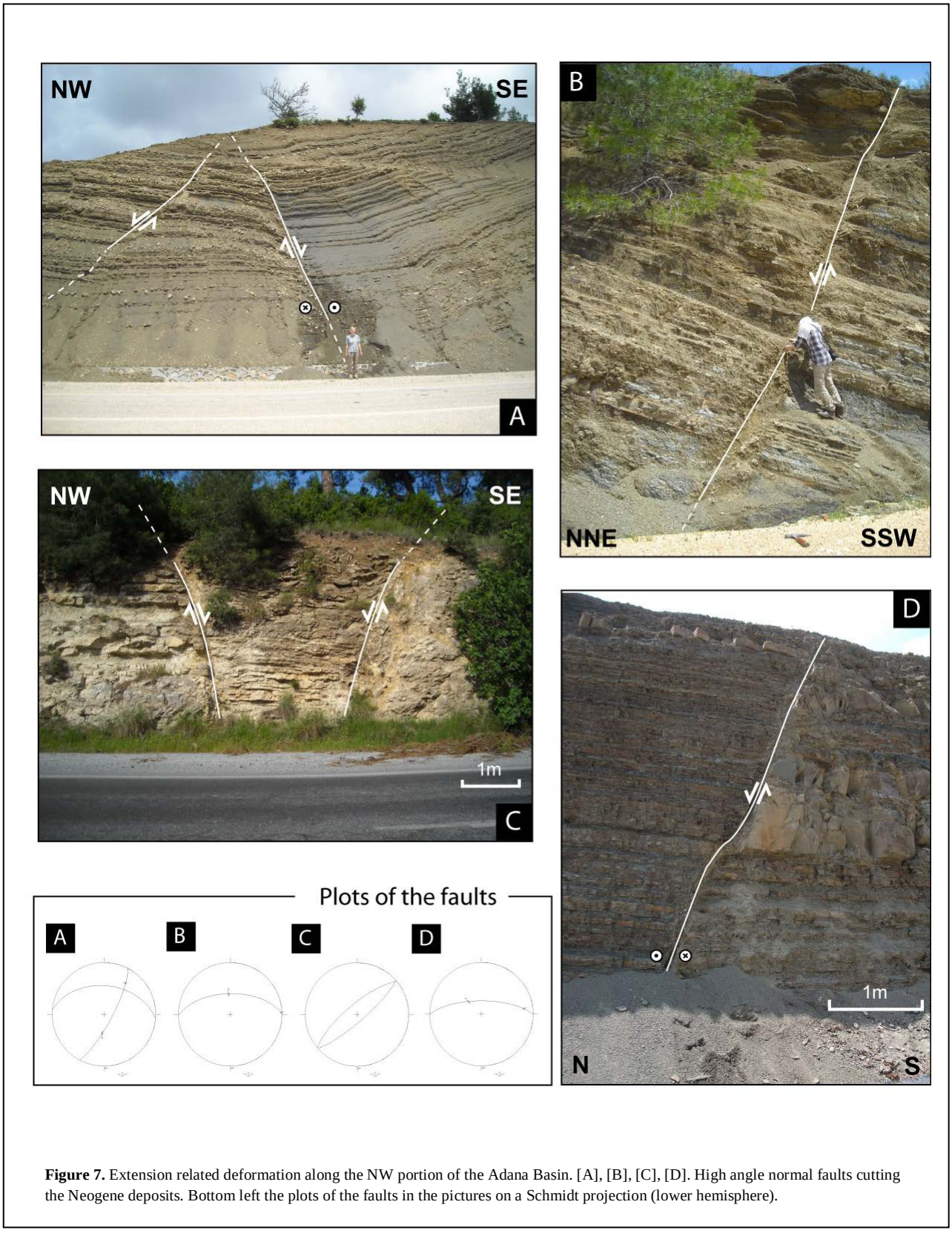

Figure 7. Extension related deformation along the NW portion of the Adana Basin. [A], [B], [C], [D]. High angle normal faults cutting the Neogene deposits. Bottom left the plots of the faults in the pictures on a Schmidt projection (lower hemisphere).

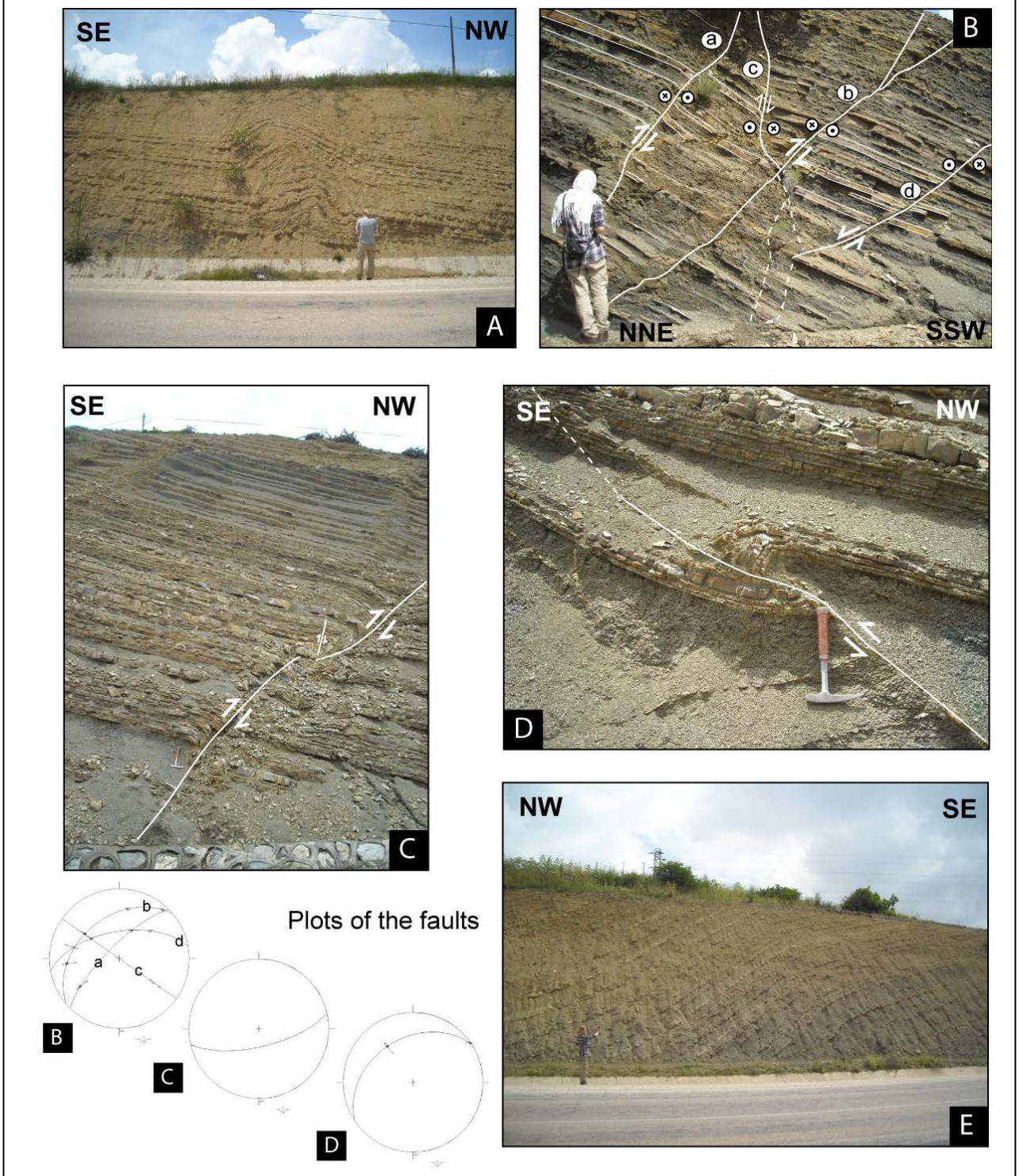

Figure 8. Transpession and/or compression related deformation along the NW portion of the Adana Basin. Structures cut the Langhian-Serravallian turbiditic sandstones. [A] Localized open to close asymmetric antiforms; [B] and [C] high and [D] low angle reverse faults; [E] long wavelength folds. Bottom left the plots of the faults in the pictures on a Schmidt projection (lower hemisphere).

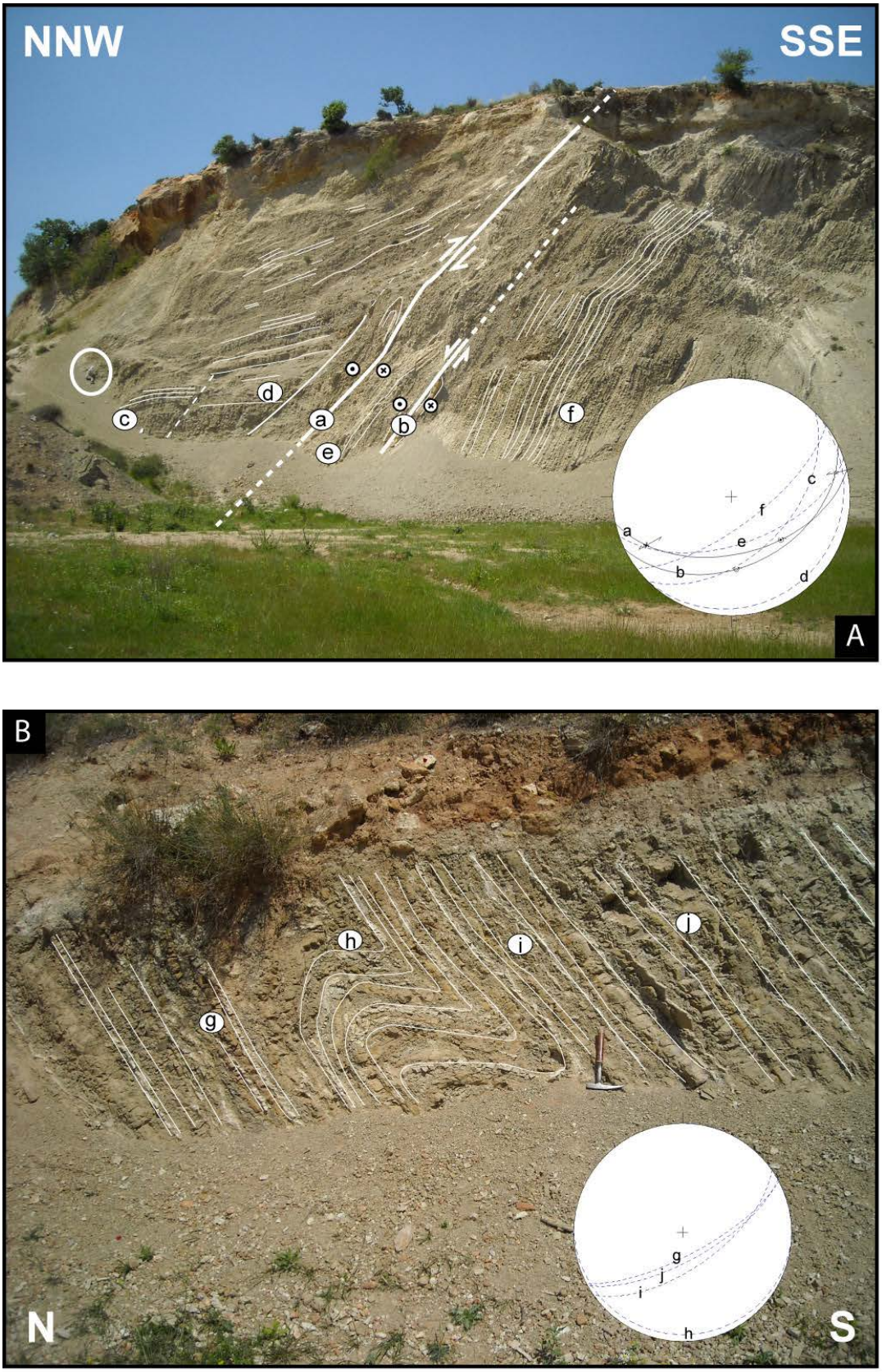

Figure 9. Compression-related deformation along the SE portion of the Adana Basin. In the circle a young geologist for reference scale. [A] and [B] Faulted and unfaulted tight recumbent folds. Bottom right of each picture, the plots of the labeled beddings and faults.

If we plot only the faults whereof the kinematic was determined with respect to both their sense of motion and the age of the deposits in which they were measured (Fig. 10), we notice that all the four populations of fault trends pertaining to the youngest measured deposits are mainly characterized by normal dip-slip and strike-slip kinematics. More specifically, the ~120° NW-SE oriented population show an almost pure dip-slip normal kinematic with a subordinate right- or (more often) left-lateral strike-slip component. The ~155° NW-SE trending population show an oblique sense of motion, with a predominant left-lateral strike-slip component and a subordinate normal dip-slip component. The ~70° WSW-ENE oriented population show an oblique left-lateral strike-slip and normal dip-slip kinematic. Unfortunately, only one fault pertaining to the NNE-SSW trending population showed clear slickenlines pointing to a normal and left-lateral oblique-slip kinematic; nevertheless, other field data, as for example left-lateral offset pebbles and offsets of the strata corroborate the hypothesis that this population is constituted by left-lateral, slightly normal faults. The presence of almost only normal faults associated with major strike-slip components allowed us to easily ascribe the kinematic of the structures measured in the late Tortonian – early Messinian and late Messinian sediments to a transtensional tectonic regime. Going back in time, Langhian-Serravallian deposits are cut by structures showing a different kinematic with respect to the site of measurement.

The SE portion of the Adana Basin is characterized by faults mostly showing a reverse dip-slip component associated with a secondary left-lateral strike slip component. The scarcity of outcrops on this side of the Adana Basin didn't allow us to discern different generations of faults; plots are therefore highly unorganized and the analysis is only quantitative.

The Langhian-Serravallian deposits along the NW side of the basin are intensely deformed by high angle normal fault associated with a subordinate both right- and left-lateral strike-slip component. The previously noticed NE-SW oriented populations (~60°-65° and ~30°) range from almost pure normal dip-slip to almost pure strike-slip. The WNW-ESE oriented population (~95°) show an oblique sense of motion characterized by either right- or, more often, left-lateral normal dip-slip. The few elements showing a reverse dip-slip component are mostly NE-SW oriented; they generally dip toward SE and show a major right-lateral strike-slip component; very few faults dipping towards NW show almost pure reverse dip-slip. The right- and left-lateral strike-slip components are overall equally distributed in all the fault-trend populations.

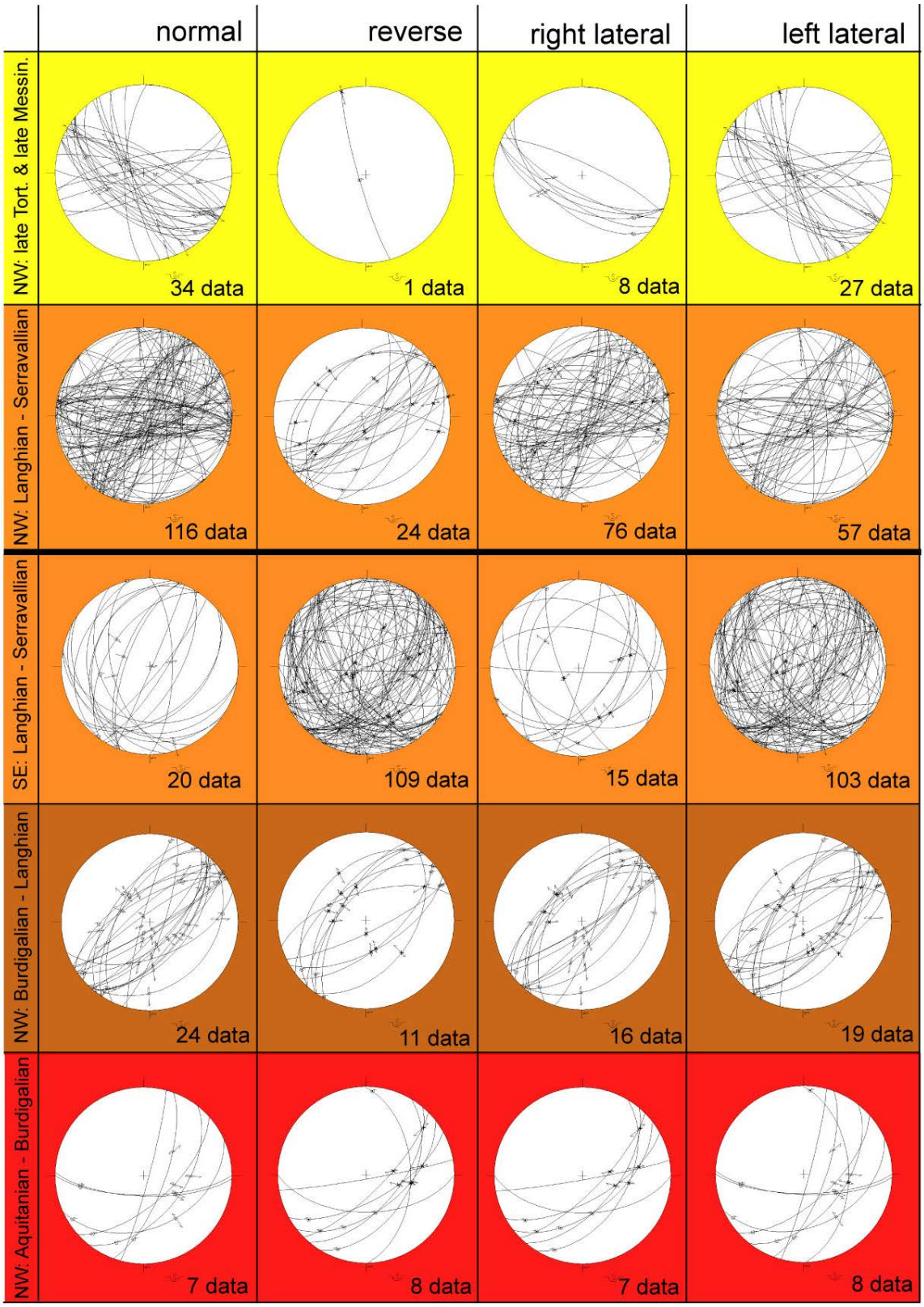

Figure 10. Fault measurements plotted on a Schmidt projection, lower hemisphere, with respect to kinematic and age of the deposits in which they were measured. Discontinuities measured in the Aquitanian – Serravallian deposits pertaining to the NW side of the Adana Basin have been filtered eliminating the structures whose trend correspond to the main trends outline in the late Messinian deposits.

Burdigalian-Langhian deposits are characterized by NE-SW trending normal and subordinate reverse, often conjugated, faults. Both the normal and reverse structures show a minor strike-slip component that doesn't show a preferential sense of motion. The northeasternmost measurement site, characterize also by the oldest deposits (Fig. 5 and 10) is cut by both reverse and normal faults mainly dipping toward SE. Normal faults show a subordinate left-lateral component, whereas reverse faults show a subordinate right-lateral component. Nor the number or the dimension of the structures allowed us to infer the predominant kinematic.

3.5. Discussion

The clearest findings obtained integrating all the data presented in this work is that the NW and SE portion of the Adana Basin behave in completely different ways. When analyzing the spatial distribution of the earthquakes with magnitude ≥ 4.0 (Harvard CMT Catalogue; Ergin et al. 2004), the only active area seems to be toward the SE margin of the basin, in correspondence of the Misis Mountains structural high, whereas the NW margin of the basin seems completely aseismic (Fig. 3). Nevertheless, when taking into account the lower magnitude events (KOERI NEMC Catalogue) we note that an almost continuous energy release presently occurs in the Adana region, with clusters of earthquakes happening along the NW margin at shallow depths (Fig. 2).

Our temporal and spatial analysis of fault kinematic shows that the area of low-magnitude seismicity coincides with an area that have been moderately deformed. The latest phase of deformation that we have surveyed dates back to late Messinian times and is characterized mainly by transtension (Fig. 10). In agreement with what reported by Aksu et al. (2005b) and Burton-Ferguson et al. (2005), these structures can be confidently related with the transtension occurring along the Kozan Fault Zone (Fig.1), currently accomodating the left-lateral motion of the East Anatolian Fault and possibly accomodating the differential uplift between the slower Adana Basin and the faster SE margin of the Central Anatolian Plateau. The absence of NE-SW oriented structures, parallel to the Kozan Fault, could be related to the position of the measurements sites, located in the internal portion of the Adana Basin, south from the Kozan Fault, in an area where, according to Aksu et al. (2005b) and Burton Ferguson et al. (2005) mainly NW-SE oriented extension occurs. The position of the youngest measurement sites, located relatively on the northwestern side

of the basin but distant from the basin margin, would also explain the absence, in the statistical analysis performed on a DEM, (and concentrated on the margins of the Adana Basin; Fig. 4a), of fault populations oriented along the main directions detected in these measurement sites. If we move north from the Kozan Fault (Fig. 5), along the NW side of the Adana Basin, several NE-SW oriented extensional and transtensional structures in the Burdigalian-Serravallian deposits are present (Fig.7 and 10), with a subordinate number of local structures related to transpession (Fig. 8 and 10). Both the trend of the structures and their kinematic can be linked to the Kozan and Ecemiş faults (e.g. Koçyiğit and Beyhan 1999; Jaffey and Robertson 2001; Piper et al. 2010). Unfortunately, since the sites where Aquitanian-Serravallian deposits outcrop are located close to the basin NW margin, relatively distant from the late Tortonian and late Messinian measurement sites, we cannot infer if the observed differences between the Aquitanian-Serravallian and late Tortonian/late Messinian stations are due to variations whether in spatial or temporal deformation. Nevertheless, the presence of diffused low-magnitude seismicity, coupled with the occurrence of several extensional and transtensional faults throughout the NW side of the Adana Basin point to a spatially variable deformation that accomodated and probably still accomodates both the extensional stresses due to the differential uplift occurring between the basin and the SE margin of the Central Anatolian Plateau (Cipollari et al. 2013) and the left-lateral stresses linked to the westward motion of the Aegean-Anatolian plate (Reilinger et al. 1997, 2006). Conversely, along the SE margin of the basin we note left-lateral transpression expressed along structures mainly trending NE-SW and cutting Langhian – Serravallian deposits (Fig. 6; Aksu et al. 2005; Burton-Ferguson et al. 2005) and current transtension outlined by the earthquake focal mechanisms (Fig. 3; Ergin et al. 2004; Over et al. 2004), with a shift from transpression to transtension occurred at Pleistocene time (Over et al. 2004).

Integrating all these observations we obtain a complex evolution of the area. An initial stage (late Oligocene – Serravallian) of deposition occurred in a subsiding area characterized by the presence of a relatively shallow topographic relief along the NW margin of the depocenter, constituted by the accreted Taurides fold-and-thrust belt (e.g. Williams et al. 1995). At the end of Serravallian the Adana region records a regressive event, probably in response to the combined effect of a major sea-level drop, coinciding with the Mi-5 isotope event and the deep-sea hiatus NH4 (Hilgen et al. 2005) and the continental collision between the Arabian and Eurasian plates. (Faranda et al. 2013). Tectonic uplift (Chapter 2) and localized

transpression faults led to the uplift of the Misis structural high (late Serravallian – Tortonian; Kelling et al. 1987; Gökçen et al. 1988; Aksu et al. 2005 Burton-Ferguson et al. 2005). Renewed subsidence occurs during rearrangement of the plates. The moderate deformation showed by the NW portion of the Adana Basin, coupled with the copious sedimentation occurred after Tortonian time and in particular at late Messinian time (Chapter 1) point to a deep-rooted mechanism responsible for the renewed subsidence. From analogue and experimental models (Bajolet et al. 2012), the most likely mechanisms leading subsidence in the Adana Basin after Tortonian time is slab delamination and possibly break-off (Chapter 1) a process that would also explain the Pn slow velocity perturbations observed east of the Cyprus slab (Şengor et al. 2003; Faccenna et al. 2006; Byriol et al. 2011) and the uplift of the SE margin of the Central Anatolian Plateau, which would be a topographic feature supported by mantle processes (Cosentino et al. 2012; Schildgen et al. 2012a). If slab delamination and break-off occurred, we can speculate that the different seismicity of the NW and SE margin of the Adana Basin could be related to different position with respect to the delaminated and possibly broken slab. The SE margin is located close to the East Anatolian Fault, currently defining the plate boundary between the Aegean-Anatolian plate and the African and Arabian plates (e.g. Aksu et al. 2005a). The relatively high magnitude, moderately deep seismicity occurring along the Misis structural high (Ergin et al. 2004; Over et al. 2004) could reflect the vicinity of the plate boundary, characterized by low frequency and relatively high magnitude energy release (Aktar et al. 2000). The shallow and low-magnitude seismicity observed along the central and NW sides of the basin (Fig. 2) could be the crustal response to the mantle upwelling triggered by slab delamination, and studying this seismicity in detail could help understanding the interaction between deep and surface processes.

3.6. Conclusions

Studying the present seismicity and the spatial and temporal deformation through time of the Adana Region we were able to define the different evolution of its NW and SE margin. The SE margin was created, after a first Oligocene-Serravallian period of deposition, by transpression related to the continental collision between the Arabian and Eurasian plates at late Serravallian – Tortonian times. The NW margin if the Adana Basin, already partially uplifted during the Alpine deformation, didn't experienced major compressive phases from Oligocene times. The extension and transtension related deformation is the evidence that the

major phase of margin deformation is due to the uplift of the SE margin of the Central Anatolian Plateau and, more specifically, to the accomodation of the differential uplift occurring between the plateau margin and the adjacent Adana Basin. We relate the high magnitude and relatively deep earthquakes occurring at the SE margin of the Adana Basin with a seismic activity occurring close to a plate boundary in correspondence of a zone of slab delamination ond possibly break-off . The low-magnitude shallow-depth earthquakes recorded in the central and NW portion of the Adana Basin would be the crustal response of a mantle upwelling triggered by the slab delamination.

References

AA.VV. (2002), Türkiye Jeoloji Haritası (Geological map of Turkey), scale 1:500,000, "KAYSERI" sheet, Maden Tetk. ve Arama, Genel Müdürlüğü, Ankara.

Agard, P., Omrani, J., Jolivet, L., and Mouthereau, F. (2005). Convergence history across Zagros (Iran): constraints from collisional and earlier deformation. International Journal of Earth Sciences, 94(3), 401-419.

Agard, P., Omrani, J., Jolivet, L., Whitechurch, H., Vrielynck, B., Spakman, W., Monié, P., Meyer, B., and Wortel, R. (2011). Zagros orogeny: a subduction-dominated process. Geological Magazine, 148(5-6), 692-725.

Akay, E., and Uysal, Ş. (1988). Post-eocene tectonics of the Central Taurus Mountains. Bull. MTA, 108, 23-34.

Aksu, A. E., Calon, T. J., Hall, J., Mansfield, S., and Yaşar, D. (2005b). The Cilicia–Adana basin complex, Eastern Mediterranean: Neogene evolution of an active fore-arc basin in an obliquely convergent margin. Marine geology, 221(1), 121-159.

Aksu, A. E., Calon, T. J., Piper, D. J. W., Turgut, S., and Izdar, E. (1992). Architecture of late orogenic Quaternary basins in northeastern Mediterranean Sea. Tectonophysics, 210(3), 191-213.

Aksu, A. E., Hall, J., and Yaltırak, C. (2005a). Miocene to Recent tectonic evolution of the eastern Mediterranean: New pieces of the old Mediterranean puzzle. Marine Geology, 221(1), 1-13.

Aktar, M., Ergin, M., Özalaybey, S., Tapirdamaz, C., Yörük, A., and Biçmen, F. (2000). A lower-crustal event in the northeastern Mediterranean: The 1998 Adana earthquake (Mw= 6.2) and its aftershocks. Geophysical research letters, 27(16), 2361-2364.

Allen, P. A., and Allen, J. R. (2009). Basin analysis: principles and applications. Wiley. com.

Allmendinger, R. W., Jordan, T. E., Kay, S. M., and Isacks, B. L. (1997). The evolution of the Altiplano-Puna plateau of the Central Andes. Annual Review of Earth and Planetary Sciences, 25(1), 139-174.

Angus, D. A., Wilson, D. C., Sandvol, E., and Ni, J. F. (2006). Lithospheric structure of the Arabian and Eurasian collision zone in eastern Turkey from S-wave receiver functions. Geophysical Journal International, 166(3), 1335-1346.Ozacar, A. A., Gilbert, H., and Zandt, G. (2008). Upper mantle discontinuity structure beneath East Anatolian Plateau (Turkey) from receiver functions. Earth and Planetary Science Letters, 269(3), 427-435.

Ates, A., and Tufan, S. (1999). New gravity and magnetic anomaly maps of Turkey. Geophysical Journal International, 136(2), 499-502.

Bache, F., Olivet, J. L., Gorini, C., Rabineau, M., Baztan, J., Aslanian, D., and Suc, J. P. (2009). Messinian erosional and salinity crises: view from the Provence Basin (Gulf of Lions, Western Mediterranean). Earth and Planetary Science Letters, 286(1), 139-157.

Bajolet, F., Galeano, J., Funiciello, F., Moroni, M., Negredo, A. M., and Faccenna, C. (2012). Continental delamination: Insights from laboratory models. Geochemistry, Geophysics, Geosystems, 13(2).

Ballato, P., Uba, C. E., Landgraf, A., Strecker, M. R., Sudo, M., Stockli, D. F., Friedrich, A., and Tabatabaei, S. H. (2011). Arabia-Eurasia continental collision: Insights from late Tertiary foreland-basin evolution in the Alborz Mountains, northern Iran. Geological Society of America Bulletin, 123(1-2), 106-131.

Bally, A. W., Price, R. A., Roberts, D. G., and Osmaston, M. F. (1982). Musings over Sedimentary Basin Evolution [and Discussion]. Philosophical Transactions of the Royal Society of London. Series A, Mathematical and Physical Sciences, 305(1489), 325-338.

Barka A.A. and Reilinger R., (1997). Active tectonics of the Mediterranean region: deduced from GPS, neotectonic and seismicity data, *Annali di Geophis*., XI, 587–610

Barka, A. A. (1992). The north Anatolian fault zone. In Annales Tectonicae (Vol. 6, No. Suppl, pp. 164-195).

Barka, A., Akyüz, H. S., Cohen, H. A., and Watchorn, F. (2000). Tectonic evolution of the Niksar and Tasova–Erbaa pull-apart basins, North Anatolian Fault Zone: their significance for the motion of the Anatolian block. Tectonophysics, 322(3), 243-264.

Bassant, P., Van Buchem, F. S. P., Strasser, A., and Görür, N. (2005). The stratigraphic architecture and evolution of the Burdigalian carbonate—siliciclastic sedimentary systems of the Mut Basin, Turkey. Sedimentary Geology, 173(1), 187-232.

Bilgiç, T. and AA.VV. (2002), Türkiye Jeoloji Haritası (Geological map of Turkey), scale 1:500,000, "SIVAS" sheet, Maden Tetk. ve Arama, Genel Müdürlüğü, Ankara.

Biryol, C.B., Beck, S. L., Zandt, G., and Özacar, A. A. (2011). Segmented African lithosphere beneath the Anatolian region inferred from teleseismic P-wave tomography. Geophysical Journal International, 184(3), 1037-1057.

Blanc-Valleron, M. M., Rouchy, J. M., Pierre, C., Badaut-Trauth, D., and Schuler, M. (1998). 34. Evidence of Messinian nonmarine deposition at Site 968 (Cyprus Lower Slope). In: Robertson, A.H.F., Emeis, K.-C., Richter, C., and Camerlenghi, A. (Eds.), 1998 Proceedings of the Ocean Drilling Program, Scientific Results, Vol. 160.

Boggs, S. (2009). Petrology of sedimentary rocks. Cambridge University Press.

Bozkurt, E. (2001). Neotectonics of Turkey–a synthesis. Geodinamica Acta, 14(1), 3-30.

Brinkmann, R. (1976). Geology of Turkey. Elsevier Scientific Publishing Company.

Burton-Ferguson, R., Aksu, A. E., Calon, T. J., and Hall, J. (2005). Seismic stratigraphy and structural evolution of the Adana Basin, eastern Mediterranean. Marine geology, 221(1), 189-222.

Carrapa, B., Strecker, M. R., and Sobel, E. R. (2006). Cenozoic orogenic growth in the Central Andes: Evidence from sedimentary rock provenance and apatite fission track thermochronology in the Fiambalá Basin, southernmost Puna Plateau margin (NW Argentina). Earth and Planetary Science Letters, 247(1), 82-100.

Chorowicz, J., Collet, B., Bonavia, F. F., and Korme, T. (1994). Northwest to north-northwest extension direction in the Ethiopian rift deduced from the orientation of extension structures and fault-slip analysis. Geological Society of America Bulletin, 106(12), 1560-1570.

Chung, S. L., Lo, C. H., Lee, T. Y., Zhang, Y., Xie, Y., Li, X., Wang, K.L. and Wang, P. L. (1998). Diachronous uplift of the Tibetan plateau starting 40 Myr ago. Nature, 394(6695), 769-773.

CIESM (Commission Internationale pour l'Exploration de la Mer Mediterranee, Monaco) 2008. The Messinian Salinity Crisis from Mega-Deposits to Microbiology: A Consensus Report. CIESM Workshop Monograph 33, 1-168.

Çíftçí, S., Haciköylü, P., Geze Kalanyuva, Y., Kansu, E., and Aktepe, A. (2012). Exploration plays in the Mersin Basin, Turkish Mediterranean Sea. The Leading Edge, 31(7), 832-845.

Cipollari, P., Cosentino, D., Radeff, G., Schildgen, T.F., Faranda, C., Grossi, F., Gliozzi, E., Smedile, A., Gennari, R., Darbaş G., Dudas, F.Ö., Gürbüz, K., Nazik, A., Echtler, H.P., (2013a). Easternmost Mediterranean evidence of the Zanclean flooding event and subsequent surface uplift: Adana Basin, southern Turkey. In: Robertson, A.H.F., Parlak, O., Ünlügenç, U.C. (Editors), Geological Development of Anatolia and the Easternmost Mediterranean Region. Geological Society of London Special Publications, 372: 473-494.

Cipollari, P., Halasova, E., Guerbuez, K., and Cosentino, D. (2013b). Middle-Upper Miocene paleogeography of southern Turkey: insights from stratigraphy and calcareous nannofossil biochronology of the Olukpınar and Başyayla sections (Mut-Ermenek Basin). Turkish Journal of Earth Sciences, 22(5), 820-838.

Cita, M. B., and Corselli, C. (1990). Messinian paleogeography and erosional surfaces in Italy: an overview. Palaeogeography, palaeoclimatology, palaeoecology, 77(1), 67-82.

Cita, M.B., Wright, R.C., Ryan, W.B.F., and Longinelli, A., (1978). Messinian paleoenvironments. In Hsü K.J., Montadert, L., et al., Init. Repts. DSDP, 42 (Pt. 1): Washington (U.S. Govt. Printing Office), 1003-1035.

Clark, M. K., and Royden, L. H. (2000). Topographic ooze: Building the eastern margin of Tibet by lower crustal flow. Geology, 28(8), 703-706.

Clark, M., and Robertson, A. (2002). The role of the Early Tertiary Ulukisla Basin, southern Turkey, in suturing of the Mesozoic Tethys ocean. Journal of the Geological Society, 159(6), 673-690.

Clark, M., and Robertson, A. (2005). Uppermost Cretaceous–Lower Tertiary Ulukışla Basin, south-central Turkey: sedimentary evolution of part of a unified basin complex within an evolving Neotethyan suture zone. Sedimentary Geology, 173(1), 15-51.

Clauzon, G. (1978). The Messinian Var canyon (Provence, southern France) - paleogeographic implications. Marine Geology, 27, 231–246.

Clauzon, G., Suc, J. P., Gautier, F., Berger, A., and Loutre, M. F. (1996). Alternate interpretation of the Messinian salinity crisis: Controversy resolved?. Geology, 24(4), 363-366.

Cloetingh, S. A. P. L., Maţenco, L., Bada, G., Dinu, C., and Mocanu, V. (2005). The evolution of the Carpathians–Pannonian system: interaction between neotectonics, deep structure, polyphase orogeny and sedimentary basins in a source to sink natural laboratory. Tectonophysics, 410(1), 1-14.

Cornée, J. J., Ferrandini, M., Saint Martin, J. P., Münch, P., Moullade, M., Ribaud-Laurenti, A., Roger, S., Saint Martin, S., and Ferrandini, J. (2006). The late Messinian erosional surface and the subsequent reflooding in the Mediterranean: New insights from the Melilla–Nador basin (Morocco). Palaeogeography, Palaeoclimatology, Palaeoecology, 230(1), 129-154.

Cosentino, D., and Cipollari, P. (2012). The Messinian Central Apennines. Rendiconti Online Società Geologica Italiana, 23, 45–51.

Cosentino, D., Buchwaldt, R., Sampalmieri, G., Iadanza, A., Cipollari, P., Schildgen, T. F., Hinnov, L.A., Ramezani, J., and Bowring, S. A. (2013). Refining the Mediterranean "Messinian gap" with high-precision U-Pb zircon geochronology, central and northern Italy. Geology, 41(3), 323-326.

Cosentino, D., Federici, I., Cipollari, P., and Gliozzi, E. (2006). Environments and tectonic instability in central Italy (Garigliano Basin) during the late Messinian *Lago–Mare* episode: New data from the onshore Mondragone 1 well. Sedimentary Geology, 188, 297-317.

Cosentino, D., Gliozzi, E., and Pipponzi, G. (2007). The late Messinian Lago-Mare episode in the Mediterranean Basin: preliminary report on the occurrence of Paratethyan ostracod fauna from central Crete (Greece). Geobios, 40(3), 339-349.

Cosentino, D., Schildgen, T. F., Cipollari, P., Faranda, C., Gliozzi, E., Hudáčková, N., Lucifora,S., and Strecker, M. R. (2012). Late Miocene surface uplift of the southern margin of the Central Anatolian Plateau, Central Taurides, Turkey. Geological Society of America Bulletin, 124(1-2), 133-145.

Cosentino, Domenico, Darbaş, G., and Gürbüz, K. (2010a). The Messinian salinity crisis in the marginal basins of the peri-Mediterranean orogenic systems: examples from the central Apennines (Italy) and the Adana Basin (Turkey). Geophysical Research Abstracts Vol. 12. EGU General Assembly 2010. (Vol. 12, pp. 2010–2462).

Cosentino, Domenico, Darbaş, G., Gliozzi, E., Grossi, F., Gürbüz, K., and Nazik, A. (2010b). How did the Messinian Salinity Crisis impact the Adana Basin? International Symposium on Eastern Mediterranean Geology; 18-22 October 2010 University of Çukurova ADANA - TURKEY (p. 145).

Costa, G.P., Colalongo, M.L., De Giuli, C., Marabini, S., Masini, F., Torre, D. and Vai, G.B., 1986. Latest Messinian vertebrate fauna preserved in a Paleokarst-neptunian dike setting. Grotte Ital., 12, 221–235.

Cronin, B. T., Gürbüz, K., Hurst, A., and Satur, N. (2000). Vertical and lateral organization of a carbonate deep-water slope marginal to a submarine fan system, Miocene, southern Turkey. Sedimentology, 47(4), 801-824.

Cronin, V. (2004). A draft primer on focal mechanism solutions for geologists. Universidad de Baylor, Texas-EE. UU.< http://serc. carleton. edu/files/NAGTWorkshops/structure, 4.

Dalkiliç H., and Balci V., 2009. Türkiye Jeoloji Haritaları (1:100 000), n° 130 Silifke-030 paftası. Maden Tetkik ve Arma Genel Müdürlüğü.

Daradich, A., Mitrovica, J. X., Pysklywec, R. N., Willett, S. D., and Forte, A. M. (2003). Mantle flow, dynamic topography, and rift-flank uplift of Arabia. Geology, 31(10), 901-904.

DeCelles, P. G., Gehrels, G. E., Quade, J., Ojha, T. P., Kapp, P. A., and Upreti, B. N. (1998). Neogene foreland basin deposits, erosional unroofing, and the kinematic history of the Himalayan fold-thrust belt, western Nepal. Geological Society of America Bulletin, 110(1), 2-21.

Decou, A., Von Eynatten, H., Mamani, M., Sempere, T., and Wörner, G. (2011). Cenozoic forearc basin sediments in Southern Peru (15–18° S): Stratigraphic and heavy mineral constraints for Eocene to Miocene evolution of the Central Andes. Sedimentary Geology, 237(1), 55-72.

Demirel, I. H. (2004). Petroleum systems in the eastern and central Taurus region, Turkey. Marine and petroleum geology, 21(8), 1061-1071.

Dewey, J. F., and Sengör, A. M. C. (1979). Aegean and surrounding regions: complex multiplate and continuum tectonics in a convergent zone. Geological Society of America Bulletin, 90(1), 84-92.

Dewey, J. F., Hempton, M. R., Kidd, W. S. F., Saroglu, F. T., and Şengör, A. M. C. (1986). Shortening of continental lithosphere: the neotectonics of Eastern Anatolia—a young collision zone. Geological Society, London, Special Publications, 19(1), 1-36.

Dilek, Y., Whitney, D. L., and Tekeli, O. (1999). Links between tectonic processes and landscape morphology in an Alpine collision zone, South-Central Turkey. Annals of Geomorphology (Zeitschrift fur Geomorphologie Supplementband), 147-164.

Druckman, Y., Buchbinder, B., Martinotti, G. M., Tov, R., and Aharon, P. (1995). The buried Afiq Canyon (eastern Mediterranean, Israel): a case study of a Tertiary submarine canyon exposed in Late Messinian times. Marine Geology, 123(3), 167-185.

Dziewonski, A. M., Chou, T. A., and Woodhouse, J. H. (1981). Determination of earthquake source parameters from waveform data for studies of global and regional seismicity. Journal of Geophysical Research: Solid Earth (1978–2012), 86(B4), 2825-2852.

Ekström, G., Nettles, M., and Dziewoński, A. M. (2012). The global CMT project 2004–2010: Centroid-moment tensors for 13,017 earthquakes. Physics of the Earth and Planetary Interiors, 200, 1-9.

Emeis, K.-C., Robertson, A.H.F., Richter, C. et al. (Eds.), 1996. Proceedings of the Ocean Drilling Program, Initial Reports 160. College Station, TX (Ocean Drilling Program), 972 pp.

Ergin, M., Aktar, M., and Eyidoğan, H. (2004). Present-day seismicity and seismotectonics of the Cilician Basin: Eastern Mediterranean Region of Turkey. Bulletin of the Seismological Society of America, 94(3), 930-939.

Eriş, K. K., Bassant, P., and Ülgen, U. B. (2005). Tectono-stratigraphic evolution of an Early Miocene incised valley-fill (Derinçay Formation) in the Mut Basin, Southern Turkey. Sedimentary Geology, 173(1), 151-185.

Escutia, C., and Maldonado, A. (1992). Palaeogeographic implications of the Messinian surface in the Valencia Trough, northwestern Mediterranean Sea. Tectonophysics, 203(1), 263-284.

Faccenna, C., Becker, T. W., Jolivet, L., and Keskin, M. (2013). Mantle convection in the Middle East: Reconciling Afar upwelling, Arabia indentation and Aegean trench rollback. Earth and Planetary Science Letters, 375, 254-269.

Faccenna, C., Bellier, O., Martinod, J., Piromallo, C., and Regard, V. (2006). Slab detachment beneath eastern Anatolia: A possible cause for the formation of the North Anatolian fault. Earth and Planetary Science Letters, 242(1), 85-97.

Faccenna, C., Molin, P., Orecchio, B., Olivetti, V., Bellier, O., Funiciello, F., Minelli, L., Piromallo, C., and Billi, A. (2011). Topography of the Calabria subduction zone (southern Italy): Clues for the origin of Mt. Etna. Tectonics, 30(1).

Faranda, C., Gliozzi, E., Cipollari, P., Grossi, F., Darbaş, G., Gürbüz, K., Nazik, A., Gennari, R., and Cosentino, D. (2013). Messinian paleoenvironmental changes in the easternmost Mediterranean Basin: Adana Basin, southern Turkey. Turkish Journal of Earth Sciences, 22(5), 839-863.

Ferguson, R., Hoey, T., Wathen, S., and Werritty, A. (1996). Field evidence for rapid downstream fining of river gravels through selective transport. Geology, 24(2), 179-182.

Fuller, C. W., Willett, S. D., and Brandon, M. T. (2006). Formation of forearc basins and their influence on subduction zone earthquakes. Geology, 34(2), 65-68.

Gans, C. R., Beck, S. L., Zandt, G., Biryol, C. B., and Ozacar, A. A. (2009). Detecting the limit of slab break-off in central Turkey: new high-resolution Pn tomography results. Geophysical Journal International, 179(3), 1566-1572.

Garcia-Castellanos, D., and Villaseñor, A. (2011). Messinian salinity crisis regulated by competing tectonics and erosion at the Gibraltar arc. Nature, 480(7377), 359-363.

Garcia-Castellanos, D., Estrada, F., Jiménez-Munt, I., Gorini, C., Fernández, M., Vergés, J., and De Vicente, R. (2009). Catastrophic flood of the Mediterranean after the Messinian salinity crisis. Nature, 462(7274), 778-781.

Gedik, A., Birgili, Ş., Yilmaz, H., and Yoldas, R. (1979). Mut-Ermenek-Silifke yöresinin jeolojisi ve petrol olanakları. Bull Geol Soc Turkey, 22, 7-26.

Gelati, R. (1975). Miocene marine sequence from Lake Van, eastern Turkey. Riv. Ital. Paleontol. Stratigr, 81, 477-490.

Gennari, R., Iaccarino, S. M., Di Stefano, A., Sturiale, G., Cipollari, P., Manzi, V., Roveri, M., and Cosentino, D. (2008). The Messinian–Zanclean boundary in the Northern Apennine. Stratigraphy, 5(3-4), 307-322.

Giese, P., Scheuber, E., Schilling, F., Schmitz, M., and Wigger, P. (1999). Crustal thickening processes in the Central Andes and the different natures of the Moho-discontinuity. Journal of South American Earth Sciences, 12(2), 201-220.

Gliozzi, E., Cosentino, D., Darbaù, G., Grossi, F., Gürbüz, K., and Nazik, A. (2010). Late Messinian ostracod biozonation: stratigraphical constraints fot the base of the Loxoconcha Mülleri zone derived from Central Apennine (Italy) and Adana Basin (Southern Turkey) successions. International Symposium on Eastern Mediterranean Geology; 18-22 October 2010 University of Çukurova ADANA - TURKEY (p. 141)

Göğüş, O. H., and Pysklywec, R. N. (2008). Mantle lithosphere delamination driving plateau uplift and synconvergent extension in eastern Anatolia. Geology, 36(9), 723-726.

Gökçen, S. L., Kelling, G., Gökçen, N., and Floyd, P. A. (1988). Sedimentology of a late Cenozoic collisional sequence: the Misis Complex, Adana, southern Turkey. Sedimentary geology, 59(3), 205-235.

Gokten, E. (1993). Geology of the southern boundary of Sivas Basin in the east of Ulas (Sivas-Central Anatolia): tectonic development related to the closure of Inner Tauride Ocean. Turkish Assoc. Petrol. Geol. Bull, 5, 35-55.

Gokten, E., and Floyd, P. A. (1987). Geochemistry and tectonic environment of the Sarkl la area volcanic rocks in central Anatolia, Turkey. Mineralogical Magazine, 51, 553-559.

Görür, N. (1992). A tectonically controlled alluvial fan which developed into a marine fan-delta at a complex triple junction: Miocene Gildirli Formation of the Adana Basin, Turkey. Sedimentary geology, 81(3), 243-252.

Görür, N. 1985. Depositional history of Miocene sediments of the NW flank of the Adana Basin. The Sixth Colloquium on the Geology of the Agean Region, pp. 185–208.

Görür, N., (1979). Karaisalı Kireçtaşının (Miyosen) sedimantolojisi. TJKB 22/2, 227–234 (in Turkish).

Görür, N., Oktay, F. Y., Seymen, I., and Şengör, A. M. C. (1984). Palaeotectonic evolution of the Tuzgölü basin complex, Central Turkey: sedimentary record of a Neo-Tethyan closure. Geological Society, London, Special Publications, 17(1), 467-482.

Görür, N., Tüysüz, O., and Celal Şengör, A. M. (1998). Tectonic evolution of the central Anatolian basins. International Geology Review, 40(9), 831-850.

Goudie, A. S. (2005). The drainage of Africa since the Cretaceous. Geomorphology, 67(3), 437-456.

Griffin, D. L. (2002). Aridity and humidity: two aspects of the late Miocene climate of North Africa and the Mediterranean. Palaeogeography, Palaeoclimatology, Palaeoecology, 182(1), 65-91.

Grossi, F., Cosentino, D., and Gliozzi, E. (2008). Late Messinian Lago-Mare ostracods and palaeoenvironments of the central and eastern Mediterranean Basin. Bollettino della Società Paleontologica Italiana, 47(2), 131-146.

Grossi, F., Gliozzi, E., and Cosentino, D. (2011). Paratethyan ostracod immigrants mark the biostratigraphy of the Messinian Salinity Crisis. Joannea Geol. Palaont, 11, 66-68.

Guennoc, P., Gorini, C., and Mauffret, A. (2000). Histoire géologique du Golfe du Lion et cartographie du rift oligo-aquitanien et de la surface messinienne. Géologie de la France, 3, 67-97.

Guillemin, M. and Honzay, J.P., (1982). Le Néogène post-nappe et le Quaternaire du Rif nord-oriental (Maroc). Stratigraphie et tectonique des bassins de Melilla, du Kert, de Boudinar et du piedmont des Kebdana. Notes Mém. Serv. Géol. Maroc, 314, 7–238.

Gürbüz, K. and Kelling, G. (1991). Evolution of Miocene submarine fans, northern Adana Basin, Turkey. EUG VI Strasbourg, 24–8 March,Terra Abstracts, 342.

Gürbüz, K. (1999). Regional implications of structural and eustatic controls in the evolution of submarine fans: an example from the Miocene Adana Basin, Southern Turkey. Geological magazine, 136(3), 311-319.

Gürbüz, K., and Kelling, G. (1993). Provenance of Miocene submarine fans in the northern Adana Basin, southern Turkey: A test of discriminant function analysis. Geological Journal, 28(3-4), 277-293.

Gürbüz, K., Ünlügenç, U.C., (2001). Field Excursion A1 Guide Book – Neogene Adana Basin (26 September 2001) In: Fourth International Turkish Geology Symposium - Çukurova University, Adana, Turkey. 24-28 September 2001.

Hall, J., Aksu, A. E., Calon, T. J., and Yaşar, D. (2005). Varying tectonic control on basin development at an active microplate margin: Latakia Basin, Eastern Mediterranean. Marine geology, 221(1), 15-60.

Hodell, D. A., Brenner, M., Curtis, J. H., and Guilderson, T. (2001). Solar forcing of drought frequency in the Maya lowlands. Science, 292(5520), 1367-1370.

Hoke, G. D., and Garzione, C. N. (2008). Paleosurfaces, paleoelevation, and the mechanisms for the late Miocene topographic development of the Altiplano plateau. Earth and Planetary Science Letters, 271(1), 192-201.

Hsü, K. J., Cita, M. B., and Ryan, W. B. F., (1973). The origin of the Mediterranean evaporites, Initial Rep. Deep Sea Drill. Proj., 13, 1203-1231.

Hsü, K. J., Montadert, L., Bernoulli, D., Bizon, G., Cita, M. B., Erickson, A., Fabricius, F., Garrison, R. E., Kidd, R.B., Mèlierés, F., Müller, C., and Wright, R. C. (1978). (Eds.), 1996. 6. Sites 375 and 376: Florence Rise. Proceedings of the Deep Sea Drilling Project, Initial Reports. 42 (1), 219-304.

Hsü, K. J., Montadert, L., Bernoulli, D., Cita, M. B., Erickson, A., Garrison, R. E., Kidd, R.B., Mèlierés, F., Müller, C., and Wright, R. C., (1977). History of the Mediterranean salinity crisis. Nature, 267(5610), 399-403.

Hüsing, S. K., Zachariasse, W. J., van Hinsbergen, D. J., Krijgsman, W., Inceöz, M., Harzhauser, M., Mandic, O., and Kroh, A. (2009). Oligocene–Miocene basin evolution in SE Anatolia, Turkey: constraints on the closure of the eastern Tethys gateway. Geological Society, London, Special Publications, 311(1), 107-132.

Iaccarino, S. M., and Bossio, A. (1999). 42. Paleoenvironment of Uppermost Messinian sequences in the Western Mediterranean (Sites 974, 975, and 978). In: Zahn, R., Comas, M.C., Klaus, A. (Eds.), Proc. O.D.P., Sci. Res., 161. Ocean Drilling Program, College Station, TX, 529 –541.

Iaccarino, S. M., Cita, M. B., Gaboardi, S., and Gruppini, G. M. (1999a). 15. High-Resolution Biostratigraphy at the Miocene/Pliocene boundary in Holes 974b and 975b, Western Mediterranean1. In Proceedings of the Ocean Drilling Program: Scientific results (Vol. 161, p. 197). The Program.

Iaccarino, S., Castradori, D., Cita, M.B., Di Stefano, E., Gaboardi, S., Mckenzie, J.A., Spezzaferri, S. and Sprovieri, R. (1999b). The Miocene–Pliocene boundary and the significance of the earliest Pliocene flooding in the Mediterranean. Mem. Soc. Geol. Ital. 54, 109–131.

Iadanza, A., Sampalmieri, G., Cipollari, P., Mola, M., and Cosentino, D. (2013). The “Brecciated Limestones” of Maiella, Italy: Rheological implications of hydrocarbon-charged fluid migration in the Messinian Mediterranean Basin. Palaeogeography, Palaeoclimatology, Palaeoecology.

Imprescia, P., Pondrelli, S., Vannucci, G., and Gresta, S. (2012). Regional centroid moment tensor solutions in Cyprus from 1977 to the present and seismotectonic implications. Journal of seismology, 16(2), 147-167.

Jackson, J. (1992). Partitioning of strike-slip and convergent motion between Eurasia and Arabia in eastern Turkey and the Caucasus. Journal of Geophysical Research: Solid Earth (1978–2012), 97(B9), 12471-12479.

Jackson, J., and McKenzie, D. (1984). Active tectonics of the Alpine—Himalayan Belt between western Turkey and Pakistan. Geophysical Journal International, 77(1), 185-264.

Jaffey, N., and Robertson, A. H. (2001). New sedimentological and structural data from the Ecemiş Fault Zone, southern Turkey: implications for its timing and offset and the Cenozoic tectonic escape of Anatolia. Journal of the Geological Society, 158(2), 367-378.

Jolivet, L., and Faccenna, C. (2000). Mediterranean extension and the Africa-Eurasia collision. Tectonics, 19(6), 1095-1106.

Jolivet, L., Faccenna, C., Huet, B., Labrousse, L., Le Pourhiet, L., Lacombe, O., Lecomte, E., Burov, E., Denèle, Y., Brun, J.P., Philippon, M., Paul, A., Salaün, G., Karabulut, H., Piromallo, C., Moniè, P., Gueydan, F., Okay, A.I., Oberhänsli, R., Pourteau, A., Augier, R., Gadenne, L., and Driussi, O. (2013). Aegean tectonics: Strain localisation, slab tearing and trench retreat. Tectonophysics, 597, 1-33.

Kalyoncuoğlu, Ü. Y., Elitok, Ö., Dolmaz, M. N., and Anadolu, N. C. (2011). Geophysical and geological imprints of southern Neotethyan subduction between Cyprus and the Isparta Angle, SW Turkey. Journal of Geodynamics, 52(1), 70-82.

Karig, D. E., and Kozlu, H. (1990). Late Palaeogene-Neogene evolution of the triple junction region near Maraş, south-central Turkey. Journal of the Geological Society, 147(6), 1023-1034.

Kelling, G. (2000). Miocene Carbonate-Fringed Basins of South Central Turkey-Correlation, Evolution and Controls. In EAGE Conference-Geology and Petroleum Geology.

Kelling, G., Gökçen, S. L., Floyd, P. A., and Gökçen, N. (1987). Neogene tectonics and plate convergence in the eastern Mediterranean: new data from southern Turkey. Geology, 15(5), 425-429.

Kelling, G., Robertson, A., and Van Buchem, F. (2005). Cenozoic sedimentary basins of southern Turkey: an introduction. Sedimentary Geology, 173(1), 1-13.

Kempler, D., and Ben-Avraham, Z. (1987). The tectonic evolution of the Cyprean Arc. In Annales Tectonicae (Vol. 1, No. 1, pp. 58-71).

Kempler, D., and Garfunkel, Z. (1994). Structures and kinematics in the northeastern Mediterranean: a study of an irregular plate boundary. Tectonophysics, 234(1), 19-32.

Keskin, M. (2003). Magma generation by slab steepening and breakoff beneath a subduction-accretion complex: An alternative model for collision-related volcanism in Eastern Anatolia, Turkey. Geophysical Research Letters, 30(24), 8046.

Keskin, M., Pearce, J. A., Kempton, P. D., and Greenwood, P. (2006). Magma-crust interactions and magma plumbing in a postcollisional setting: Geochemical evidence from the Erzurum-Kars volcanic plateau, eastern Turkey. Special Papers-Geological Society of America, 409, 475.

Ketin, I. (1948). Über die tektonisch-mechanischen Folgerungen aus den grossen anatolischen Erdbeben des letzten Dezenniums: Geologische Rundschau,v. 36, p. 77–83.

Koç, A., Kaymakci, N., van Hinsbergen, D. J., Kuiper, K. F., and Vissers, R. L. (2012). Tectono-Sedimentary evolution and geochronology of the Middle Miocene Altınapa Basin, and implications for the Late Cenozoic uplift history of the Taurides, southern Turkey. Tectonophysics, 532, 134-155.

Koçyiğit, A., and Beyhan, A. (1998). A new intracontinental transcurrent structure: the Central Anatolian Fault Zone, Turkey. Tectonophysics, 284(3), 317-336.

Kodama, Y. (1994). Downstream changes in the lithology and grain size of fluvial gravels, the Watarase River, Japan; evidence of the role of abrasion in downstream fining. Journal of Sedimentary Research, 64(1a), 68-75.

Krijgsman, W., Hilgen, F. J., Raffi, I., Sierro, F. J., and Wilson, D. S. (1999). Chronology, causes and progression of the Messinian salinity crisis. Nature, 400(6745), 652-655.

Kuscu, G. G., and Geneli, F. (2010). Review of post-collisional volcanism in the Central Anatolian Volcanic Province (Turkey), with special reference to the Tepekoy Volcanic Complex. International journal of earth sciences, 99(3), 593-621.

Le Pichon, X. L., and Angelier, J. (1979). The Hellenic arc and trench system: a key to the neotectonic evolution of the eastern Mediterranean area. Tectonophysics, 60(1), 1-42.

Le Pichon, X., and Angelier, J. (1981). The Aegean Sea. Royal Society of London Philosophical Transactions Series A, 300, 357-372.

Li, J. J., Fang, X. M., Van der Voo, R., Zhu, J. J., Niocaill, C. M., Ono, Y., Pan, B.T., Zhong, W., Wang, J.L., Sasaki, T., Zhang, Y.T., Cao, J.X., Kang, S.C., and Wang, J. M. (1997). Magnetostratigraphic dating of river terraces: Rapid and intermittent incision by the Yellow River of the northeastern margin of the Tibetan Plateau during the Quaternary. Journal of Geophysical Research: Solid Earth (1978–2012), 102(B5), 10121-10132.

Lofi, J., Gorini, C., Berné, S., Clauzon, G., Tadeu Dos Reis, A., Ryan, W. B., and Steckler, M. S. (2005). Erosional processes and paleo-environmental changes in the Western Gulf of Lions (SW France) during the Messinian Salinity Crisis. Marine Geology, 217(1), 1-30.

Lofi, J., Sage, F., Déverchère, J., Loncke, L., Maillard, A., Gaullier, V., Thinon, I., Gillet, H., Guennoc, P., and Gorini, C. (2011). Refining our knowledge of the Messinian salinity crisis records in the offshore domain through multi-site seismic analysis. Bulletin de la Société géologique de France, 182(2), 163-180.

Lüdecke, T., Mikes, T., Rojay, F. B., Cosca, M. A., Mulch, A., and Eriksfiord, A. S. (2013). Stable isotope-based reconstruction of Oligo-Miocene paleoenvironment and paleohydrology of Central Anatolian lake basins (Turkey). Turkish Journal of Earth Sciences, 22(5), 793-819.

Maillard, A., Gorini, C., Mauffret, A., Sage, F., Lofi, J., and Gaullier, V. (2006). Offshore evidence of polyphase erosion in the Valencia Basin (Northwestern Mediterranean): scenario for the Messinian Salinity Crisis. Sedimentary Geology, 188, 69-91.

Manzi, V., Gennari, R., Hilgen, F., Krijgsman, W., Lugli, S., Roveri, M., and Sierro, F. J. (2013). Age refinement of the Messinian salinity crisis onset in the Mediterranean. Terra Nova.

Mart, Y. (2013). Geodynamics of the Middle East domain since the Oligocene: research summary. Journal of the Geological Society, 170(3), 483-496.

Mart, Y., and Ryan, W. B. F. (2002). The Tectonic Effect of The Rollback of The Hellenic Trenches On The Westward Motion of Anatolian. In EGS General Assembly Conference Abstracts (Vol. 27, p. 1345).

Mazzini, I., Hudáčková, N., Joniak, P., Kováčová, M., Mikes, T., Mulch, A., Rojay, B., Lucifora, S., Esu, D., and Soulie-Maersche, I. (2013). Palaeoenvironmental and chronological constraints on the Tuğlu Formation (Çankiri Basin, Central Anatolia, Turkey). Turkish Journal of Earth Sciences, 22.

McClusky, S., Balassanian, S., Barka, A., Demir, C., Ergintav, S., Georgiev, I., Gurkan, O., Hamburger, M., Hurst, K., Kahle, H., Kastens, K., Kekelidze, G., King, R., Kotzev, V., Lenk, O., Mahmoud, S., Mishin, A., Nadariya, M., Ouzounis, A., Paradissis, D., Peter, Y., Prilepin, M., Reilinger, R., Sanli, I., Seeger, H., Tealeb, A., Toksöz, M.N. and Veis, G. (2000). Global Positioning System constraints on plate kinematics and dynamics in the eastern Mediterranean and Caucasus. Journal of Geophysical Research: Solid Earth (1978–2012), 105(B3), 5695-5719.

McKenzie, D. (1972). Active tectonics of the Mediterranean region. Geophysical Journal of the Royal Astronomical Society, 30(2), 109-185.

McKenzie, D. (1978). Active tectonics of the Alpine—Himalayan belt: the Aegean Sea and surrounding regions. Geophysical Journal of the Royal Astronomical Society, 55(1), 217-254.

McKenzie, D. P. (1970). Plate tectonics of the Mediterranean region. Nature, 226, 239-243.

McQuarrie, N., and van Hinsbergen, D. J. (2013). Retrodeforming the Arabia-Eurasia collision zone: Age of collision versus magnitude of continental subduction. Geology, 41(3), 315-318.

Meissner, R., and Mooney, W. (1998). Weakness of the lower continental crust: a condition for delamination, uplift, and escape. Tectonophysics, 296(1), 47-60.

Métivier, F., Gaudemer, Y., Tapponnier, P., and Meyer, B. (1998). Northeastward growth of the Tibet plateau deduced from balanced reconstruction of two depositional areas: The Qaidam and Hexi Corridor basins, China. Tectonics, 17(6), 823-842.

Miller, K. G., Kominz, M. A., Browning, J. V., Wright, J. D., Mountain, G. S., Katz, M. E., Sugarman, P. J., Cramer, B.S., Christie-Blick, N., and Pekar, S. F. (2005). The Phanerozoic record of global sea-level change. science, 310(5752), 1293-1298.

Mocochain, L., Audra, P., Clauzon, G., Bellier, O., Bigot, J. Y., Parize, O., and Monteil, P. (2009). The effect of river dynamics induced by the Messinian Salinity Crisis on karst landscape and caves: Example of the Lower Ardèche river (mid Rhône valley). Geomorphology, 106(1), 46-61.

Molnar, P., England, P., and Martinod, J. (1993). Mantle dynamics, uplift of the Tibetan Plateau, and the Indian monsoon. Reviews of Geophysics, 31(4), 357-396.

Monod, O. (1977). Recherches géologiques dans le Taurus occidental au sud de Beysehir (Turquie) (Doctoral dissertation).

Mulder, C. J., Lehner, P., and Allen, D. C. K. (1975). Structural evolution of the Neogene salt basins in the eastern Mediterranean and the Red Sea. Geol. Mijnbouw, 54(3-4), 208-221.

Najman, Y., and Garzanti, E. (2000). Reconstructing early Himalayan tectonic evolution and paleogeography from Tertiary foreland basin sedimentary rocks, northern India. Geological Society of America Bulletin, 112(3), 435-449.

Nazik, A. (2004). Planktonic foraminiferal biostratigraphy of the Neogene sequence in the Adana Basin, Turkey, and its correlation with standard biozones. Geological Magazine, 141(3), 379-387.

Nazik, A., and Gürbüz, K. (1992). Karaisalı-Çatalan-Egner yöresinin (KB-Adana) alt-orta Miyosen istifinin planktonik foraminifer giyostratigrafisi. Turkiye Jeoloji Bulteni, 35(1), 67-80.(In Turkish)

Okay, A. I., Satir, M., Zattin, M., Cavazza, W., and Topuz, G. (2008). An Oligocene ductile strike-slip shear zone: The Uludağ Massif, northwest Turkey—Implications for the westward translation of Anatolia. Geological Society of America Bulletin, 120(7-8), 893-911.

Okay, A. I., Zattin, M., and Cavazza, W. (2010). Apatite fission-track data for the Miocene Arabia-Eurasia collision. Geology, 38(1), 35-38.

Orszag-Sperber, F. (2006). Changing perspectives in the concept of "Lago-Mare" in Mediterranean Late Miocene evolution. Sedimentary Geology, 188, 259-277.

Orszag-Sperber, F., Rouchy, J. M., and Blanc-Valleron, M. M. (2000). La transition Messinien–Pliocène en Méditerranée orientale (Chypre): la période du *Lago-Mare* et sa signification. Comptes Rendus de l'Académie des Sciences-Series IIA-Earth and Planetary Science, 331(7), 483-490.

Over, S., Ozden, S., and Can Unlugenc, U. (2004). Late Cenozoic stress distribution along the Misis Range in the Anatolian, Arabian, and African plate intersection region, SE Turkey. Tectonics, 23(3).

Ozacar, A. A., Gilbert, H., and Zandt, G. (2008). Upper mantle discontinuity structure beneath East Anatolian Plateau (Turkey) from receiver functions. Earth and Planetary Science Letters, 269(3), 427-435.

Özgül, N. (1976). Toroslar'm bazı temel jeoloji özellikleri. Bulletin of the Geological Society of Turkey, 19, 65-78.

Pearce, J. A., Bender, J. F., De Long, S. E., Kidd, W. S. F., Low, P. J., Güner, Y., Saroglu, Y., Yilmaz, S., Moorbath, S., and Mitchell, J. G. (1990). Genesis of collision volcanism in Eastern Anatolia, Turkey. Journal of Volcanology and Geothermal Research, 44(1), 189-229.

Pierre, C., Caruso, A., Blanc-Valleron, M. M., Rouchy, J. M., and Orzsag-Sperber, F. (2006). Reconstruction of the paleoenvironmental changes around the Miocene–Pliocene boundary along a West–East transect across the Mediterranean. Sedimentary Geology, 188, 319-340.

Piper, J. D. A., Gürsoy, H., Tatar, O., Beck, M. E., Rao, A., Koçbulut, F., and Mesci, B. L. (2010). Distributed neotectonic deformation in the Anatolides of Turkey: A palaeomagnetic analysis. Tectonophysics, 488(1), 31-50.

Poisson, A. (1977). Recherches géologiques dans les Taurides occidentales (Turquie) (Doctoral dissertation).

Poole, A., and Robertson, A. (1998). Pleistocene fanglomerate deposition related to uplift of the Troodos Ophiolite, Cyprus. In Proceedings of the Ocean Drilling Program. Scientific results (Vol. 160, pp. 545-566). Ocean Drilling Program.

Reilinger, R. E., McClusky, S. C., Oral, M. B., King, R. W., Toksoz, M. N., Barka, A. A., Kinik, I., Lenk, O. and Sanli, I. (1997). Global Positioning System measurements of present-day crustal movements in the Arabia-Africa-Eurasia plate collision zone. Journal of Geophysical Research: Solid Earth (1978–2012), 102(B5), 9983-9999.

Reilinger, R., McClusky, S., Vernant, P., Lawrence, S., Ergintav, S., Cakmak, R., Ozener,H., Kadirov, F., Guliev,I., Stepanyan, R., Nadariya,M., Hahubia,G., Mahmoud, S., Sakr, K., ArRajehi, A., Paradissis,D., Al-Aydrus, A., Prilepin, M., Guseva, T., Evren, E., Dmitrotsa, A., Filikov, S. V., Gomez, F., Al-Ghazzi, R., and Karam, G. (2006). GPS constraints on continental deformation in the Africa-Arabia-Eurasia continental collision zone and implications for the dynamics of plate interactions. Journal of Geophysical Research: Solid Earth (1978–2012), 111(B5).

Reuter, M., Brachert, T. C., and Grunert, P. (2011). Fossil round karren from Cyprus: a latest Miocene record of a humid-temperate climate in the eastern Mediterranean. Facies, 57(1), 39-50.

Riding, R., Braga, J. C., and Martín, J. M. (1999). Late Miocene Mediterranean desiccation: topography and significance of theSalinity Crisis' erosion surface on-land in southeast Spain. Sedimentary Geology, 123(1), 1-7.

Robertson, A. H. (2000). Mesozoic-Tertiary tectonic-sedimentary evolution of a south Tethyan oceanic basin and its margins in southern Turkey. Geological Society, London, Special Publications, 173(1), 97-138.

Robertson, A. H. F., and Woodcock, N. H. (1986). The role of the Kyrenia Range Lineament, Cyprus, in the geological evolution of the eastern Mediterranean area. Philosophical Transactions of the Royal Society of London. Series A, Mathematical and Physical Sciences, 317(1539), 141-177.

Robertson, A. H. F., Dixon, J. E., Brown, S., Collins, A., Morris, A., Pickett, E., Sharp, I., and Ustaömer, T. (1996). Alternative tectonic models for the Late Palaeozoic-Early Tertiary development of Tethys in the Eastern Mediterranean region. Geological Society, London, Special Publications, 105(1), 239-263.

Robertson, A. H., and Dixon, J. E. (1984). Introduction: aspects of the geological evolution of the Eastern Mediterranean. Geological Society, London, Special Publications, 17(1), 1-74.

Robertson, A. H., and Mountrakis, D. (2006). Tectonic development of the Eastern Mediterranean region: an introduction. Geological Society, London, Special Publications, 260(1), 1-9.

Robertson, A., Unlügenç, Ü. C., İnan, N., and Taśli, K. (2004). The Misis–Andırın Complex: a Mid-Tertiary melange related to late-stage subduction of the Southern Neotethys in S Turkey. Journal of Asian Earth Sciences, 22(5), 413-453.

Rouchy, J. M., Orszag-Sperber, F., Blanc-Valleron, M. M., Pierre, C., Rivière, M., Combourieu-Nebout, N., and Panayides, I. (2001). Paleoenvironmental changes at the Messinian–Pliocene boundary in the eastern Mediterranean (southern Cyprus basins): significance of the Messinian Lago-Mare. Sedimentary Geology, 145(1), 93-117.

Rouchy, J. M., Pierre, C., Et-Touhami, M., Kerzazi, K., Caruso, A., and Blanc-Valleron, M. M. (2003). Late Messinian to Early Pliocene paleoenvironmental changes in the Melilla Basin (NE Morocco) and their relation to Mediterranean evolution. Sedimentary Geology, 163(1), 1-27.

Rouchy, J.M., (1982). La genèse des évaporites messiniennes de Méditerranée. Mem. Mus. Nat. Hist. Nat., 50:1-267.

Roveri M., Lugli S., Manzi V., Gennari R., Iaccarino S. M., Grossi F., Taviani M., (2006) – The record of Messinian events in the Northern Apennines foredeep basins. Acta Naturalia de "L'Ateneo Parmense". 42 (1): 65 pp.

Roveri, M., Bassetti, M. A., and Ricci Lucchi, F. (2001). The Mediterranean Messinian salinity crisis: an Apennine foredeep perspective. Sedimentary Geology, 140(3), 201-214.

Roveri, M., Lugli, S., Manzi, V., and Schreiber, B. C. (2008). The Messinian Sicilian stratigraphy revisited: new insights for the Messinian salinity crisis. Terra Nova, 20(6), 483-488.

Roveri, M., Manzi, V., Bassetti, M. A., Merini, M., and Ricci Lucchi, F. (1998). Stratigraphy of the Messinian post-evaporitic stage in eastern-Romagna (northern Apennines, Italy). Giornale di Geologia, 60, 119-142.

Ryan, W. B. (2009). Decoding the Mediterranean salinity crisis. Sedimentology, 56(1), 95-136.

Şafak, Ü., Kelling, G., Gökçen, N. S., and Gürbüz, K. (2005). The mid-Cenozoic succession and evolution of the Mut basin, southern Turkey, and its regional significance. Sedimentary Geology, 173(1), 121-150.

Salvini, F. (2008). Daisy software. Università Roma Tre, Italy.

Salvini, F., Billi, A., and Wise, D. U. (1999). Strike-slip fault-propagation cleavage in carbonate rocks: the Mattinata Fault Zone, Southern Apennines, Italy. Journal of Structural Geology, 21(12), 1731-1749.

Sampalmieri, G., Cipollari, P., Cosentino, D., Iadanza, A., Lugli, S. and Soligo, M., (2008). Evaporites of the Messinian salinity crisis: natural radioactivity of the Gessoso-Solfifera Fm in the Maiella Mts (Abruzzi, central Italy). Bollettino della Societa Geologica Italiana 127 (1), 25–36.

Sampalmieri, G., Iadanza, A., Cipollari, P., Cosentino, D., and Lo Mastro, S. (2010). Palaeoenvironments of the Mediterranean Basin at the Messinian hypersaline/hyposaline transition: evidence from natural radioactivity and microfacies of post-evaporitic successions of the Adriatic sub-basin. Terra Nova, 22(4), 239-250.

Scheidegger, A. E., and Ai, N. S. (1986). Tectonic processes and geomorphological design. Tectonophysics, 126(2), 285-300.

Schildgen, T. F., Cosentino, D., Bookhagen, B., Niedermann, S., Yıldırım, C., Echtler, H., Wittmann, H., and Strecker, M. R. (2012a). Multi-phased uplift of the southern margin of the Central Anatolian plateau, Turkey: A record of tectonic and upper mantle processes. Earth and Planetary Science Letters, 317, 85-95.

Schildgen, T. F., Cosentino, D., Caruso, A., Buchwaldt, R., Yıldırım, C., Bowring, S. A., Rojay,B., Echtler, H., and Strecker, M. R. (2012b). Surface expression of eastern Mediterranean slab dynamics: Neogene topographic and structural evolution of the southwest margin of the Central Anatolian Plateau, Turkey. Tectonics, 31(2).

Schildgen, T. F., Hodges, K. V., Whipple, K. X., Pringle, M. S., van Soest, M., and Cornell, K. (2009). Late Cenozoic structural and tectonic development of the western margin of the central Andean Plateau in southwest Peru. Tectonics, 28(4).

Schildgen, T. F., Hodges, K. V., Whipple, K. X., Reiners, P. W., and Pringle, M. S. (2007). Uplift of the western margin of the Andean plateau revealed from canyon incision history, southern Peru. Geology, 35(6), 523-526.

Schildgen, T.F., Yildirim, C., Cosentino, D., Strecker, M.R., in press. Linking slab break-off, Hellenic trench retreat, and uplift of the Central and Eastern Anatolian plateaus. Earth-Science Reviews.

Schmidt, G. C. (1961). Stratigraphic nomenclature for the Adana region petroleum district VII. Petroleum Administration Bulletin, 6, 47-63.

Schurr, B., Rietbrock, A., Asch, G., Kind, R., and Oncken, O. (2006). Evidence for lithospheric detachment in the central Andes from local earthquake tomography. Tectonophysics, 415(1), 203-223.

Sclater, J. G., and Christie, P. (1980). Continental stretching: An explanation of the post-Mid-Cretaceous subsidence of the central North Sea Basin. Journal of Geophysical Research: Solid Earth (1978–2012), 85(B7), 3711-3739.

Sengör, A. M. C. (1979). The North Anatolian transform fault: its age, offset and tectonic significance. Journal of the Geological Society, 136(3), 269-282.

Şengör, A. M. C., Büyükaşikoğlu, S., and Canitez, N. (1983). Neotectonics of the Pontides: Implications for 'incompatible'structures along the North Anatolian Fault. Journal of Structural Geology, 5(2), 211-216.

Şengör, A. M. C., Görür, N., and Şaroğlu, F. (1985). Strike-slip deformation basin formation and sedimentation: Strike-slip faulting and related basin formation in zones of tectonic escape: Turkey as a case

study. Strike-slip faulting and basin formation. Society of EconomicPaleontologists and Mineralogist, Special Publication, 37, 227-264.

Şengör, A. M. C., Özeren, S., Genç, T., and Zor, E. (2003). East Anatolian high plateau as a mantle-supported, north-south shortened domal structure. Geophysical Research Letters, 30(24).

Sengör, A. M. C., Tüysüz, O., Imren, C., Sakinç, M., Eyidogan, H., Görür, N., Le Pichon, X., and Rangin, C. (2005). The North Anatolian fault: A new look. Annu. Rev. Earth Planet. Sci., 33, 37-112.

Şengör, A. M. C., Yılmaz, Y., and Sungurlu, O. (1984). Tectonics of the Mediterranean Cimmerides: nature and evolution of the western termination of Palaeo-Tethys. Geological Society, London, Special Publications, 17(1), 77-112.

Şengör, A. M., and Yilmaz, Y. (1981). Tethyan evolution of Turkey: a plate tectonic approach. Tectonophysics, 75(3), 181-241.

Şengör, A.M.C. (1980), Türkiye'nin Neotektoniginin Esaslari, Türk. Jeol. Kur., Konf. Serisi, 2, 40 pp. (In turkish)

Shackleton, N. J. (1995). Pliocene stable isotope stratigraphy of Site 846. In Proc. ODP, Sci. Results (Vol. 138, pp. 337-355). College Station, TX (Ocean Drilling Program).

Soria, J. M., Caracuel, J. E., Yébenes, A., Fernández, J., and Viseras, C. (2005). The stratigraphic record of the Messinian salinity crisis in the northern margin of the Bajo Segura Basin (SE Spain). Sedimentary Geology, 179(3), 225-247.

Speranza, G., Cosentino, D., Tecce, F., and Faccenna, C. (2013). Palaeoclimate reconstruction during the Messinian evaporative drawdown of the mediterranean basin: Insights from microthermometry on halite fluid inclusions. Geochemistry, Geophysics, Geosystems.

Steckler, M. S., and Watts, A. B. (1978). Subsidence of the Atlantic-type continental margin off New York. Earth and Planetary Science Letters, 41(1), 1-13.

Strecker, M. R., Alonso, R. N., Bookhagen, B., Carrapa, B., Hilley, G. E., Sobel, E. R., and Trauth, M. H. (2007). Tectonics and climate of the southern central Andes. Annu. Rev. Earth Planet. Sci., 35, 747-787.

Strecker, M. R., Alonso, R., Bookhagen, B., Carrapa, B., Coutand, I., Hain, M. P., Hilley, G.E., Mortimer, E., Schoenbohm, L., and Sobel, E. R. (2009). Does the topographic distribution of the central Andean Puna Plateau result from climatic or geodynamic processes?. Geology, 37(7), 643-646.

Tanar, U. (1989). Mut Havzasi Tersiyer istifinin stratigrafik ve mikropaleontolojik (Ostrakod ve Foraminifer) incelemesi. CU Fen Bilimleri Enstitusu, Adana.

Tanar, U., and Gökçen, N. (1990). Mut-Ermenek Tersiyer istifinin stratigrafisi ve mikropaleontolojisi. MTA Dergisi, 110, 175-180.

Tapponier, P. (1977). Evolution tectonique du system Alpin en Mediterraean: Poinconnement et ecrasement rigide-plastique. Bull. Soc. Géol. France, 19, 437-460.

Tapponnier, P., Zhiqin, X., Roger, F., Meyer, B., Arnaud, N., Wittlinger, G., and Jingsui, Y. (2001). Oblique stepwise rise and growth of the Tibet Plateau. science, 294(5547), 1671-1677.

Uba, C. E., Strecker, M. R., and Schmitt, A. K. (2007). Increased sediment accumulation rates and climatic forcing in the central Andes during the late Miocene. Geology, 35(11), 979-982.

Ulu, Ü. and AA.VV. (2002a), Türkiye Jeoloji Haritası (Geological map of Turkey), scale 1:500,000, "ADANA" sheet, Maden Tetk. ve Arama, Genel Müdürlüğü, Ankara.

Ulu, Ü. and AA.VV. (2002b), Türkiye Jeoloji Haritası (Geological map of Turkey), scale 1:500,000, "HATAY" sheet, Maden Tetk. ve Arama, Genel Müdürlüğü, Ankara.

Ünlügenç, U. C. (1993). Controls on Cenozoic sedimentation in the Adana Basin, southern Turkey. University of Kent at Canterbury.

Ünlügenç, U. C., Demirkol, C., and Safak, U. (1991). Stratigraphical and sedimentological characteristics of the Karsanti Basin fill to the NE of the Adana Basin. In Proc. A. Suat Erk Geology Symposium, Ankara (pp. 215-227).

Van der Laan, E., Snel, E., De Kaenel, E., Hilgen, F. J., and Krijgsman, W. (2006). No major deglaciation across the Miocene-Pliocene boundary: Integrated stratigraphy and astronomical tuning of the Loulja sections (Bou Regreg area, NW Morocco). Paleoceanography, 21(3).

Vandervoort, D. S., Jordan, T. E., Zeitler, P. K., and Alonso, R. N. (1995). Chronology of internal drainage development and uplift, southern Puna plateau, Argentine central Andes. Geology, 23(2), 145-148.

Wandres, A. M., Bradshaw, J. D., Weaver, S., Maas, R., Ireland, T., and Eby, N. (2004). Provenance analysis using conglomerate clast lithologies: a case study from the Pahau terrane of New Zealand. Sedimentary Geology, 167(1), 57-89.

Wells, S. G., Bullard, T. F., Menges, C. M., Drake, P. G., Karas, P. A., Kelson, K. I., Ritter, J.B., and Wesling, J. R. (1988). Regional variations in tectonic geomorphology along a segmented convergent plate boundary pacific coast of Costa Rica. Geomorphology, 1(3), 239-265.

Whitney, D. L., and Dilek, Y. (1997). Core complex development in central Anatolia, Turkey. Geology, 25(11), 1023-1026.

Willett, S. D., Schlunegger, F., and Picotti, V. (2006). Messinian climate change and erosional destruction of the central European Alps. Geology, 34(8), 613-616.

Williams, G. D., Ünlügenç, U. C., Kelling, G., and Demirkol, C. (1995). Tectonic controls on stratigraphic evolution of the Adana Basin, Turkey. Journal of the Geological Society, 152(5), 873-882.

Woodcock, N. H., and Robertson, A. H. F. (1982). Wrench and thrust tectonics along a Mesozoic–Cenozoic continental margin: Antalya Complex, SW Turkey. Journal of the Geological Society, 139(2), 147-163.

Wörner, G., Uhlig, D., Kohler, I., and Seyfried, H. (2002). Evolution of the West Andean Escarpment at 18 S (N. Chile) during the last 25 Ma: uplift, erosion and collapse through time. Tectonophysics, 345(1), 183-198.

Yalcın, M., and Gorur, N. (1984). Sedimentological evolution of the Adana Basin. In Geology of the Taurus belt. International symposium (pp. 165-172).

Yang, Y., and Liu, M. (2002). Cenozoic deformation of the Tarim plate and the implications for mountain building in the Tibetan Plateau and the Tian Shan. Tectonics, 21(6), 1059.

Yetis, C. (1988). Reorganization of the Tertiary stratigraphy in the Adana Basin, southern Turkey. Newsletters on Stratigraphy, 20(1), 43-58.

Yetiş, C., and Demirkol, C. (1986). Adana baseni batı kesiminin detay jeoloji etüdü. MTA Enstitüsü, Derleme, (8037) (in Turkish).

Yetiş, C., Kelling, G., Gökçen, S. L., and Baroz, F. (1995). A revised stratigraphic framework for later Cenozoic sequences in the northeastern Mediterranean region. Geologische Rundschau, 84(4), 794-812.

Yıldız, A., Toker, V., Demircan, H., and Sevim, S. (2003). Paleoenvironmental interpretation and findings of Pliocene–Pleistocene nannoplankton, planktic foraminifera, trace fossil in the Mut Basin. Yerbilimleri, 28, 123-144.

Yilmaz, Y., Tüysüz, O., Yigitbas, E., Can Genç, S., and Sengör, A. M. C. (1998). Geology and tectonic evolution of the Pontides. Memoirs-American Association of Petroleum Geologists, 183-226.

Yin, A. (2010). Cenozoic tectonic evolution of Asia: A preliminary synthesis. Tectonophysics, 488(1), 293-325.

Yuan, D. Y., Ge, W. P., Chen, Z. W., Li, C. Y., Wang, Z. C., Zhang, H. P., Zhang, P.Z., Zheng, D.W., Zheng, W.J., W.H., Craddock, Dayem, K.E., Duvall, A.R., Hough, B.G., Lease, R.O., Champagnac, J.D., Burbank, D.W., Clark, M.K., Farley, K.A., Garzione, C.N., Kirby, E., Molnar, P., and Roe, G. H. (2013). The growth of northeastern Tibet and its relevance to large-scale continental geodynamics: A review of recent studies. Tectonics.

Yuan, X., Sobolev, S. V., Kind, R., Oncken, O., Bock, G., Asch, G., .Schurr, F. Graeber, A. Rudloff, W. Hanka, K. Wylegalla, R. Tibi, Ch. Haberland, A. Rietbrock, P. Giese, P. Wigger, P. Röwer, G. Zandt, S. Beck, T. Wallace, M. Pardo and Comte, D. (2000). Subduction and collision processes in the Central Andes constrained by converted seismic phases. Nature, 408(6815), 958-961.

Zapata, S., Weber, M., Cardona, A., Valencia, V., Guzmán, G., and Tabón, M. (2010). Provenance of Oligocene conglomerates and associated sandstones from the Siamaná formation, Serraníade Jarara, Guajira, Colombia: implications for Oligocene Caribbean-South American tectonics. Boletín de Ciencias de la Tierra, (27), 07-24.

Zattin, M., Cavazza, W., Okay, A. I., Federici, I., Fellin, M. G., Pignalosa, A., and Reiners, P. (2010). A precursor of the North Anatolian Fault in the Marmara Sea region. Journal of Asian Earth Sciences, 39(3), 97-108.

Zattin, M., Okay, A. I., and Cavazza, W. (2005). Fission-track evidence for late Oligocene and mid-Miocene activity along the North Anatolian Fault in south-western Thrace. Terra Nova, 17(2), 95-101.

Zhisheng, A., Kutzbach, J. E., Prell, W. L., and Porter, S. C. (2001). Evolution of Asian monsoons and phased uplift of the Himalaya–Tibetan plateau since Late Miocene times. Nature, 411(6833), 62-66.

Zor, E., Sandvol, E., Gürbüz, C., Türkelli, N., Seber, D., and Barazangi, M. (2003). The crustal structure of the East Anatolian plateau (Turkey) from receiver functions. Geophysical Research Letters, 30(24), 8044.

Acknowledgements

I think that the art of thanking is better expressed in one's own mother tongue.
If you find your name in these pages you probably know why.

(...) afinal bem se pode afirmar que o destino existe, o destino de cada um é nas mãos dos outros que está.

(...) in fondo si può ben dire che il fato esiste, il destino di ognuno è proprio nelle mani degli altri.

(...) when all is said and done, we can confidently say that destiny exists and each man's destiny is in the hands of others.
"O Evangelho segundo Jesus Cristo" , José Saramago

Se è vero quel che scrive Saramago il mio destino, viaggiando sulle prorompenti note del gagliardo Ludwig van, deve essere passato per mani di probe persone: ardimentosi che con le loro parole ed i loro consigli, hanno "*temperato la mia natura intemperante e impedito di farmi arrivare a livelli di depressione da suicidio o a manie di grandezza napoleoniche" (Niccolò Ammaniti*).

Tra i ringraziamenti ufficiali compare il Boss, Domenico Cosentino, sempre presente e mai invadente; Taylor Schildgen, irreprensibile correttrice di testi; Manfred Strecker, impeccabile coordinatore; Kemal Gürbüz, ospitale professore e "nostro agente ad Adana".

In pole-position sono, ovviamente, il signor Christian, la signora Florià ed Elli, che mi hanno spesso sfamata, curata, ascoltata ed accudita. La signora Concetta, che mi ha accompagnata mentre terminavo questa tesi.

Un grazie di imprecisato chilometraggio a Valerio ed Itala, gioie (e qualche piccolo dolore) di questi tre anni.

Un arzillo omaggio ai fantastici coinquis, che sì, sono supereroi ninja ma soprattutto degnissimi abitanti della remota Villa Arzilla.

Ai compagni di merende (e non): Annalisa, che imperturbabile coniuga scienza ed esoterismo; Francesco, serio naturalista con l'hobby del gossip; Paolo, "chiedetemi tutto ma non di lunedì"; Paola, quasi compagna di stanza; Chiaramadori, che ha una timetable più fitta di Laura Palmer; Martina dalla voce melodica; Martamarchegiano da Ortona; Stephanie, severa critica dell'odiosa estate tedesca; Veronica, sempre sorridente; Eren, cinefilo determinato; Micha, compagno di caffè; Scampa, compagna di ventura; Becci, compagna di campagna: denghiù, siete stati croccantissimi.

Un "Grazie, grazie che c'eri!" a Laura e ZaraZara, sulla strada per la felicità; a Federico Bussoni, un gioioso migrante; a Vittoria e Teresa, colonne portanti. Grazie mille a Chiaramarocco, Margherita, Gabriella, Tiglio, Anita, Emanuzz, Mary, Jayne, Valentina e Valeria, erranti nel mondo o di ritorno a casa.

Grazie per i ripetuti aiuti a Barbara Norrito, Tanja, Andrea Franceschini, Claudio e Steffy, chiavi di qualsiasi ricerca.

Sentiti ossequi a Luigi, Giacomo, Filippo, Kristian, Vinci, Valerio Drago, Mozart, Samuele, Benedetta, Leonardo, Tommaso e Pietro, che me l'hanno fatta prende – tendenzialmente - bene. E grazie mille a Daniela, Giordano, Gino, la Signorina Margherita, Carola, Elena, Silverio e Rossella, per l'affetto e l'accoglienza.

In ordine sparso vorrei anche ringraziare Francesca Cifelli, Elsa Gliozzi, Cengiz Yildirim, Matteo Maggi, Gerold Zeilinger, Jhosnella, Gianluca, Matteo e Michele a Potsdam, Angela, Andrea, Emanuele, Sarah, Erpiastra, Fabio del bar Zazie, il bar Bri tutto e Zerocalcare: forse vi sfugge, ma ognuno di voi ha

pronunciato saggia frase, o ha dato degno consiglio o fornito un essenziale appoggio al momento giusto (e se si tratta di un consiglio non ancora seguito, lo sarà in futuro).

Il grazie più deciso va ovviamente a tutti coloro che non sono menzionati ma dovrebbero esserlo: neppure con tre anni di dottorato sono riuscita a moderare la mia inguaribile smemoratezza.